pt. 1

This is to certify that the

dissertation entitled

ASSESSING A GEOGRAPHIC INFORMATION SYSTEM AND ANN-AGNPS WATER QUALITY MODEL: A CASE STUDY

presented by

Scott E. Needham

has been accepted towards fulfillment
of the requirements for

Ph.D. degree in Resource Development

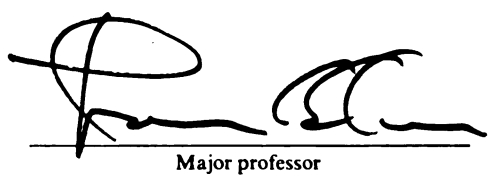

Major professor

Date August 2, 1994

ASSESSING A GEOGRAPHIC INFORMATION SYSTEM AND ANN-AGNPS WATER QUALITY MODEL: A CASE STUDY

By

Scott E. Needham

A DISSERTATION

Submitted to
Michigan State University
in partial fulfillment of the requirements
for the degree of

DOCTOR OF PHILOSOPHY

Department of Resource Development

1994

ABSTRACT

ASSESSING A GEOGRAPHIC INFORMATION SYSTEM AND ANN-AGNPS WATER QUALITY MODEL: A CASE STUDY

By

Scott E. Needham

Geographic Information Systems (GIS) and nonpoint source (NPS) water quality simulation models have been identified as important tools for supporting the development of agricultural resource conservation and water quality management plans. It is anticipated that by integrating these two technologies, conservation planners will operate more efficiently towards mitigating the impacts of agricultural NPS water pollution. The basic goal of this research is to assess the capabilities of the integrated GIS/simulation model computer technology prior to its adoption into mainstream agricultural water quality planning and management.

The research is divided into two separate areas. Each area addresses one half of the identified technology: GIS, and the distributed-parameter grid-based NPS pollution simulation model ANN-AGNPS. The first half of the research focuses on the capabilities of the GIS to generate input parameters for the ANN-AGNPS model from identified available digital data sources, as compared to typically used map interpretation/field survey methods. The capabilities of GIS parameter generation were further tested by assessing model output results, including hydrology, suspended sediment and soluble nitrogen, for the two parameter generation methods. This

research showed that the two parameter generation methods produced significantly different model input parameter values for 40- and 10-acre grid cell sizes. Divergence between the two sets of parameter values were attributed to the inappropriate resolution of digital elevation data and the limitation of GIS terrain analysis in a flat agricultural watershed. However, the model output results using the two sets of input parameters were shown to be statistically similar. The ANN-AGNPS model is less sensitive to variable topographic-based parameters than soil- and field management- based parameters, which were the same for the two parameter generation methods.

The second half of the research focused on the predictive capabilities of the ANN-AGNPS water model. The research goal was to determine the type of NPS pollution contribution description the model is best capable of providing: a quantitative estimation of NPS pollution loading, a ranking of sub-watershed loading, or the identification of lands contributing significant amounts of NPS pollutants. The research watershed was divided into sub-watersheds with gauging and sampling equipment installed to record hydrologic characteristics and sample suspended sediment and soluble nitrogen. It was concluded that the model cannot accurately predict quantitative contributions of identified NPS pollutants for rainstorms during the 1992 growing season in western Minnesota. The model, however, is capable of ranking the order of hydrologic, sediment and nutrient contribution, as well as identifying those sub-watersheds which generated more than 25% of total watershed loading.

To my wife and editor Johanna, and my son Matthias

ACKNOWLEDGEMENTS

This dissertation was not possible without the support, cooperation, urging, and understanding of a host of people. First and foremost I must thank my wife Johanna. Without her support and help this endeavor would not have been possible. Next I wish to thank my major advisor Tom Edens. He never gave up on me, although at times I came close. I thank Bob Young at USDA's Agricultural Research Station in Morris, Minnesota for the opportunities he provided me to carry out this research. I also thank Steve Gloss, director of the Wyoming Water Resources Center, who allowed me to finish my dissertation while working.

There are, of course, many others who aided me directly or indirectly in my research. First I would like to thank the remaining members of my committee; Baxter Vieux, Jon Bartholic and Stuart Gage. Their input and patience was appreciated. Second I wish to thank the technical staff at the ARS lab in Morris, including Jim Eckland, Alan Wilts, John Witte, Mike Kahler and Basil Meyer. Finally I want to thank Jeff Hamerlinck and Chris Arneson at the Wyoming Water Resources Center's GIS lab for filling in when I was busy.

TABLE OF CONTENTS

LIST OF TABLES

LIST OF FIGURES

CHAPTER 1

INTRODUCTION

1.1 Problem Setting

1.1.1 The Severity of NPS Pollution

Nonpoint Source (NPS) water pollution has been recognized as the major remaining obstacle in obtaining water quality goals espoused in the National "Clean Water Act" (CWA) (USEPA, 1988). Considerable governmental and private resources have been invested in reducing point source effluence. However, decreases in point source pollution have not significantly improved overall national water quality. In fact, the last 20 years of point source pollution abatement programs have resulted in an overall maintenance of water quality (Lattenmaier et al., 1991; USEPA, 1988). Achieving the water quality standards defined in the CWA requires a comprehensive and coordinated effort to reduce NPS pollutants, similar to that expended on point source pollution.

Of all activities that create NPS water pollution, agriculture generates by far the largest share. USEPA (1986) estimated that 50% to 70% of the nation's assessed surface waters are "adversely impacted" by agricultural NPS pollutants. In the intensely cultivated upper midwest over 90% of the basins are impaired (Braden, 1985). Research has demonstrated that between 33% and 50% of the nitrogen and 10% of the pesticides applied to croplands find their way to surface waters or into

aquifers in states where NPS pollution is recognized as a serious problem (Crowder et al., 1988). Chemicals are not the only agricultural NPS contaminants. Clark (1985) estimates that between 25% and 40% of the sediments that run off fields end up in surface waters.

1.1.2 New NPS Pollution Policy Directions

A new paradigm in agricultural resource management for reducing NPS pollutants is currently being formulated. This new direction is replacing field-based erosion control with a more holistic watershed management approach. Two recent pieces of legislation have adopted a watershed-based strategy for implementing NPS abatement programs; the 1990 Food, Agriculture, Conservation and Trade Act (FACTA), and the 1990 amendment to the Coastal Zone Management Act (CZMA), the Coastal Zone Act Re-authorization Amendments (CZARA).

FACTA's primary vehicle is found in the new Water Quality Initiative Program (WQIP). WQIP calls for the development and implementation of water quality protection plans on 10 million NPS pollution generating or impacted agricultural acres. Compensation for installing new management practices will come from federal cost sharing of up to $2500 per year per farm for the 3- to 5-year life-span of the program. Qualification for cost sharing will be based upon the location of farm acreage in "critical cropland" areas. Critical areas are defined in the bill (section 1238C) as "lands located within hydrologic units, identified by the state under section 319 of the Federal Water Pollution Control Act, that contribute to an identifiable water quality problem" (Center for Resource Economics, 1990, p. 247).

The re-authorization of the CZMA requires that states implement management practices for each category of land use that individually or cumulatively contributes to the degradation of coastal waters (USEPA, 1991a). Using the most current land use information, the land area in the watershed that threatens a water body must be identified. Management measures that are economically achievable for the control of pollution must have quantitative estimates of the pollution reduction effect and cost measures.

The implementation of agricultural NPS pollution programs is occurring simultaneously with an emerging trend of restructuring and downsizing within USDA. The Secretary of Agriculture has proposed combining four existing farm support agencies, the Soil Conservation Service (SCS), the Agricultural Stabilization and Conservation Service (ASCS), the Farm Home Administration (FHA), and the Federal Crop Insurance Program (FCIP), into one consumer-based service agency to provide educational, technical and financial resources required by the farm community (Associated Press, 1993). The consolidation of agencies is an attempt to streamline and coordinate a multitude of farm support and conservation programs presently occurring within and across services. The goals of agricultural NPS pollution abatement articulated in recent legislation are not necessarily at odds with the changes in farm conservation agency structure.

Achieving the policy goals defined in the WQIP and CZARA and operating within the new USDA institutional environment requires developing programs that are effective in reducing NPS pollution loading and cost efficient for farmers, farm

community and government agencies. First, the program must be capable of reducing agricultural NPS pollution loading of sediment, nutrients and pesticides to a naturally assimilative level. EPA's designation of Total Daily Maximum Load (TDML) is one definition of a target level for determining effective reductions in loading (USEPA, 1991b). Second, the program must achieve economic efficiency by targeting and cooperating with only those land owners and operators who contribute significant amounts of pollutants to water bodies. Targeting of contributing lands minimizes financial cost sharing as well as the technical and educational support required of the federal, state and local conservation agencies. Further, any individual costs of implementing best management practices (BMPs) are borne only by those designated land owners whose practices and/or location within the watershed lead to significant contribution of NPS pollutants. Finally, the cost to local agricultural-based businesses from large-scale reduction in commodity production is alleviated.

1.1.3 Tools for NPS Pollution Abatement Strategies

Numerous methods, procedures and tools are available to conservation agents for identifying lands and practices generating significant levels of NPS pollutants. Methods enlisted over the years include: establishing a water quality monitoring network, applying basic "rules of thumb" and expert opinion, interpreting and measuring mapped information, and enlisting mathematical computer models. The method which has recently gained considerable attention is the use of computer models. In fact, the SCS has committed itself to the use of computer models to assist conservation planners in resource management decision making (Shaw, 1991).

NPS water pollution computer models simulate, with quantitative analytic techniques, the effect of hydrologic processes on state variables such as soil, applied nutrients and pesticides. Distributed parameter physical-based models are capable of generating this information for a particular time and space within a given watershed. Agricultural NPS pollution models can thus be used to determine the amount of sediment eroded, and subsequently the amount transported and deposited along flow paths. Further, changes in the concentration of nutrients, pesticides and bacteria can be estimated as these constituents are transported off the fields and feedlots, then routed down through the watershed's channel network.

Given this simulated information provided by the model, the conservation agent can draw a number of conclusions about NPS pollution generation within the watershed. First, it can be determined which fields are generating significant contributions of sediments, nutrients and pesticides: a targeting or identification description. Second, fields in the watershed can be ranked relative to each other based upon the contribution of pollutants: a ranking description. Third, the amount of loading being generated from the various fields within the watershed can be determined: a quantitative description.

Simulation models can also be used as proactive planning tools, testing alternative field management practices apriori. The conservation planner interacts with a computer model, modifying parameter input values representing changes in management practices within the farm field, along flow paths between fields and channels, or within channels. Alternative BMP scenarios can thus be created and

modelled to compare and contrast their potential impacts on water quality.

A Geographic Information System (GIS) is a computer tool that can greatly facilitate decision making in agricultural resource conservation and water quality planning and management. The SCS has identified GIS as the "wave of the future", a "fundamental technology for all facets of SCS work" (Shaw, 1991, p. 407). A GIS is capable of spatial data capture, management, manipulation, analysis and output. The spatial data processing capabilities of the GIS can enable the conservation planner to analyze and assess considerably larger land areas than conventional map interpretation and field reconnaissance surveys. The GIS has proven useful in providing parameter input to physical-based distributed process models. Hydrologic and related agricultural NPS pollution water quality models are one subset of distributed process models into which GIS-generated parameters have been incorporated in recent years. This is evident in the number of GIS-water quality modeling projects and paper presentations (Harlin and Lanfear, 1993; Moore et al., 1993).

Digital spatial data required for GIS-generation of NPS pollution model input parameters are becoming more available to conservation planners. Digital data that can be used in NPS pollution water quality modeling include: SCS 1:24,000 scale SSURGO county-wide soils survey data, USGS 1:24,000 scale Digital Line Graph (DLG) feature files for hydrography, transportation and political boundaries, USGS 1:24,000 scale Digital Elevation Module (DEM) topographic data, and SCS/USGS 1:24,000 scale digital orthophoto quad. aerial photography.

1.2 Research Questions

Fundamental questions concerning the use of these NPS modeling tools must be answered before they are implemented. The most basic questions are: How well will this integrated technology and data perform? Has there been adequate testing to determine capabilities and limitations? By using these methods, are NPS programs more capable of achieving the above-mentioned goals of effectiveness and efficiency within a smaller farm/conservation service agency? This research deals with two separate yet related research questions evolving from these general concerns, each relating to the two technologies that will eventually be utilized in NPS pollution abatement programs, computer models and GIS.

The first question relates to the capabilities of a GIS to manage and manipulate the above-mentioned spatial data sets for use as input parameters to a distributed-parameter NPS pollution model. Input values for a distributed parameter NPS pollution water quality model will by nature contain inherent error. Model parameter error can originate from two distinct sources: data compilation and data representation. Data compilation error occurs because of the inability to collect physical landscape information continuously throughout a watershed. Most resource management modeling tools use secondary data sources, such as soil survey maps and contour elevation maps. These maps have been created using spatial interpolation techniques to assign values to areas between data collection points. Data representation error results when the landscape is delineated into computational elements for collecting and then inputting parameter data to a distributed-parameter

model (Beven, 1989). The commonly used grid cell element imposes artificial "straight-line" boundaries to represent landscape features. Within the grid cell, spatial complexity of physical or agronomic land features is replaced with either a homogeneous average, weighted average or dominant characteristic.

Question 1: How much error is introduced to the input parameters of a distributed-parameter NPS water quality model when values are generated using a GIS as compared to a standard set of input parameters utilizing more costly and time-consuming conventional methods of map interpretation and field reconnaissance surveys? How does the error influence NPS pollution model simulation results?

The SCS has identified both the single rainfall event version AGNPS (Young et al., 1987) and the expanded continuous simulation model ANN-AGNPS (Needham and Young, 1993), as NPS pollution models they intend to use as part of their agricultural NPS program (USDA-SCS, 1991). The second set of research questions is concerned with the predictive capabilities of ANN-AGNPS, and the influence of potential GIS-generated parameter error on simulation results.

Question 2: How well does the ANN-AGNPS model predict NPS pollution loading from an agricultural watershed? Given the resulting level of simulation accuracy, what kind of description can be made concerning NPS pollution loading out of an agricultural watershed as well as within it: (1) a targeting or identification description, (2) a ranking description, or (3) a quantitative estimation description?

1.3 Research Hypotheses

To gain insight into the capabilities of these technologies as well as address the research questions posed, the following hypotheses have been forwarded to formally focus the research.

Hypothesis 1: The input parameter error introduced using GIS-based spatial data manipulation methods is insignificant as compared to model input data values generated from conventional map interpretation and reconnaissance field surveys. Thus the simulation results utilizing the two sets of model input parameters will be comparable.

This first hypothesis states that GIS-generated parameters incorporated into the ANN-AGNPS water quality simulation model, on the whole, will not differ significantly from parameter values that would be generated if GIS technology was not available. The parameters generated from map interpretation and field survey are the standard for comparing GIS-generated parameters. GIS-related error is thus the

difference in the two parameter values. Given the similarities in parameter sets, simulation results from ANN-AGNPS will not significantly differ.

Hypothesis 2: The ANN-AGNPS model cannot accurately predict quantitative contributions of NPS pollutants from sub-watersheds within a larger agricultural watershed. The model is only capable of providing identification and ranking description.

The single rainstorm event and the continuous AGNPS model were developed to "analyze nonpoint source pollution and to prioritize potential water quality problems in rural areas" (Young et al., 1989). Because of their basic analytic approach, the AGNPS models are limited in the accuracy of predictions, and thus should be limited to the type of applied uses. Most major processes represented in the AGNPS models are based on empirical equations developed from inherently limited sets of observations. The models are also intended for use by local conservation planners in ungauged watersheds and thus do not allow for calibration. Quantitative results produced by the AGNPS models should thus only be used in identifying and rating contributing lands within a watershed.

1.4 Research Approach

The testing of the research hypotheses was carried out on an agricultural watershed in West-Central Minnesota. The Moyer watershed is a small sub-basin to the larger Pomme de Terre watershed system, which in turn is a tributary to the Minnesota River. The Minnesota River, throughout its course, flows through intensely cultivated agriculture landscape and experiences considerable water quality

degradation from agricultural NPS pollution.

The 1076-acre Moyer watershed has been subdivided into sub-watershed units nested hierarchically throughout the overall watershed (Figure 1.1). Stage recorder and automated water samplers have been set up at the outlet of each sub-watershed. The sampling design enables determination of pollutant loading for each individual sub-watershed, an intermediate location and the watershed outlet.

Watershed modeling to estimate and isolate contributing areas requires the delineation of the watershed into computational areas. ANN-AGNPS requires a spatial framework for re-sampling real-world physical and agronomic information into a homogeneous computational unit. Grid cell sizes of 40 and 10 acres will be used for testing potential parameter error generation. This research does not directly address the issue of determining optimal grid cell size. However, it intends to assess the ability of the GIS to generate parameter error for these resolutions.

Agricultural NPS pollutants encompass a wide range of organic, inorganic, and water characteristics changes which degrade the quality of water relative to an established standard or a particular use. Sediments, nutrients, pesticides and bacteria are NPS pollutants typically associated with agricultural activity, and constitute the majority of contaminants NPS pollution abatement programs address. This research only addresses two of the major NPS pollutants; suspended sediments and soluble nitrogen. The ANN-AGNPS model can predict soluble phosphorus as well as sediment-absorbed nitrogen and phosphorus, however only suspended sediments and soluble nitrogen were collected and analyzed. It is clearly recognized that other NPS

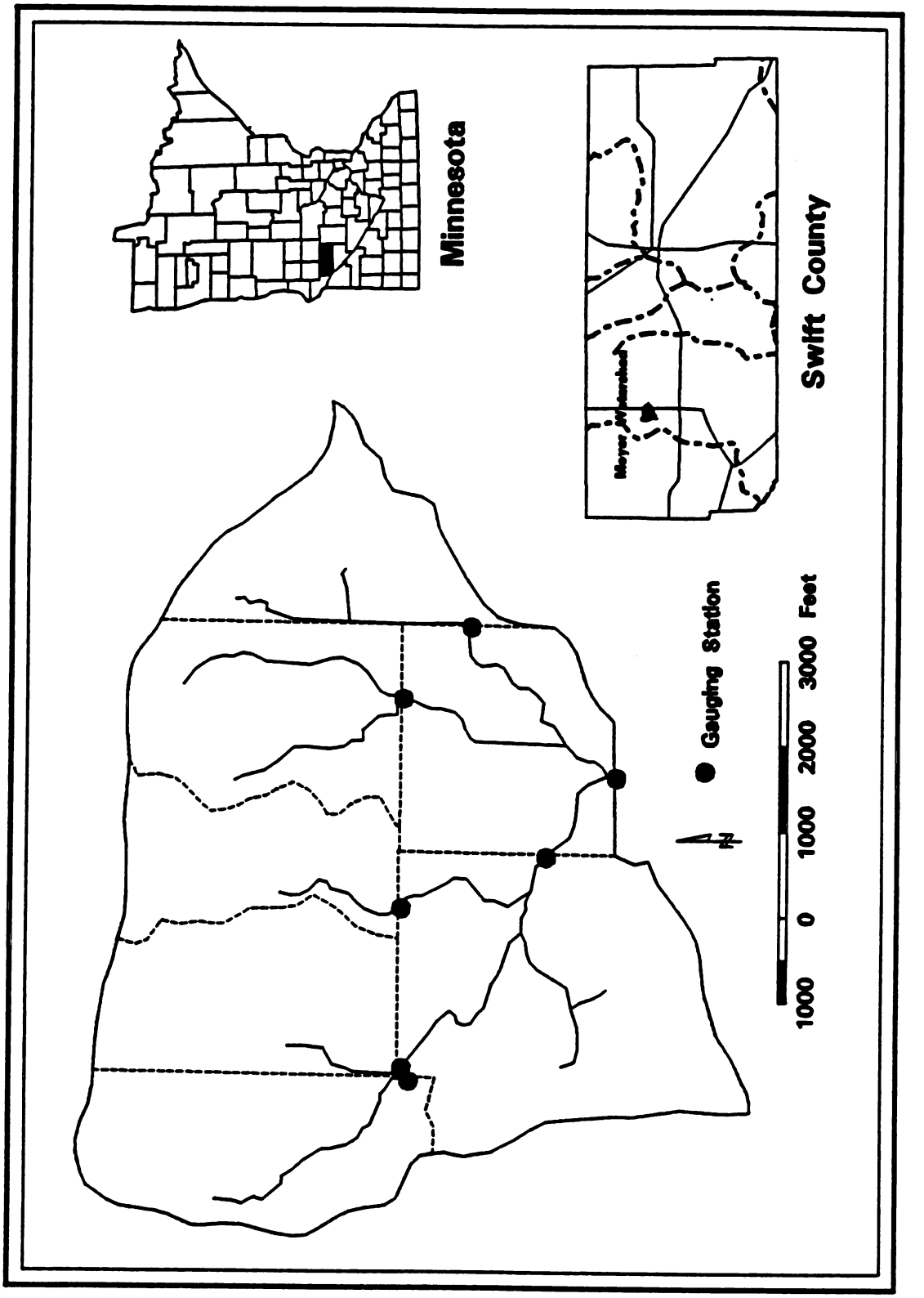

Figure 1.1 Moyer Watershed, Sub-Watersheds and Gauging Stations

pollutants are also serious agriculture-generated constituents, and must be considered in agricultural NPS pollution abatement programs.

A GIS-based interface program has been created for assisting in model parameter generation. The GIS program is capable of manipulating the entered spatial data sets as well as querying the user for farm management practices in generating a complete set of parameter data required by ANN-AGNPS. The GIS used is ESRI's UNIX version of ARC/INFO version 6.1 (ESRI, 1991). The source code for ANN-AGNPS has been re-compiled within the UNIX environment with minor modifications made to the input/output routines to enable direct linkage with the GIS.

The final analysis will consist of comparing the GIS-generated and the map interpreted/field observation input parameter values and then operating the ANN-AGNPS model with the two sets of model input parameters at two different cell resolutions for the 1992 growing season. The model input values for the two parameter sets and two cell sizes will first be statistically evaluated to determine if there are significant differences between the two parameter sets. Next the ANN-AGNPS model will be operated for the two parameter sets for each cell size to determine if there are significant differences in output results. Model outputs to be evaluated include runoff volume, peak flow rate, suspended sediment load and soluble Total-Nitrogen load for each individual cell and at each of the sampling sites for two runoff events. Finally, model output results will be compared using map interpretation/field survey parameter generation methods to determine what type of

contributing land description can accurately be ascribed: (1) a targeting or identification description, (2) a ranking description, or (3) a quantitative estimation description.

1.5 Thesis Organization

The thesis is divided into five further chapters; (2) a review of the literature, (3) a description of the experimental watershed, (4) a description of the experimental design and statistical techniques, (5) a presentation and explanation of results, and (6) a discussion of the significance of those results relative to the stated hypotheses and research questions, as well as final conclusions. The literature review chapter (2) is further divided into two sections. The first section reviews research and applied hydrologic and NPS pollution models presented in the literature. It identifies and then discusses the major procedures for mathematically representing hydrologic, sediment transport and nutrient fate processes. The primary processes covered include infiltration, overland runoff, soil erosion, channel flow and sediment transport. The second section reviews past work of linking hydrologic and agricultural NPS pollution water quality models with GIS to facilitate the generation of model parameters and decision support in water resources planning and management.

Chapter three describes the physical characteristics of the watershed as well as the agricultural activity taking place. Chapter four describes the experimental design. Data collection methods will be explained, including a description of the techniques for processing recordings and samples. Included in the description of data collection methods will be a discussion of model parameter generation by both traditional map

interpretation and field observation as well as GIS processing of digital spatial data. Also covered are the statistical techniques in data analysis.

The fifth chapter presents the results for both watershed data collection and model simulation runs. The sixth chapter assesses the results in terms of the hypotheses and provides answers to the research questions. The final chapter will also discuss the implications of this research to current water quality policies and outline future research needs.

CHAPTER 2

LITERATURE REVIEW

2.1 Modeling Agricultural NPS Pollutants

2.1.1 Introduction

The presence of water-borne NPS pollutants in harmful concentrations is due to the capacity of water to dissolve, entrain and then transport soil, nutrients, bacteria and other chemical constituents. These potential pollutants can be transported via surface overland and stream channel flows, as well as subsurface flows through organic and inorganic residues, soils, vadoze and saturated geologic media. Novotny and Chesters (1981, p. 77) thus refer to contamination from nonpoint sources as a "hydrologic problem". Estimating NPS pollution concentrations through mathematical simulation therefore requires models based upon principles of hydrology.

The complexity of the hydrologic system is vast both in terms of its dimension and detail. Representing the hydrologic system through conceptual, analog or mathematical means requires a simplification of the hydrologic processes into discrete and definable components. Incorporating a systems perspective, Chow (1988, p. 7) forwards a definition of the hydrologic phenomenon as "a structure or volume in space, surrounded by a boundary, that accepts water and other inputs, operates on them internally, and produces them as output". He defines the structure or volume of the system as the "totality of flow paths through which water may pass as throughput

from the point it enters the system to the point it leaves". The system boundary represents "a continuous surface defined in three-dimensions, enclosing the volume or structure". The working media are defined as constituents "enter[ing] the system as input, interact[ing] with the structure and other media and leav[ing] as output".

Implementing the systems approach is a prerequisite for distributed-parameter process-based hydrologic watershed modeling. The watershed fixes the physical and spatial boundary conditions for isolating dominant processes. The complexity of the watershed structure is then delineated into separate sub-processes represented by mathematical functions relating the modification of water and water-borne constituents from inflow to outflow. Once each of the sub-systems is accounted for through quantitative methods, the complexity of the larger watershed system is reconstructed by combining the results according to the interaction between sub-systems (Chow, 1988).

Within the upland watershed, the emphasis of this research, basic processes can be subdivided into two sub-systems; overland flow and stream channel flow systems. For both sub-systems, the working media of water and agricultural inputs move through the natural and man-modified structures of soil, vegetation and topography. The working media is thus modified and redistributed as it moves down through the structure paths. Dimensions of space and time must be included within the analytic framework. The inherent spatial variability of the watershed's structure leads to variation in the rate and timing of processes. Watershed structures change relative to temporal dynamics of weather and agronomic practices thus influencing the

transformation of systems inputs to outputs.

Section one of the literature review details the major processes represented in agricultural NPS water quality models by reviewing methods of mathematical representation. The processes examined for overland and channel sub-systems include: (1) hydrology, including infiltration and surface flow, (2) soil erosion, including detachment, transport and deposition of soil sediments, and (3) nutrient fate covering soluble and sediment-attached forms of nitrogen and phosphorus entrainment and transport.

To organize a review of distributed parameter models and the mathematical representation of processes, a list of NPS water quality and hydrological models has been compiled (Table 2.1). The models in the following table are a subset of available operational models applied to water resource planning and management. For each of these models, the mathematical representation of the major processes contributing to NPS pollutant loading will be reviewed. Various methods of delineating a watershed for generating distributed parameters will also be discussed.

Table 2.1 NPS and Hydrologic Models

MODEL	INFILTRATION	SURFACE RUNOFF	EROSION	CHANNEL FLOW	SEDIMENT TRANSPORT	NUTRIENT FATE
ACTMO Frere et al. 1975	Holtan	Kinematic Wave	USLE, R Factor Modification	Kinematic Wave	Continuity: Yalin Transport Capacity	Soluble and Attached N and P, Area Surface Proportionality
AGNPS/ANN-AGNPS Young et al. 1987/ Needham and Young, 1993	SCS CurveNumber/ SCS Curve Number	SCS Curve Number/ SCS Curve Number: CREAMS modification	USLE/ RUSLE: Daily Increment	CREAMS: Geomorphic Peak Runoff	Continuity: Bagnold Transport Capacity	Soluble and Attached N and P. CREAMS : Extraction Coefficient and Enrichment Ratio
ANSWERS Beasley et al. 1980 Storm et al. 1988 Dillaha and Beasley, 1983	Modified Holtan	Rainfall excess	Pundamental: Meyer and Wischmeier	Continuity: Manningn	Continuity: Beasley, et al. Transport Capacity	Soluble and Attached P. Sharpley Kinetics and Specific Surface Area Proportionality
CPS Steenhuis, 1979	SCS Curve Number	SCS Curve Number	USLE	———	———	———
CREAMS Knisel et al. 1980	SCS Curve Number /Green and Ampt	SCS Curve Number/ Kinematic Wave	Pundamental: Foster and Meyer	Geomorphic Peak Runoff/ Kinematic Wave	Continuity: Yalin Transport Capacity	Soluble and Attached N and P. Extraction Coefficient and Enrichment Ratio
GAMES Rudra et al. 1986	———	Manningn: Velocity	USLE: Seasonally Adjusted	———	Delivery Ratio	Enrichment Ratio
GWLF Haith and Shoemaker, 1987	———	SCS Curve Number	USLE	———	Delivery Ratio	Enrichment Ratio
HSPF/NPS/ARM Donigian and Crawford, 1976	Philip	Kinematic Wave	Modified Negev	Kinematic Wave	Continuity: Yalin Transport Capacity	Soluble and Attached N and P. Adsorption/ Desporption Freundlich Isotherms

Table 2.1 NPS and Hydrologic Models (continued)

MODEL	INFILTRATION	SURFACE RUNOFF	EROSION	CHANNEL FLOW	SEDIMENT TRANSPORT	NUTRIENT FATE
HYMO Williams and Haan, 1972	Green and Ampt	Kinematic Wave	———	Variable Storage	———	———
KINEROS Woolhiser et al. 1990	Smith and Parlange	Kinematic Wave	Continuity: Bennett	Kinematic Wave	Continuity: Multiple Selection Transport Capacity	———
LANDRUN Novotny et al. 1978	Holtan or Philip	Rainfall Excess	MUSLE	Instantaneous Unit Hydrograph	Delivery Ratio	Enrichment Ratio
SHE Abbott et al. 1986	Richards	Diffusion Wave	———	Diffusion Wave	———	———
SWRBB-WQ Williams et al. 1985 Arnold et al. 1990	SCS Curve Number	SCS Curve Number	MUSLE	Rational Formula: Peak Runoff	Continuity: Bagnold Transport Capacity	Soluble and Attached N and P. Equilibrium Soluble Concentration and Enrichment Ratio
USDAHL Holtan et al. 1975	Holtan	Kinematic Wave	———	Kinematic Wave	———	———
WEPP Lane and Nearing, 1989	Green and Ampt	Kinematic Wave	Continuity: Foster, et al.	Kinematic Wave	Continuity: Yalin Transport Capacity	———

2.1.2 Distributed-Parameter Models

Distributed-parameter watershed models delineate the watershed into dimensional units representing physical homogeneity of landscape components such as soils, slope, and land use as well as hydrologic processes, including infiltration, runoff and soil erosion. Woolhiser (1982) adds that the distributed parameter spatial abstraction of the water must also represent natural flow patterns. The distributed-parameter model is required to identify partial area contribution of runoff, sediment and nutrients to the watershed. This can only be achieved when interactions between the area of interest and the rest of the watershed are known. Beven (1985) has identified three major reasons for using distributed-parameter models:

1. forecasting the effects of land use changes
2. forecasting the effects of spatially variable inputs and outputs
3. forecasting the movement of pollution and sediment

A number of distributed watershed representations have been developed for model parameter delineation. Moore et al. (1993) divide the representations into grid, triangular irregular networks (TIN), hydrologic response units (HRU) and contour-based elements. Two more types can be added: plane/channel and sub-watershed.

2.1.2.1 Grids

Bernard (Hjelmfelt and Amerman, 1980) formulated the earliest version of a distributed watershed model. He incorporated a simple regular grid cell method (Figure 2.1a) for partitioning the watershed and collecting landscape data. The parameter data represented a homogeneous value for the grid cell. His model utilized the physical-based kinematic wave method to route water across grid cells to a

channel, and then through the channels to the watershed outlet. Presently the regular grid cell framework is incorporated in a number of hydrologic and NPS water quality computer programs, including ANSWERS (Beasley et al., 1980), AGNPS (Young et al., 1987), SHE (Abbott et al., 1986). Changing grid cell size enables more realistic representation of natural features. However, it also increases data collection and computational time.

2.1.2.2 Planes/Channels

Networks of planes and channel elements (Figure 2.1b) (Loague and Freeze, 1985) have been used to segment a watershed into the two primary hydrologic processes; overland and channel flow. The relative size of the overland element and the location of the channels to the elements can be maintained with this system. Overland elements can flow onto overland elements or into channels. Woolhiser (1982, p. 197) notes the advantage of this watershed representation over grid cells: "it may require fewer elements and the programming logic and storage requirements are not so severe". Examples of models using this watershed geometry include: KINEROS (Woolhiser et al., 1990) and the Watershed Version of WEPP (Lane and Nearing, 1989).

2.1.2.3 Triangular Irregular Network

A configuration of irregularly shaped and sized triangles or TINs (triangular irregular network) (Figure 2.1c) has been used to delineate a watershed. The TIN representation was developed in part to fit more flexible triangular geometries to irregular topographies as well as to provide a numerical structure for finite element

solutions. Overland flow can occur across TIN elements and the downhill intersection of two TIN elements can form a channel. TIN-based hydrologic models have been used primarily in research, including: Vieux (1988), Maidment et al. (1989), and Goodrich et al. (1991).

2.1.2.4 Hydrologic Response Unit

A Hydrologic Response Unit (HRU) delineation of a watershed (Figure 2.1d) (Ross et al., 1979) is created by identifying common land units with similar landscape characteristics. For example, all areas with similar slope, soil, and land cover type would constitute a HRU. The purpose of creating HRUs is to minimize differences within the delineation and to maximize differences across delineations. Water flow can take place across several HRUs or through a super-imposed channel network. A watershed model representative of the HRU structure is FESHM (Ross et al., 1979).

2.1.2.5 Sub-Watersheds

A watershed can be divided into smaller, topographically independent sub-watersheds (Figure 2.1e) (Wood et al., 1988). The sub-watersheds are then connected by the network of natural channels. This type of delineation cannot be considered a "true" distributed parameter (Larson et al., 1982). Considerable variability of input parameter values may exist within the sub-units. Representing these sub-watersheds with one value introduces the potential for considerable input parameter error. Models with this type of structure include SWRRB (Williams et al., 1985), HSPF/NPS/ARM (Crawford and Donigian, 1973).

Figure 2.1 Distributed Parameter Representation

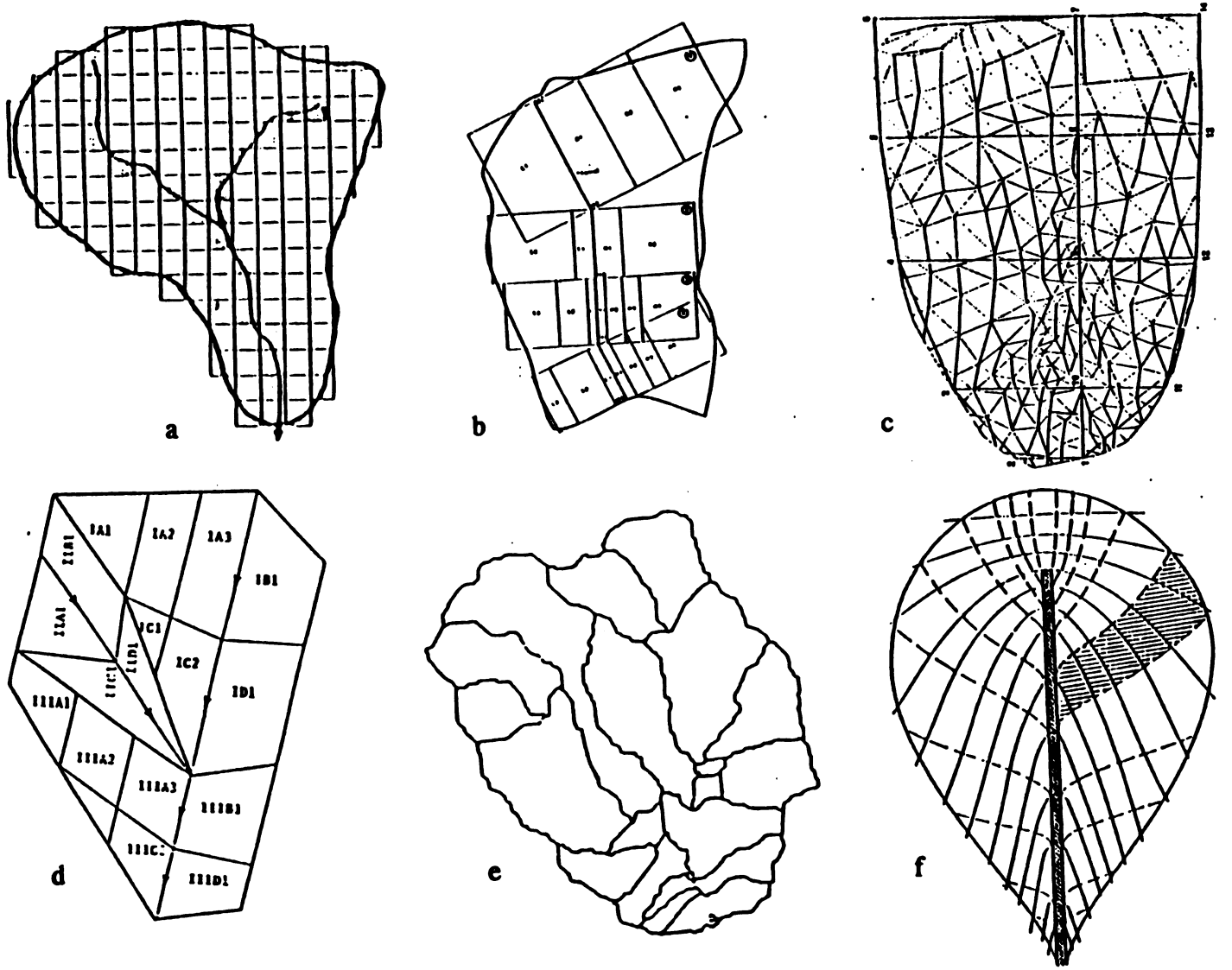

2.1.2.6 Contour-based Elements

The contour-based method (Figure 2.1f) (Moore and Grayson, 1991) attempts to spatially delineate land based on the direction of overland flow. Onstad and Brakensiek (1968) first proposed the technique, calling it stream path or stream tube delineation. Contour lines are assumed to be lines of equal flow potential. Elemental units are created by drawing element boundaries orthogonal to the contour lines. Several experimental hydrologic models have incorporated this spatial delineation, including THALES (Grayson et al., 1992) and TOPOG (Davies and Short, 1988).

Any attempt to delineate the watershed into smaller units for capturing data and modeling the processes will by nature include a certain degree of physical variability within that defined unit. This is true for both arbitrary grid cell as well as physical-based HRU delineations. Arriving at one representative parameter value for the computational unit requires averaging or selecting of dominant physical characteristics. Beven (1989) states that all distributed-parameter models are "lumped" models at the scale of the individual area delineation. An unknown quantity of error will be introduced at this scale because the theory for sub-unit data integration is incomplete.

2.1.3 Hydrology

2.1.3.1 Infiltration

Infiltration is the process of water penetration from the soil surface into the soil profile. It is the first stage of terrestrial water movement and is responsible for partitioning water to potential aquifer recharge, lateral interflow and surface runoff.

Accurately accounting for infiltration is key to successful hydrologic modeling and estimating soil erosion and nutrient transport.

Soil water movement, including infiltration, is the consequence of hydraulic gradients created by gravity and capillary suction. Under the combined gradients, water progressively relocates from a lower to a higher potential. For gravity this movement is always vertical, and it is the dominant force in saturated soils. For capillary suction, it is in all directions and is dominant in drier soils. Basic properties of the soil in relation to antecedent moisture conditions define the influence of gradients. A soil's textural properties determine the size and distribution of pores and macro-spaces. The density, size and distribution of pores in turn influence a soil's ability to transmit water (hydraulic conductivity), as well as its ability to store and release water (water-retention capacity) (Rawls et al., 1993). Antecedent soil moisture conditions modify the rate of soil water movement. Drier soils with larger capillary suction potential draw water quickly through the soil, whereas water in wetter soils moves more slowly under diminishing capillary suction which eventually evolves into a weak gravitational gradient.

Bodman and Coleman (1944) described the migration of water through a homogeneous soil profile delineating the vertical characteristic of soil moisture into four zones: (1) a saturated zone a few millimeters in thickness located at the soil surface, (2) a transmission zone of nearly saturated soil with uniform water content, (3) a wetting zone underneath which soil moisture decreases with depth to a wetting front, and (4) a wetting front which separates below drier soils from oncoming soil

water. This descriptive model serves as the basis for many physical-based mathematical models.

Mathematical models of infiltration have been developed to quantify water movement into the soil and estimate excess rainfall leading to runoff. The list of models from Table 2.1 can be classified by whether they represent the infiltration process with empirical or physical-based sets of mathematical equations. The empirical models presented in the list include the SCS Curve Number (CN) method, and Holtan's model. Three approximate physical models are implemented within the listed models, including: Green and Ampt, Philip, and Smith and Parlange. The complete physical-based infiltration model or Richards equation is implemented in the SHE model.

A. Empirical Infiltration Models

a. Holton

Holton's model (1961) relates pre-steady state infiltration capacity to unsaturated pore space in the soil, which is represented by the volume of potential storage.

(2.1) $$f = a F_p^n + f_c$$

where:

f = infiltration rate

f_c = steady-state infiltration capacity

F_p = potential infiltration or available storage up to time of steady-state infiltration capacity rate

a and n = constants related to a soil-vegetation complex.

Holtan and Lopez (1971) refined the base equation to incorporate the influence of growing crops.

(2.2) $$f = GI\ A\ F_p^{1.4} + f_c$$

where:

GI = crop growth indicator, relating to crop maturity (0.0-1.0)

A = index of root connectivity between ground surface and soil

The ANSWERS model incorporates a modified form of Holtan's equation:

(2.3) $$f = f_c + D\ [(F_p - F)/T_p]^P$$

where:

D = difference between maximum and steady-state infiltration rate

F = total volume of infiltrated water

T_p = total porosity

P = dimensionless coefficient relating rate of infiltration decrease with increasing soil moisture content

Holtan's model can be integrated relative to time for determining the infiltration rate. Tables have been created to help model users determine input parameters for a given soil type and land use (Musgrave, 1955; Frere et al., 1975).

b. SCS Curve Number (CN) Method

The CN method (USDA-SCS, 1972) incorporates a rainfall excess equation. A runoff volume is the calculated result, and infiltration is then the difference between rainfall and runoff. Infiltration generated from the CN method is a total volume generated from one rainstorm. The Curve Number method is covered in

detail in the surface runoff section below.

B. Physical-Based Infiltration Models

The physical or conceptual model of infiltration is developed by applying physics to assess the movement of water into the soil. Parameter input data is determined from measuring physical characteristics of the soil-water environment. This model type is derived by combining the equation for water flow derived from Darcy's Law:

(2.4) $$-q=-K\frac{\partial H}{\partial z}$$

where:

K = saturated conductivity or unsaturated conductivity.

H = hydraulic head loss due to gravitational and pressure head, or suction pressure in unsaturated soils

z = distance from surface

with the continuity equation for water flow:

(2.5) $$\frac{\partial \theta}{\partial t}=-\frac{\partial q}{\partial x}$$

where:

θ = soil moisture

t = time

q = flow rate

x = distance

The resulting combined equation is:

$$\frac{\partial \theta}{\partial t} = \frac{\partial}{\partial t}\left[K\theta \frac{\partial H}{\partial x}\right] \tag{2.6}$$

Equation 2.6 is representative of one-dimensional flow, and is the "water content equation" or Richards equation (Richards, 1931). It is a non-linear partial differential equation with two unknowns; soil moisture and hydraulic gradient. A numerical solution incorporating either finite methods or finite elements is required. Known relationships for soil moisture and hydraulic conductivity as well as soil moisture and suction potential are required input parameters. Richards equation has proven to be a useful research tool. However, it is impractical to use as an operation model (Rawls et al., 1993).

Approximate solutions to Richards equation have been developed and used as practical alternatives. Models from Table 2.1 include: the Green and Ampt equation, Philip's Two Term equation and the Smith-Parlange equation. These models are considered approximate physical models because they do not incorporate the partial differential solution approach of Richards equation, and thus can be solved analytically. Physical parameter input values can be obtained more easily from either field observation or developed soil characteristic descriptions (Rawls and Brakensiek, 1983).

a. Green and Ampt

Green and Ampt (1911) proposed a simplified description of water penetration into soil based upon Darcy's equation. The soil profile is represented by two zones of distinct soil-water conditions. The upper transmission zone consists of saturated soils with a moisture content equal to the soil porosity. Water movement through this zone occurs at saturated hydraulic conductivity. The lower drier zone exists at initial soil water conditions. An abrupt wetting front separates the two soil conditions. At the wetting front, the above soil water is drawn into the drier soils through capillary suction forces. The Green and Ampt equation is presented as:

(2.7) $$f = K\left[1 + \frac{(\Phi - \Theta_i) S_f}{F}\right]$$

where:

f = infiltration rate

K = effective hydraulic conductivity

ϕ = soil porosity

θ_i = initial water content ($\phi - \theta_i = M_d$: the initial moisture deficit)

S_f = effective suction at wetting front

F = accumulated infiltration

Practical application of the Green and Ampt model for simulating infiltration and runoff requires the incorporation of a rainfall rate at the soil surface. Using the basic concepts of Green and Ampt, Mein and Larson (1973) forwarded a three-stage procedure to model infiltration under steady rate rainfall conditions and determine the

time it takes for surface ponding to occur. In stage one, infiltration is equal to rainfall intensity (rainfall rate is less than saturated hydraulic conductivity). In stage two, infiltration continues at the rainfall intensity and the soil moisture content at the surface continues to increase (rainfall rate surpasses the saturated hydraulic conductivity, however, it is less than infiltration capacity). In stage three, the infiltration rate is at its capacity, which is less than the rainfall rate . Water thus begins ponding at the soil surface. The amount of infiltration prior to runoff and the time to the beginning of runoff are calculated by:

(2.8) $$F = S_f M_d/[(I/K)-1]$$

where:

I = rainfall rate

Rainfall rates are not constant through a storm. Rain intensity can drop below infiltration capacity and hydraulic conductivity after infiltration capacity has already been achieved. Chu (1978) enhances the Mein and Larson procedure by developing a "pseudotime" shift in the ponding timescale to determine if ponding has occurred.

b. Philip Two Term

Philip two term model for infiltration (1957) is a derivative of an infinite power series equation, generated by solving Richards equation after converting it to an ordinary differential equation (Chow et al., 1988). The Philip equation is represented as:

(2.9) $$q(t) = 1/2\ st^{1/2} + A$$

where:

s = Philip parameter of soil sorptivity

t = time

A = constant dependent of soil hydraulic properties K(θ) and h(θ)

Initial stages of water infiltration are represented with the first half of the equation : $q(t) = 1/2\ st^{1/2}$, where sorptivity is the basic process moving water into the initially dry soil surface. As infiltration progresses, sorptivity becomes less of an influencing factor and gravity flow, represented by the saturated hydraulic conductivity, becomes more of an influence. The two basic parameters s and A have physical meaning and can be determined from field data.

c. Smith and Parlange

The Smith and Parlange model of infiltration (1978) is a one-dimensional approximation of the Richards equation simulating flow into a homogeneous unsaturated medium. The basic form of the equation is:

(2.10) $$f = K \exp(F/B)/[\exp(f/B-1)]$$

where:

B = saturation deficit parameter

The B parameter relates the effective net capillary drive (G) to the difference between initial (θ_i) and saturated (θ_s) soil water conditions:

(2.11) $$B = G(\theta_s - \theta_i)$$

The smaller the moisture difference, the smaller the effect of suction capacity in drawing water through the soil profile. For a short time period after the beginning

of rainfall, equation 2.11 can be approximated by: f=BK/F. When moisture content approaches saturation, the infiltration capacity approximates saturated hydraulic conductivity.

C. Parameter Estimation

Studies have related soil physical characteristics to quantifiable hydrologic descriptions required by physical-based infiltration models. Brooks and Corey (1964) determined that suction head is logarithmically related to an effective saturation (S_e): $S_e = (\theta - \theta_r)/(\phi - \theta_r)$, where θ_r = residual water content. Brakensiek et al. (1981) developed methods implementing the Brooks-Corey relationship to estimate required Green and Ampt input parameter of S_f, K and ϕ. Rawls et al. (1983) then generated hydraulic data for a large range of soil classes by applying the developed procedure.

2.1.3.2 Surface Runoff

Surface flow begins with the ponding of water at the soil surface when rainfall intensity becomes greater than infiltration capacity. However, before gravity takes hold moving water downhill, water fills the surficial detention and soil depressional storage of the soil surface. With the accumulation of more water at the surface, gravity eventually overcomes storage and runoff begins to flow downhill.

Horton (1933) described these mechanics of overland flow, referring to this as "rainfall excess", which is equal to rainfall minus infiltration. Research since has demonstrated that water flows parallel to the hillslope through sub-surface unsaturated zones. If the water re-surfaces at hill side cuts or stream banks, it is called unsaturated lateral flow (Freeze, 1974; Dunne et al., 1975). If sub-surface water

settles into depressions or near the bottom of a slope causing the groundwater level to rise to the surface it is called saturated lateral flow (Betson, 1964; Hewlett and Hibbert, 1967). In both cases, surface runoff is not a result of Hortonian runoff, where rainfall is greater than infiltration capacity.

Lateral flow or interflow processes are dominant processes existing on vegetated slopes in humid environments, while Hortonian flow occurs in more arid climates with impervious soil layers (Chorley, 1978). However, the complexity and spatial variability of soils, slopes, vegetative cover and antecedent soil moisture conditions within a watershed lead to both processes occurring somewhere in the watershed (Chow, 1988). In upland agricultural cultivated watersheds, Huggins and Burney (1982) have found that interflow processes are negligible. Therefore, in this research, only Hortonian surface flow is incorporated into the NPS water quality model to be tested.

Overland flow begins as millimeter-thin sheets when water overcomes surface tension forces (Chow, 1988). The irregular two-dimension flow is influenced by spatial changes in soil tension, frictional forces and infiltration. Surface irregularities eventually focus sheets into discrete small-scale rills (Foster, 1982). Obstacles to rill flow, including soil aggregates, vegetation and plant residue, create tortuous flow paths that are capable of returning the water to sheet flow. Foster and Meyer (1972) describe this process as broad uniform areas of sheet flow dissected by concentrated rills. This pattern of flow in shallow sheet and rill occurs for only very short distances down the hillslope - 100 meters or less (Woolhiser, 1982) - before more

permanent and structured rill flow is achieved. The total process of flow described above is referred to as overland flow.

Channel flow begins with the confluence of overland rill flow into a relatively more stable network of channels and gullies. Moving downslope through a watershed, channels converge together adding to the size and volume of the flow. Feeding into channels are lateral contributions from overland rill and sheet flow. Factors influencing the development of channels include larger-scale topographic features such as hillside slope, length of slope, vegetation, and large-scale obstructions (Emmett, 1978). The distinction between rills and channels is sometimes subtle. Foster (1982, p. 299) forwards the following definition: "rills infer a large number of small flow concentrations uniformly distributed over an area whereas the number of gullies or channels is small".

The models presented in Table 2.1 mathematically represent water flow by empirical and physical-based equations. Empirical models are represented by the SCS CN Method for estimating a single storm-related runoff volume. Empirical equations are also utilized in calculating characteristics of flow. The Rational Formula and the CREAMS geomorphic equations are used to estimate peak runoff rate. Physical-based models incorporate physical principles, including the laws for the conservation of mass and momentum. The two physical-based models from the table include the Kinematic and Diffusion Wave models.

A. Empirical Flow Models

a. SCS Curve Number (CN) Method

The CN method (USDA-SCS, 1972) is a rainfall excess equation which calculates runoff on a rainstorm basis. It is used primarily as a planning tool for designing upland water retention structures. It is represented as:

(2.12) $$Q = \frac{(P - I_a)^2}{(P - I_a) + S}$$

where:

Q = runoff volume from a rainstorm

P = total rainstorm precipitation

I_a = initial abstraction coefficient

S = potential maximum retention

The initial abstraction coefficient (I_a) represents losses of rain water to surface depression, interception, evaporation, and infiltration and was determined through research to equal 0.2S (SCS, 1972), thus:

(2.13) $$Q = \frac{(P - 0.2S)^2}{P + 0.8S}$$

The SCS (1972) has created tables to determine a curve number value which in turn is related to the S value. A particular curve number is based upon configuration of soil hydrologic type, vegetative cover and antecedent soil moisture conditions. S is related to the curve number by:

(2.14) $$S = 1000/CN - 10.$$

b. Rational Formula

A modification of the rational formula is used in the SWRBB (Williams et al. 1985) model to estimate peak flow rates. In its original form, the rational formula is expressed as Q = CPA, where Q is the peak discharge, C is the runoff coefficient reflecting drainage characteristics, and P is the average intensity of rainfall of specified frequency for a duration equal to the time of concentration (Singh, 1988). The SWRBB modification is represented by:

(2.15) $$q_p = \frac{(\alpha)\ (Q)\ (A)}{360\ (t_c)}$$

where:

q_p = peak runoff rate

α = dimensionless parameter that expresses the fraction of total rainfall that occurs during the watershed time of concentration (t_c)

t_c = total time to concentration for both overland and channel flow

Q = runoff volume calculated using CN method

A = watershed area

Time to concentration is calculated separately for channel and overland flow with the following empirical equations:

(2.16) $$t_{cc} = \frac{0.62\ (L)\ (n)^{0.75}}{(A)^{0.125}\ (S)^{0.375}}$$

(2.17) $$t_{cs} = \frac{(ln)^{0.6}}{18(s)^{0.3}}$$

where:

t_{cc} = time to concentration for channel flow

t_{sc} = time to concentration for overland flow

L = length of channel

l = length of overland flow

n = Mannings roughness coefficient

s = average channel slope

s = average overland slope

c. Geomorphic Peak Equation

ANN-AGNPS incorporates an empirical peak flow calculation (Smith and Williams, 1980) used by the CREAMS model to calculate Peak runoff rate. The equation was created from 304 storms occurring on 56 watersheds located in fourteen states. The watershed sizes ranged from 0.275 to 24 square miles. The equation incorporates watershed geomorphic features including the drainage area, channel slope, length-width ratio for the watershed together with runoff calculated by using the CN method.

(2.18) $$q_p = 200\,(DA)^{0.7}\,(CS)^{0.159}\,(Q)^{(0.917DA^{0.0166})}\,(LW)^{-0.187}$$

where:

q_p = peak flow

DA = drainage area

CS = channel slope

Q = runoff volume

LW = ratio of watershed length to width

B. Physical-Based Flow Models

The physical-based flow models represented in the list are derivatives of the St. Venant equations which combine laws of continuity and momentum for flow in one and two dimension (Chow, 1988). The continuity equation is:

(2.19) $$\frac{\partial h}{\partial t}+\frac{\partial q}{\partial x}=v_p$$

and the momentum equation is:

(2.20) $$\frac{\partial u}{\partial t}+u\frac{\partial u}{\partial x}+g\frac{\partial h}{\partial x}=g(S_o-S_f)$$

where:

h = local depth of flow

q = discharge per unit width

v_p = lateral inflow rate

u = velocity of flow

g = acceleration of gravity

S_o = bed slope

S_f = friction slope

x = distance

t = time

The derivative models represented in Table 2.1 include the Kinematic Wave and the Diffusion Wave models. Both models incorporate fewer than the complete set of parameters from the momentum equation to represent overland and channel flow.

a. Kinematic Wave

The Kinematic representation of flow depth and velocity (Lighthill and Witham, 1955; Henderson and Wooding, 1965; Wooding, 1965) assumes that the friction slope and the overland or channel slope from the momentum equation are equal. In assuming $S_0 = S_f$, the momentum equation can be replaced with a depth discharge relationship for every point along the overland or channel segment:

(2.21) $$q = \alpha_p h^m$$

where:

q = flow discharge

α_p = surface friction constant

h = flow depth

m = constant power parameter.

The Chezy or Mannings resistance law can be employed to determine the surface friction constant. Surface friction is calculated with: $\alpha_p = c_z(S_o)^{0.5}$, where m = 3/2 and c_z is the Chezy friction factor. It is also calulated with $\alpha_p = 1/n_m S_o^{0.5}$,

where m = 5/3 and n_m is the Manning friction factor.

A number of studies determined that the Kinematic approach was appropriate for use in modeling overland flow as well as channel flow in upland watersheds (Brakensiek, 1966, Woolhiser and Liggett, 1967). Overland and upland small channel flow experience minimal backflow and eddying effects on wave propagation. The Kinematic model's representation of channel slope from the momentum equation is a sufficient approximation of flow (Woolhiser and Liggett, 1967; Chow, 1988).

b. Diffusion Wave

Flow in channels with milder bed slopes that are located further down into the watershed can be impacted by the above-mentioned factors of backflow and eddying. The diffusion form of the St. Venant flow model accounts for these effects (Chow, 1988) by including the pressure force term from the continuity equation:

(2.22) $$g\frac{\partial h}{\partial x}$$

The SHE model utilizes a two-dimensional form of the diffusion equation for overland flow and a one-dimensional form for channel flow (Abbott et al. 1986).

2.1.4 Soil Erosion

Soil detachment and soil transport are the two basic soil erosion processes identified by Ellison (1947). Both processes are associated with identifiable upland watershed features of interrill overland flow areas and rills (Foster, 1971; Meyer et al., 1975). Detachment and transport processes also occur in concentrated flow

channels (Foster, 1982).

Within the interrill sediment source area, soil particles are detached by rain drop impact. The rainfall detached soil particles become available to rainwater entrainment and are transported to rills by thin layers of surface flow. Overland flow in the interrill area transports sediments to the rills rather than causing additional detachment from shear stress forces (Young and Wiersma, 1973). When shear stress associated with concentrated flow in rills exceeds soil critical shear, detachment of soil particles along the flow path occurs, thus forming ever-larger rills. Deposition of sediments originating from interrill areas and up-slope rills occurs within the rill if the transport capacity of the flow falls below the sediment concentration. Factors which influence the rate of interrill and rill erosion include: soil erodibility, soil transportability, antecedent soil moisture, slope, slope length, vegetative cover, litter, rainfall amount, rainfall intensity, rainfall duration, and human factors (Bennett, 1974).

Channels and gullies are considered a separate feature from rills. One definition forwarded is that rills, as opposed to channels and gullies, can be obliterated by normal field management practices (Hutchinson et al., 1976). Foster (1982) however, states that distinction of the three features must be based on the dominant process taking place within each feature. One major process distinction forwarded by Foster (1982, p. 252) is that concentrated channel flow can erode the channel bed toward an "equilibrium shape" defined in part by depth to a less erodible soil layer. Because of the complexity of channel erosion processes, most models

represent rills and channels in a similar fashion. Factors which influence channel erosion processes include; inflow from upstream areas, soil erodibility, soil transportability, nonerodible layer, vegetative cover, channel sidewall stability, channel alignment and channel control structures (Foster, 1982).

The list of models in Table 2.1 contains empirical and physical-based models for representing the erosion process in overland and channel features. Most all the physical-based erosion models implement essentially the same mathematical representation for rill and channel flow. CREAMS is the only model that accounts for dynamic channel cutting processes. One of the models, AGNPS, combines a statistical overland erosion model with a physical-based channel transport model. The physical-based models can be subdivided into those which incorporate empirical-generated parameters to represent physical features (fundamental erosion models) and those using physical parameters. Fundamental erosion models are represented by the CREAMS and ANSWERS models, while KINEROS and WEPP implement a more physical-based approach.

A. Empirical Erosion Models

a. Universal Soil Loss Equation (USLE)

The Universal Soil Loss Equation (USLE) is an empirical-based formula developed from regression analysis of over 10,000 plot years of data from both natural and artificial rainfall simulation (Wishmeier and Smith, 1978). The USLE was developed as a resource planning tool to estimate average annual soil erosion when comparing agricultural management plans to control erosion and protect soil

productivity. The average annual erosion value is calculated by cross-multiplying five empirical-based coefficients:

(2.23) $$A = R K LS C P$$

where:

A = average annual erosion

R = rainfall energy factor, which combines erosivity of rainfall and runoff

K = soil erodibility

LS = length slope factor

C = cropping management or vegetative cover factor

P = erosion control factor

The USLE has been widely applied in both soil conservation and water quality management. However, the predicting capabilities of the model are limited and thus it should only be applied to conservation planning efforts. Foster (1982) summarizes the limitations of the USLE:

(1) it does not calculate soil loss for a single storm event, (2) because it is an erosion equation, it does not estimate deposition anywhere within the field, and (3) gully and channel erosion are not included.

Several adjustments to the basic model have been made so that it is more capable of representing single storm erosion required for water quality modeling. ACTMO incorporates a modification to the USLE developed by Foster et al. (1977) where the USLE R factor is updated to account for the influence of individual storm runoff:

(2.24) $$R_m = 0.5\, R_{ei} + 0.35\, V_s\, Q_p^{1/3}$$

where:

R_m = modified R factor

R_{ei} = EI_{30} the storm maximum 30 minute rainfall intensity

V_s = runoff volume

Q_p = peak runoff rate

The R factor is removed completely in the Modified USLE (MUSLE) (Williams, 1975) used in LANDRUN and SWRBB. The R factor is replaced by a runoff-erosivity factor, which emphasizes the importance of runoff causing erosion over rainfall.

(2.25) $$A = 11.8(V_s\, Q_p)^{0.56}\, K\, C\, P\, LS$$

Both modifications to the USLE require the pre-calculation of hydrologic parameters for overland runoff.

b. Revised Universal Soil Loss Equation (RUSLE)

The Revised Universal Soil Loss Equation (RUSLE) represents a recent update in the USLE technology (Renard et al., 1991). RUSLE retains the five USLE empirical-based factors, utilizing them in the same multiplicative procedure. The final factor values used in calculating average annual erosion, however, are derived by summing fifteen-day sub-factor values that better represent temporal changes in climatic patterns and farm management practices. Table 2.2 represents the major modifications made in RUSLE.

Table 2.2 RUSLE Changes

R Factor	Accounts for seasonal variability of rain storms. More complete and detailed isoerodent maps derived from more recording stations.
K Factor	Factor now varies seasonally, reflecting the influence of freeze thaw cycles, rainfall compaction. Rocks within the soil profile addressed and adjustments made to reflect soil permeability.
LS Factor	Incorporates complex multi-segmented hillsides with varying slope.
C Factor	Four C sub-factors incorporated: prior land use, canopy, ground cover and surface roughness. Soil loss ratio (SLR) determined on 15-day basis, with final C value based on weighted distribution of SLRs through year.
P Factor	More accurate factor based on better description of conservation practice.

The R factor in RUSLE reflects the impact of rainfall on two separate erosion mechanisms, erosion from rainsplash and erosion occurring due to runoff generated from the rain event. The energy intensity value (EI) is the product of the total storm energy (E) and the 30 minute intensity of the rain event (I_{30}): ($EI = I_{30}E$). In RUSLE E is calculated with the following equation:

(2.26) $$E = 1099[1-0.72e^{(-1.27i)}]$$

where:

i = the total storm rainfall intensity.

Long-term rainfall erosivity R values are calculated with:

(2.27) $$R = \frac{\sum_{i=1}^{j} (EI_{30})_i}{N}$$

where:

i = values of EI_{30} for a particular storm

j = number of storms

N = year period

The K factor in RUSLE represents the capacity of the soil to erode under natural forces of rainfall impact, runoff and infiltration. A K factor value can be determined by relating the physical characteristics of the soil to soil loss per rainfall erosion index unit (Römkens et al., 1991). A K factor value has been determined for many of the mapped soils in the US. These values can be found in USDA county soil surveys. Empirical relationships have been developed using physical soil characteristics to estimate K. RUSLE utilizes the equation forwarded by Wischmeier and Smith (1978) to calculate K given the availability of soil textural information. This equation approximates the soil erodibility nomograph developed by Wischmeier et al. (1971).

(2.28) $$K = [2.1*10^{-4}(12-OM)M^{1.14}+3.25(s-2)+2.5(p-3)]/100$$

where:

OM = percent organic matter

M = the product of the primary particle size fractions

s = code for structure

p = code for permeability

The presence of rock fragments in the soil profile alters the saturated hydraulic conductivity of the soil which in turn influences infiltration, runoff and soil erosion by overland flow. The K factor includes the impact of rock fragments with the following relationship (Brakensiek et al., 1986):

(2.29) $$K_s/K_f = (1-R_w)$$

where:

K_b = saturated hydraulic conductivity of soil with rock fragments

K_f = saturated hydraulic conductivity of the fine soil fraction

R_w = percent by weight of rock fragments

Change in hydraulic conductivity can be related to a change in permeability class (Rawls et al., 1982), which in turn is related to a change in K factor value. A shift to a larger permeability class from a decrease in saturated hydraulic conductivity will cause an increase in K factor value.

K factor values in RUSLE are seasonal, varying depending upon the influence of soil freezing, soil texture and antecedent soil water (Römkens et al., 1991). K factor value is highest following soil thaw and the beginning of the frost-free season, and decreases exponentially to a minimum value close to the first frost date at the end of the frost-free growing season. In locations with minimal or no soil freezing, maximum and minimum erodibility values are related to low and high rainfall periods.

Calculating seasonal K values in RUSLE requires knowing when maximum and minimum soil erodibility occurs, the corresponding K values and a base K value determined from the soil erodibility nomograph. These values can be calculated with the following relationships:

(2.30) $$t_{max} = 154\text{-}0.44(R)$$

(2.31) $$t_{min} = t_{max} + GS$$

(2.32) $$K_{max}/K_{nom} = 3.0\text{-}0.005(R)$$

(2.33) $$K_{max}/K_{min} = 8.60\text{-}0.019(R)$$

where:

t_{max} = julien date of maximum K value

t_{min} = julien date of minimum K value

K_{max} = maximum K value

K_{min} = minimum K value

K_{nom} = K value from soil erodibility nomograph

R = Rainfall-Runoff erosivity factor value

GS = number of frost-free days

Two different K factor scenarios can be calculated based upon when in the year the maximum date K value occurs relative to the minimum value. In the northern US, where a frost period is experienced, t_{max} will be less than t_{min}. In areas of the US not experiencing frost, t_{max} can be greater than t_{min} depending on the timing of wet and dry periods of the year. The calculations for both scenarios are outlined below:

A. when $t_{max} < t_{min}$

(1) $t_{max} < t_i < t_{min}$

(2.34) $$K_i = K_{max}(K_{min}/K_{max})^{(t_i - t_{max})/\Delta t}$$

(2) $t_i < t_{max}$ or $t_i > t_{min}$

when average temperature > 27 deg. F

(2.35) $$K_i = K_{min}e^{(0.009(t_i - t_{min} + 365\delta)}$$

(2.36) $$\delta = 1 \text{ if } (t_i - t_{min}) \leq 0$$

(2.37) $\delta = 0$ if $(t_i - t_{min}) > 0$

when average temperature < 27 deg. F: $K_i = K_{min}$

B. when $t_{max} > t_{min}$

(1) $t_{max} > t_i > t_{min}$

when average temperature > 27 deg. F

(2.38) $$K_i = K_{min} e^{(0.009(t_i - t_{min})}$$

when average temperature < 27 deg. F: $K_i = K_{min}$

(2) $t_i > t_{max}$ or $t_i < t_{min}$

(2.39) $$K_i = K_{max}(K_{min}/K_{max})^{(t_i - t_{max} + 365\delta)/\Delta t}$$

(2.40) $\delta = 1$ if $(t_i - t_{max}) \leq 0$

(2.41) $\delta = 0$ if $(t_i - t_{max}) > 0$

If however:

$K_i > K_{max}$ then $K_i = K_{max}$

$K_i < K_{min}$ then $K_i = K_{min}$

RUSLE is capable of determining the LS factor for both simple slopes represented by one constant percent slope, as well as hillsides with multiple slope segments (McCool et al., 1991). The simple case LS factor is calculated by first determining the L subfactor:

(2.42) $$L = (\lambda/72.6)^m$$

where:

L = USLE L factor

λ = slope length

m = variable slope length exponent

The S subfactor is calculated differently for slopes less than and greater than 9 percent:

(2.43) $$S = 10.8\sin\theta+0.03 \quad s < 9\%$$

(2.44) $$S = 16.8\sin\theta=0.50 \quad s > 9\%$$

The final LS factor for the simple slope is determined by multiplying L * S.

Complex hillsides with multiple slopes of varying lengths are calculated first by delineating the hillside into segments with equal lengths. The following equation is then used to determine LS for each segment. LS for the entire hillslope is the sum of LS for each segment.

(2.45) $$LS_i = S_i x^m[i^{m+1}-(i-1)^{m+1}]/(72.6)^m$$

where:

LS_i = the effective LS for the ith segment

x = length of each segment

The RUSLE C factor calculations are the most detailed. Management and vegetative impacts on erosion rates are represented through the soil loss ratio (SLR). The SLR value is reflective of daily field condition changes brought about by a particular management practice and modified by weather conditions. The SLR is derived from four subfactors (Yoder et al., 1991):

(2.46) $$SLR = PLU * CC * SC * SR$$

where the PLU is the prior land use subfactor, CC is the canopy cover subfactor, SC is the surface cover subfactor, and SR is the surface roughness subfactor.

The PLU represents the impact of subsurface residue from pervious crops and the effect of previous tillage practices on soil consolidation. PLU is calculated by:

(2.47) $$PLU = c_f \exp(-c\, B_u)$$

where:

c_f = surface soil consolidation factor decreasing exponentially from a value of 1.0 at a tillage practice to 0.45 seven years later (Dissmeyer and Foster, 1981)

B_u = mass of live and dead roots and buried residue found in the upper four inches of the soil

The CC subfactor represents the ability of crop cover to protect the soil surface from erosive powers of raindrops. CC is determined with the equation:

(2.48) $$CC = 1 - F_c \exp(-0.1H)$$

where:

F_c = the fraction of land surface covered by canopy

H = the height of the canopy

The SC subfactor influences erosion rates by reducing the transport capacity of water flowing over the soil surface by creating barriers to flow. Surface cover also acts as a protection to the soil from raindrop impact.

(2.49) $$SC = \exp[-bS_p(0.24/R_c)^{0.08}]$$

where:

b = coefficient representing the effectiveness of surface cover in reducing soil erosion

S_p = percentage of land area covered by surface cover

R_c = soil surface roughness

The SR subfactor represents the roughness of the surface and its ability to dampen soil erosion. Soils that have been tilled contain depressions and barriers inhibiting the flow of water and the transport of sediments. SR is calculated by:

(2.50) $$SR = \exp[-0.0265(R_c - 1.24)]$$

The P factor is calculated based upon the type of conservation practice taking place on the hillside. Conservation practices modeled in RUSLE include contouring, stripcropping, and terracing. P factor calculations are based upon placement and configuration of the practice within the hillslope and how it affects the hydraulics of overland flow, which in turn influences the sediment transport capacity of the runoff. The P factor algorithms for RUSLE were developed by combining physical-based erosion theory with analysis of experimental data (Foster et al., 1991).

The contour plowing P subfactor was developed by considering ridge height, the effects of rainstorm intensity and the impact of off-contour tillage. A base P value is first determined for three separate ridge height conditions using equations derived from fitting curves to observed data (Foster et al. 1991) :

(2.51) $$P_b = a(s_m - s_c)^b + P_{mb} \qquad s_c < s_m$$

(2.52) $$P_b = c(s_c - s_m)^d + P_{mb} \qquad s_c \geq s_m$$

(2.53) $$P_b = 1.0 \qquad s_c \geq s_c$$

where:

P_b = base P value

s_m = slope where contouring has greatest effect

s_c = actual slope

s_o = slope above which contouring is ineffective

P_{mb} = minimum P value for a given ridge height

a,b,c,d = coefficients

The base P value is then adjusted according to the severity of rainstorm as represented in the energy intensity value (EI).

(2.54) $$P_a = 1.0 - e^{\log(1.0-P)/100.0 EI}$$

where:

P_a = adjusted base P factor value

P = base P factor value

The P factor is next adjusted to account for the off-grade contouring utilizing the equation:

(2.55) $$P_g = P_a + (1-P_a)(S_f/S_l)^{1/2}$$

where:

P_g = P factor accounting for off-grade effect

S_f = grade along the furrows

S_l = slope of hillside

P factor values for stripcropping were determined with an empirical equation representing simulated output results from a simple erosion-depositional model (Renard and Foster, 1983). Three cases of strip effectiveness were determined: (1) erosion occurring everywhere along the slope, (2) both deposition and erosion occurring within a strip, and (3) deposition occurring over the entire slope. Model

input data required as parameters in the empirical equation include: type of tillage practice for area between strips, number of strips in field, strip width, land slope, and number of crop years associated with strip (Foster et al., 1991).

A P factor value for terraces is determined with the following equations:

(2.56) $Py = 0.1e^{2.4s}$ $s < 0.9\%$

(2.57) $Py = 1.0$ $s \geq 0.9\%$

where:

Py = sediment delivery factor

s = the terrace slope grade

The sediment delivery factor is incorporated into:

(2.58) $P = 1 - B(1-Py)$

where B is a parameter reflecting depositional capacity as a function of terrace spacing and 1-Py is the amount of deposition occurring.

P subfactor values for ridge height, stripcrops and terraces are multiplied together to arrive at a final P factor value.

c. Delivery Ratios

The sediment delivery ratio (DR) represents mathematically the ratio of the sediment yield at the watershed outlet to the sum of eroded sediments within the watershed. It is shown in its simplest form as:

(2.59) $DR = S_y/E_s$

where:

DR = delivery ratio

S_y = sediment yield

E_g = gross erosion

Renfro (1975) and Roehl (1962) have identified a number of factors controlling sediment delivery, including sediment source, magnitude and proximity of sediment sources relative to channels and drainage basin characteristics. The basic delivery equation can be enhanced to represent major physical influences in sediment generation and its transport to the outlet. Parameters that have been incorporated in the delivery ratio representing upland processes include rainfall characteristics, soil characteristics, vegetation, topography and human activities. Parameters that represent channel processes include velocity, depth of flow, channel slope, hydraulic roughness, and cross-section area (Singh, 1989). Drainage basin characteristics can also be included as model parameters, such as size of basin, relief-length ratio, channel density and bifurcation ratio (Renfro, 1975).

Physical-based assumptions are incorporated into the GAMES (Guelph model for evaluating the effects of Agricultural Management systems on Erosion and Sedimentation) (Rudra et al., 1986) delivery ratio where sediment transport is related to flow velocity and the overland flow path length. The flow paths are determined by connecting farm fields in a downslope fashion throughout the watershed. The GAMES DR is represented by the following equation:

(2.60) $$DR = \alpha(V/L)$$

where:

α = calibrated watershed parameter

V = velocity of flow between location, determined with a modified Mannings equation

L = length of flow between fields

An upland erosion amount is calculated for each field using the USLE. The delivery ratio is then applied to a field's sediment to determine how much arrives at the downslope field. Sediment is thus cascaded down through the watershed to the watershed outlet.

d. Negev Soil Erosion Model

The Negev soil erosion model (Negev, 1967), incorporated into the LANDRUN and HSPF models, is an empirical-based set of two equations representing rainfall impact on the soil and overland flow detachment and transport. Erosion of the smaller particle size silts and clay fractions by rainsplash is represented by:

(2.61) $$A(t) = (1\text{-}COV)K_a P(t)^{PER}$$

where:

A = erosion produced for period (t)

COV = fraction of vegetation cover at rainfall

K_a = coefficient for soil property

P = precipitation during time interval

PER = exponent

The finer particles detached become available to overland transport if precipitation is sufficient to generate overland flow. If overland flow is not achieved,

sediments remain as a potential source for the next runoff event. Overland flow transport of rain-eroded particles is represented with the equation:

(2.62) $$SER(t) = KSER\ SRER(t-1)\ ROSB(t)^{SR}$$

SER = particles transported during time period (t)

KSER = coefficient of transport

SRER(t-1) = source of potential sediment at beginning of time period

ROSB = overland flow volume

SR = exponent

Coefficients for both rainsplash erosion and overland flow soil detachment must be determined by incorporating field data with model calibration.

B. Physical-Based Erosion Models

a. Chemicals, Runoff, and Erosion From Agricultural Management Systems Program (CREAMS)

The CREAMS model is an approximation of the quasi-steady state continuity equation representing sediment transport downslope (Foster et al., 1980):

(2.63) $$\frac{dq_s}{dx} = D_L + D_F$$

where:

q_s = sediment load per unit width per unit time

x = distance

D_L = lateral inflow of sediment

D_F = detachment or deposition by flow

The general process is divided among interrill, rill and channel elements. The CREAMS model is not a true physical-based model because it incorporates many of the empirical-based parameters forwarded in the USLE model. The empirical/ fundamental CREAMS is, however, an improvement over a completely empirical model such as the USLE. Foster (1982) lists several of the empirical/fundamental improvements: (1) is more physically based and consequently can be more accurately extrapolated, (2) more accurately represents processes by considering interrill and rill erosion separately, (3) is more accurate for a single storm event, (4) can consider more complex areas, (5) overland deposition processes are accounted for directly, (6) channel erosion and deposition are accounted for directly.

Detachment of soil particles begins in interrill areas from the combination of rainsplash and water flow. It is represented in the form:

(2.64) $$D_{Li} = 0.210\ EI(S+0.014)KCP(Q_p/V_s)$$

where:

D_{Li} = Detachment in interrill area

EI = USLE rainfall erosivity factor

S = sine of slope angle

K = USLE soil erodibility factor

C = USLE cropping factor

P = USLE conservation practice factor

Q_p = peak runoff flow

V_s = flow volume

Interrill-generated sediments, or lateral flow concentrations, combine with upslope rill eroded sediments. If the resulting calculated transport capacity is sufficiently large to entrain soil particles in the rill, detachment occurs at the following rate:

(2.65) $$D_{Fr} = 37983 m V_s Q_p^{1/3} (x/72.6)^{m-1} S^2 KCP(Q_p/V_s)$$

where:

D_{Fr} = Detachment rate in rill area

m = slope length exponent

x = distance downslope

Transport capacity is solved implementing the Yalin equation (1963) modified to account for a distributed capacity among five defined particle classes (Foster et al., 1980). Particles are then routed across the overland flow and channel elements. Sediments can be deposited within the rills depending upon whether the capacity to transport the previously entrained material is less than the potential sediment load. Deposition is represented by the equation:

(2.66) $$D = \alpha(T_c - q_s)$$

where:

D = the deposition rate

α = first order reaction coefficient

where: $\alpha = \epsilon V_f / q L_x$.

ϵ = parameter equal to 0.5 for overland flow and 1.0 for channel flow.

V_f = particle fall velocity

qL_x = runoff discharge per unit width

T_c = transport capacity

q_s = sediment load

The CREAMS model simulates the channel element similar to a rill where upslope sediment input is from an above channel segment and lateral inflow is from the entire overland element. In addition, the channel model component of CREAMS can estimate the degradation of a channel to a non-erosive soil layer, which is usually assumed to be the depth of primary tillage. The channel erosion rate before a non-erodible layer is reached is expressed as:

(2.67) $$E_{ch} = W_{ac}K_{ch}\,(1.35\tau-\tau_{cr})^{1.05}t_b$$

where:

E_{ch} = soil loss per unit channel length of the storm

W_{ac} = width of the channel

K_{ch} = USLE soil erodibility factor

τ = average shear stress around wetted perimeter of channel

τ_{cr} = critical shear stress, below which erosion is negligible

t_b = time at which shear stress exceeds critical shear stress

Once the non-erodible layer is reached, the channel sides become the source of channel erosion. Erosion from channel sides is:

(2.68) $$E_{ch} = \Delta W H_{sw}\rho_{soil}$$

where:

ΔW = change in channel width, where $(dW/dt)_i = 2K_{ch}(\tau_b-\tau_{cr})^{1.05}/\rho_{soil}$

τ_b = shear stress in channel at non-erodible boundary

H_{sw} = height of channel sidewall

ρ_{soil} = mass density of soil in the channel sidewall

Channel width increases until shear stress at the non-erodible boundary equals the critical shear stress.

b. Areal Nonpoint Source Watershed Environment Response Simulation (ANSWERS)

The ANSWERS model utilizes separate equations to represent soil detachment processes for raindrop impact (Meyer and Wischmeier, 1969) and overland flow (Meyer and Wischmeier, 1969; Foster, 1976). The form and parameters utilized are similar to the CREAMS procedure. Raindrop detachment is calculated with:

(2.69) $$D_r = 0.027CKA_iI^2$$

where:

C = USLE cropping factor

K = USLE soil erodibility factor

A_i = area increment

I = rainfall intensity

Detachment by overland flow is represented by:

(2.70) $$D_f = 0.018CKA_iSQ$$

where:

S = slope steepness

Q = flow rate per unit width

A transport capacity value is required in a steady-state continuity equation to determine if deposition or detachment occur in overland and channel routing. Potential transport capacity is calculated with the following equations:

(2.71) $T_c = 161(SQ^{1/2})$ $Q \leq 0.046$ m^2/minute

(2.72) $T_c = 16320(SQ^2)$ $Q > 0.046$

c. Agricultural Nonpoint Source Pollution Model (AGNPS)

AGNPS and ANN-AGNPS model channel sediment transport and deposited sediment entrainment utilizing the same form of steady-state continuity expression forwarded in the CREAMS model (Foster et al., 1980). The sediment deposition rate in the channel is given as:

(2.73) $D = (V_f/qL_x)(T_c - G)$

Transport capacity is determined with the Bagnold stream power equation (1966):

(2.73) $g_s = k\tau v^2/V_f$

where:

g_s = transport capacity

k = transport capacity factor

τ = shear stress

v = flow velocity

Upland as well as channel erosion is broken down into the five particle classes defined by Foster et al. (1980).

d. Water Erosion Prediction Program (WEPP)

The erosion model within WEPP (Foster et al., 1989) incorporates many of the same physical concepts of erosion processes and mathematical algorithms presented in the CREAMS model. The similarities include: the delineation of overland areas into interrills and rills for defining erosional processes, the use of the steady-state sediment continuity equation for transporting sediments across overland elements and through channels. The major difference between the two erosion models is the use of more physical-based parameters in WEPP.

Interrill detachment is calculated with the following equation:

(2.75) $$D_i = K_i I_e^2 C_e G_e (R_s/W)$$

where:

K_i = baseline interrill erodibility factor

I_e = effective rainfall intensity

C_e = effect of canopy cover

G_e = effect of ground cover

R_s = spacing of rills

W = rill width

Rill detachment is calculated with the following equation:

(2.76) $$D_f = D_c(1-G/T_c)$$

where:

D_c = detachment capacity by rill flow, where $D_c = K_r(\tau_f - \tau_c)$

K_r = rill erodibility parameter

τ_f = flow shear stress

τ_c = critical shear stress

T_c = transport capacity

Deposition within the rill occurs when transport capacity is less than the sediment load. It is represented as:

(2.77) $$D_f = (\beta V_f/q)(T_c-G)$$

where:

V_f = effective fall velocity for the sediment

q = flow discharge

β = raindrop turbulence coefficient (=0.5)

The overland transport capacity in WEPP is determined by the following simplified transport equation:

(2.78) $$T_c = k_t \tau_f^{3/2}$$

T_c is calculated for rills throughout the slope utilizing a calibrated transport coefficient (k_t) and the hydraulic shear stress (τ_f). The transport coefficient is determined by using the above relationship together with a calculated Yalin-derived transport capacity at the end of the slope and a slope bottom shear stress value.

Erodibility parameters K_i and K_r for interrill and rill features are calculated with empirical equations developed from data collected for 36 cropland soils (Alberts et al., 1989). The two equations developed represent the relationship of the soil erodibility parameter as a function of physical and chemical soil parameters. Channel erosion in the WEPP models incorporates the same mathematical routines for channel

down-grading and bank cutting as presented in CREAMS.

e. Kinematic Runoff and Erosion Model (KINEROS)

The erosion component of KINEROS is based upon a form of the continuity equation forwarded by Bennett (1974):

(2.79) $$\frac{\partial}{\partial t} + \frac{\partial}{\partial x}(QC_s) - e(x, t) = q_s(x, t)$$

where:

C_s = sediment concentration

A = cross sectional area of flow

e = erosion rate of the soil bed

q_s = lateral sediment inflow for channel

The erosion rate of the soil bed is derived from two separate erosion sources; rainsplash erosion and hydraulic erosion. Rainsplash erosion is calculated with the equation:

(2.80) $$g_s = c_f k(h) r q$$

where:

g_s = rainsplash erosion

c_f = constant

k(h) = reduction factor related to increasing depth of ponded water

r = rainfall

q = runoff volume

Hydraulic erosion is linearly dependent on the difference between the transport capacity and the current sediment concentration.

(2.81) $$g_h = c_g(c_{max}-c_s)A$$

where:

g_h = hydraulic erosion

c_{max} = sediment concentration at equilibrium

c_s = current sediment concentration

c_g = transfer rate coefficient, when detachment is occurring

c_g represents erodibility constrained by cohesiveness in the soil. When deposition is occurring, c_g is related to the fall velocity of the entrained soil particles.

Channel erosion is represented by the hydraulic erosion principles presented above for upland erosion.

2.1.5 Nutrient Fate

The processes involved in the transport of nutrients from a watershed are extremely complex. Nutrients are transformed from different forms and states under environmental conditions which change across both time and space. Bailey et al. (1974) divide the processes of chemical (including nutrient) transport into four mechanisms: (1) diffusion and turbulent transport of dissolved chemicals from soil by movement of soil water into overland flow, (2) chemical desorption from solid phase adsorption into soil water or directly into overland flow, (3) dissolution of chemicals from solid phases into the soil water or overland flow, and (4) detachment and transport of chemicals attached to soil particles or organic matter by hydraulic forces

and the subsequent release of the chemical to overland flow by dissolution or desorption. The relative importance of transport processes is controlled by a particular chemical, its application method, as well as soil characteristics, vegetation, climate and recent hydraulic characteristics (Bailey et al., 1974).

Two agricultural nutrients that have been proven to affect water quality and have become a primary focus of best management practices are nitrogen (N) and phosphorus (P) (Sharpley and Menzel, 1987). Soils generally contain 0.05-0.3% N (Novotny and Chesters, 1981) and 0.01-0.13% P within the top 15 cm of the profile (Frere et al., 1980). In intensive mono-culture cropping systems, nutrients are depleted from the soil by plant uptake, sediment erosion, overland and subsurface drainage, or immobilized within the soil itself. Thus in order to supplement crops, farmers apply additional sources of nutrients to fields. Nutrient forms applied include inorganic fertilizers, manures and plant residue. Commercial fertilizers comprise 46% and manures 7% of the N input (Steward et al., 1975).

N and P are the two primary nutrients incorporated into NPS water quality models for estimating loadings and identifying sources of significant contribution. Models represent the two nutrients in their basic transportable states: water soluble state N_{sol} and P_{sol} , and sediment/particulate bound N_{sb} and P_{sb}. The sediment absorbed state of P and the soluble form of N are the major pollutants and draw the most attention in BMP formulation. However, the dissolved state of P can become a significant source of nutrients under local environmental conditions (Ahuja, 1982). It is therefore important that NPS water quality models account for each form of the

chemicals.

2.1.5.1 Dissolved Nutrient Transport

Fertilizers applied to the field are either in liquid or solid forms that easily convert to a soluble form with rainfall or irrigation. Soluble forms of nutrients thus become available to plant uptake. Nitrogen fertilizers primarily take the form of ammonium salts which are readily nitrified to Nitrates (NO_3) under normal field conditions (Novotny and Chesters, 1981). Dissolved inorganic phosphates (HPO_4 and H_2PO_4) are applied to enable direct plant uptake before particulate absorption can occur (Wendt and Alberts, 1984). Organically bound nutrients in manures and plant materials are leachable to soluble forms, with residues providing more P, in the form of orthophosphate (PO_4), than mineralized ammonium (NH_4) (Novotny and Chesters, 1981).

Representing the transport of dissolved nutrients from their origin at the soil surface into overland flow is the weakest aspect of nutrient modeling due to the "variety of nutrient sources and processes of extraction" (Frere et al., 1980, p. 69). A number of approaches have been forwarded by the different nutrient models listed in Table 2.1. These methods include; equivalent soil water/runoff concentrations: SWRBB, extraction coefficients: CREAMS and AGNPS, and kinetics: ANSWERS.

A. Extraction Coefficients

The extraction coefficients forwarded in CREAMS are determined with the following relationship:

(2.82) $$EXK = d\ POR\ K$$

where:

EXK = surface runoff extraction coefficient

d = 100 mm depth of surface layer

POR = soil porosity

K = rate constant for movement into runoff

The movement of dissolved nutrients from the soil surface, including the soil and soil-water, is calculated incorporating the extraction coefficients.

(2.83) $$ROC = C\ EXK\ Q\ 0.01$$

where:

ROC = concentration of nutrients in surface flow

C = mean concentration during runoff

Q = runoff volume

Concentrations for dissolved N and P will differ, with N concentration including Nitrogen originating from rainfall, whereas P concentrations exclude rainfall additions and incorporate a base concentration that accounts for the P buffering capacity of soils (Frere et al., 1980)

B. Kinetic Desorption

The release of attached P to runoff can be described through an empirically derived kinetic-based equation (Sharpley et al., 1981; Sharpley, 1985). This desorption of nutrients to soil-water and surface runoff water is due to turbulent raindrop impact, flow at the soil-water interface and disequilibrium of concentrations attached to the soil and dissolved in the surrounding water. The kinetic equation

presented by Sharpley for P is as follows:

(2.84) $$P_d = K P_a t^{\alpha} W^{\beta}$$

where:

P_d = amount of P released from the soil

t = average time of contact between soil surface and runoff

P_a = initial available P content in soil

W = water/soil ratio

K α β = constants for a given soil

An important feature in the loss of nutrients from the soil surface is the depth of interaction between rainfall, soil-water and the soil. This soil region of interaction is called the mixing zone. CREAMS, SWRBB and HSPF assume a constant depth where complete mixing of nutrients occurs. Ingram and Woolhiser (1980) determined that concentrations of soluble chemicals mix completely for infiltrating water. However, water ponding at the soil surface and flowing overland does not mix completely with dissolved chemicals. Concentrations within the mixing zone are highest at the water-soil contact and decrease exponentially with depth (Ingram and Woolhiser, 1980). Ahuja (1982) forwarded the concept of an effective depth of interaction (EDI) which integrates concentration differences into a representative depth approximate to chemical concentration. The EDI varies based upon soil, topography and rainfall characteristics. The ANSWERS model incorporates the EDI concept in determining soluble P desorption.

Several nutrient transport research models have applied conservation of mass equations to chemical mixing and transport by overland flow (Emmerich et al., 1989; Ingram and Woolhiser, 1981; Ashof and Borah, 1992; and Lee et al., 1989). Similar to runoff and sediment routing, a distributed process modeling approach for nutrients represents the spatially and temporally dynamic environment for overland and channel flows. Emmerich et al. (1989) found that the timing of chemical arrival and peak concentrations were better represented with a distributed model than a spatially lumped model. However, predictions of total chemical concentrations were similar.

2.1.5.2 Sediment Bound Nutrient Transport

Forms of N and P bound to soil or incorporated within organic matter comprise the largest source of nutrients (Novotny and Chesters, 1981). The control of soil erosion and sediment transport has thus been the primary means of controlling nutrient loading to water (Daniel et al., 1993). Of the two nutrients, soluble forms of P are more readily fixed by soils than soluble forms of N. P primarily precipitates in combination with calcium (Ca), however in soils with pH less than 7, precipitation occurs with ions of iron (Fe) and aluminum (Al) (Novotny and Chesters, 1981). Soluble ammonium is also capable of adhering to soil particles, primarily with layers of expanding clay such as montmorillonite. Further, both N and P exist as organic forms in plant residue. The low density of residues allows them to be easily transported in overland flow.

The sorption of soluble forms of N and P and their transport is a selective process (Massey and Jackson, 1952). It begins with nutrients more readily adhering

to smaller particles with larger surface areas. A larger portion of smaller soil particles is then detached by rainsplash and overland flow and transported downslope/channel. Sediment deposition selectively deposits the larger particles under decreasing transport capacity, whereas smaller particles continue on in the flow. This process results in downstream sediments having greater nutrient concentrations than the originally eroded soils. Two methods of modeling absorbed nutrient movement are contained in the model list (Table 2.1). The first method is the empirical-based enrichment ratio which relates mathematically the concentration of nutrients in the transported sediments to the originally eroded sediments. The CREAMS, SWRBB, AGNPS, GAMES and GWLF models implement this procedure. The second method is based upon incorporating a spatially distributed erosion and sediment transport model with nutrient absorption and desorption equations. ANSWERS, HSPF and ACTMO utilize this procedure.

A. Nutrient Enrichment Ratio

The enrichment ratio (ER) describes the ratio of nutrient content of transported soil to that of the sediment source. Menzel (1980) and Sharpley (1985) have found the ER to be a negatively linear relationship between the logarithm of ER and sediment loss. Both CREAMS and AGNPS use the following method:

(2.85) $$SEDN = SOILN\ SED^{ERN}$$

(2.86) $$SEDP = SOILP\ SED^{ERP}$$

where:

(2.87) $$ERN = AN\ SED^{BN}$$

(2.88) $$ERP = AP\ SED^{BP}$$

Based on evaluating available data for a number of soil and vegetative conditions, CREAMS assigns AN and AP equal to 7.4 and BN and BP to -0.2. Sharpley (1985) forwards an empirical-based relationship for determining ER:

(2.89) $$\ln(ER) = 1.21 - 0.16 \ln(SED)$$

SWRBB determines the enrichment ratio based upon an empirical relationship between an upper bound enrichment ratio value, which is assumed to be the inverse of the sediment delivery ratio, and a lower bound ER delivery ratio value:

(2.90) $$ER = x_1 c_s^{x2}$$

where:

(2.91) $$x_2 = \log(1/DR)/2.699$$

(2.92) $$x_1 = 1/(0.25)^{x2}$$

c_s = sediment concentration

DR = sediment delivery ratio

B. Erosion / Sediment Transport

A more physical-based method of calculating concentrations of sediment - absorbed N and P is to determine sediment size distribution in runoff originating from overland erosion (Foster et al., 1980). Attached nutrient concentrations at a given point in the watershed are represented by the sum of particle class concentrations present in the runoff after selective deposition and erosion take place.

Several methods have been used in models to represent the absorption of soluble nutrients to sediments. Non-linear absorptive isotherms relate disequilibrium

exchange potential between concentrations of absorbed and dissolved nutrients within the mixing zone (Bolan et al., 1985; Chien and Clayton, 1980). The specific surface areas of soil particles have been used in determining attached nutrient concentrations (Storm et al., 1988; Williams, 1980; Frere et al., 1975). Absorbed nutrient concentrations are empirically related to the original soil concentration based upon the specific surface characteristics of the soil. The specific area characteristics can be quantified by determining the distribution of specific surface areas for all particle classes in the soil (Williams, 1980).

2.2 Geographic Information Systems and Hydrologic Modeling

2.2.1 Introduction

A Geographic Information System (GIS) can be defined as a spatial data management system which processes geographically referenced spatial data (maps) and relational attribute information (descriptions). The digital structure of spatial data can be represented as topologically related nodes, arcs and polygons or grids of uniform squares, TINs, and other geometric shapes (Goodchild, 1993). The digital structure enables computer processing of individual and multiple data sets in carrying out geographic-based analysis. GIS routines typically used in data analysis include; connectivity operations, neighborhood operations, measurement operations, statistical analysis and cartographic modeling or overlay operations (Star and Estes, 1990). Traditional data management utilities can also be performed on the relational data base of attributes. Data management operations include; Boolean searches, queries and arithmetic operations (ESRI, 1991). Changes made in the relational data base

will be reflected in the spatial data.

The utility of a GIS for decision making has been well articulated over the years. Unwin and Wilson (1990) identify the versatility and capabilities of a GIS accordingly:

1. Integrates spatial and other information within a single system;
2. Offers a consistent framework for analyzing the spatial variation across areas;
3. Permits geographic knowledge to be manipulated and displayed in new and exciting ways by putting maps and other kinds of spatial information into digital form;
4. Allows connections to be made between activities based on geographic proximity and characteristics which can be vital to understanding and managing activities and resources;
5. Allows access to administrative, financial and other sociological records via their geographical positions.

Descriptive and mathematical definitions of hydrologic / NPS pollutant transport models were provided in the previous section. The connection between GIS and hydrologic modeling relative to spatial data location and description for parameterization of input data is obvious. However, the ability of a GIS to manage temporal changes in those land features is not straight forward (Maidment, 1993).

Maidment (1993) identifies the following five levels of GIS and hydrologic modeling integration: (1) hydrologic assessment, (2) hydrologic parameter determination, (3) linking GIS and hydrologic models, (4) hydrologic modeling inside

GIS, and (5) object-oriented linkage. The remainder of the literature review will utilize these above levels of GIS/model integration to organize the discussion. Also covered will be the GIS methods employed for generating model parameter values.

2.2.2 Hydrologic Assessment

Hydrologic assessment is the simplest form of hydrologic modeling/GIS integration. This procedure does not incorporate explicit physical laws into its analysis (Maidment, 1993). Rather, ratings are assigned to map classes based upon expert opinion and experience as to how an individual feature (distance from a river) will influence the overall impact (chemical transport). The hydrologic assessment procedure is primarily used as a planning tool (National Research Council, 1993) where the relative ratings of the final map help prioritize and target resources for addressing potential impact.

Hydrologic assessment procedures utilize multiple GIS coverages of physical features and cultural activities in combination to determine the potential impact of hydrologic-related phenomena such as flooding, erosion, and contaminant fate. The GIS is first used to generate map coverages on features which influence the degree of potential impact. GIS's spatial data manipulation capabilities are next incorporated to delineate mapped areas into different descriptive classifications, such as distance from rivers and pesticide application rates, and then assign ratings describing the feature's influence on potential impact. Finally, the GIS is used to combine individual rating coverages to generate an overall rating representing the combined influence of all individual coverages (Aller et al., 1985).

The most popular use of this procedure has been associated with assessing potential groundwater vulnerability. The DRASTIC ground water vulnerability assessment procedure (Aller et al., 1985) assesses the likelihood of ground water contamination from chemicals based upon the makeup of the hydrogeologic environment. GIS-DRASTIC applications include intermediate-scale vulnerability assessment of regional aquifers (Griner, 1993; Hearne et al., 1991; Evans and Myers, 1990) and small-scale assessment of state-wide groundwater resources (Halliday and Wolfe, 1991; Rundquist et al., 1991).

Hamlett and Petersen (1992) generated an indexing procedure, which they referred to as the Agricultural Pollution Index (API), to rank watersheds throughout the state of Pennsylvania based on their potential to contribute agricultural nonpoint source pollutants. Four index coverages were generated from base coverages of soils, land use/land cover, precipitation, slope, and animal density. The four index coverages are: (1) a runoff index based on use of the SCS CN method to calculate a total watershed runoff value, (2) a sediment production index generated by calculating erosion with the Modified USLE (MUSLE) equation and applying a sediment delivery ratio, (3) an animal loading index determined with a loading factor for the total number of animals in a watershed, and (4) a chemical use index based upon potential loading of agricultural chemicals from each watershed. The runoff index and sediment production index are generated by crudely applying the empirical CN method and MUSLE erosion equation with a sediment delivery ratio.

2.2.3 Hydrologic Parameter Determination

Hydrologic parameter determination requires identifying GIS data that can be used as parameter input into the hydrologic/NPS model. Spatial data within the GIS is passed out of GIS data format to an intermediate ASCII file which is then read into the hydrologic/NPS model program. The reverse process occurs once the model has generated its results. The GIS reads model output files and converts them back into GIS data format for displaying. The hydrologic/NPS program's I/O routines are not modified. The GIS or an intermediate data processing program formats the input parameter data so that it is readable by the model. Many of the efforts carried out at this level of integration have been either research projects investigating the use of GIS-generated parameters in hydrologic/NPS models or isolated watershed projects for identifying potential NPS pollution contribution and testing the effectiveness of BMPs. Most of the work in GIS/model integration has been done in this area (Maidment, 1993).

Needham and Vieux (1989) generated parameter values for the grid-based AGNPS model utilizing the vector-based PC ARC/INFO. A polygon coverage of square grids was created extracting the required parameter information from soils, land use/cover and topographic coverages. Wolfe and Neale (1988) generated input data for the distributed parameter HRU-based FESHM model utilizing the grid-base VIRGIS GIS. Hession and Shanholtz (1988) generated required input data from the VIRGIS GIS for a distributed parameter grid-based USLE-erosion/delivery ratio model to estimate sediment loading. Steube and Johnston (1990) used a GIS to

generate parameters required in the SCS CN method for estimating runoff. Rousseau et al. (1988) utilized PC ARC/INFO to calculate sediment and nutrient loading based upon the GAMES field-based network routing scheme.

2.2.4 Linking GIS and Hydrologic Models

Model linkage with GIS represents the improvement of a fragmented process of hydrologic parameter generation, parameter output and model simulation to a more integrated and "seamless" approach. The I/O procedures of the model are modified, eliminating the need to generate intermediate files. The relational attribute data structure of the GIS now directly provides data input parameters to the model. After the model is run, the GIS relational data base is appended with the output results. This level of GIS/model integration is considered a "toolbox" approach which enhances the functionality of the GIS (Saghafian, 1993). The GIS/model becomes a decision support tool for water resource planners and managers (Engel et al., 1993) whereby the user interacts with the software, creating and testing alternative management scenarios.

Examples of linking GIS with models include, Engel et al. (1993), who have integrated AGNPS with the GRASS GIS, and the Soil Conservation Service who is currently linking AGNPS and GRASS (Cronshey et al., 1993). Yoon et al. (1993) have integrated AGNPS and ARC/ORACLE, and Rewerts and Engel (1991) have integrated GRASS GIS with ANSWERS. Vieux et al. (1993) have integrated a grid-based rainfall-runoff model called **r.water.fea**, which utilizes the Green and Ampt equation for infiltration and a Finite Element solution to the kinematic wave for

overland and channel flow, with GRASS. The Corps of Engineers has developed a linkage between CASC2D (Saghafian, 1993), a grid-based watershed rainfall-runoff model which incorporates Green and Ampt infiltration and a diffusion wave overland and channel routing routine implementing finite difference solutions, with the raster-based GRASS GIS.

2.2.5 Hydrologic Modeling Inside GIS

Modeling hydrologic/NPS processes inside the GIS requires imbedding the hydrologic algorithms within the actual GIS code. The GIS routines and the model thus become one single compiled program. Maidment (1993) points out the limitations of such a linkage because the representation of time is not an explicit part of the GIS data structure. The representation of dynamic hydrologic processes with partial differential equations generates incremental changes in the characteristics of geographic entities, such as soil moisture content or the concentration of sediment in channel flow. A completely integrated GIS/hydrologic model would be able to record and display changes in the spatial distribution of hydrologic phenomena over time.

Because of this temporal limitation only static average annual or peak flow models employing closed form analytic or empirical-based equations can be represented within existing GIS (Maidment, 1993). Several of the more popular GIS systems; ARC/INFO, GRASS, ERDAS, have integrated into their programs simple grid algebra functionality. This enables the user to encode basic hydrologic equations into the GIS structure (ESRI, 1991). The parameter variables in the algorithms are directly linked to data from the GIS coverages. When the model runs, required

values, such as slope, soil erodibility and channel slope, are directly extracted from the GIS coverages.

2.2.6 Object-Oriented Linkage

Object-oriented linkage of GIS and hydrologic/NPS models represents a programming approach to developing a spatial decision support system (SDSS) (Loucks et al., 1985; Djokic, 1993) which incorporates the principles of Object-Oriented Programming (Aha et al., 1983). The SDSS consists of a graphical interface linked to a GIS, an expert system, numerical models, and utility software (Djokic, 1993). Hydrologic/NPS models are programmed so that the individual hydrologic processes are represented as objects. Objects can access both locational feature data from the GIS and non-locational data, such as reaction rates, from a data base (Maidment, 1993). Modeling a hydrologic system is accomplished by selecting and configuring the appropriate hydrologic processes (objects) in representing a particular watershed or basin. For example, a simple watershed can be represented by two overland flow objects joined to a channel runoff object which can then be joined to a reservoir object.

The development of SDSS utilizing object-oriented linkage to GIS has primarily addressed basin-wide hydrologic modeling, where the system is a complex structure of rivers reservoirs and diversions. Boyer (1993) describes a SDSS developed by the Bureau of Reclamation referred to as CALIDAD. One of CALIDAD's tasks has been to assist in the management of the Central Valley Project in California . 151 separate objects represented by 18 object classes were created to

represent the complex hydrologic structure of the Central Valley. The US Geological Survey is developing the Modular Hydrologic Modeling System (MHMS) based upon the Object-Oriented Approach (Leavesley et al., 1993). The computer tool will be used in evaluating alternative resource management policies in short and long term resource management plans. Djokic (1993) is developing a SDSS which utilizes the expert system Nexpert Object to integrate the Corps of Engineers' HEC-1 hydrologic model with the ARC/INFO GIS.

2.2.7 Required Hydrologic/NPS Parameter Data

The input parameters for hydrologic/NPS models are derived from a number of key physical features, including soils, land cover or land use, topography and channels. Once in digital GIS format, the feature coverages can be manipulated implementing GIS routines to generate the required model parameter inputs. The following sections discuss GIS manipulation of feature coverages for hydrologic/NPS model parameter generation.

2.2.7.1 Soils Coverage

Soils data required in hydrologic modeling are derived from USDA Soil Conservation Service county-wide soil survey maps. These maps exist at scales ranging from 1:15,000 to 1:20,000. The SCS in cooperation with the individual states are converting these hardcopy maps to digital format. This new digital spatial data base is referred to as SSURGO (USDA-SCS, 1991). Description of the soil physical and chemical characteristics associated with the mapping units is contained in tabular digital files called SOILS-5.

Hydrologic/NPS models that implement the CN method for estimating runoff, such as AGNPS (Needham and Vieux, 1989; Cronshey et al., 1993; Yoon et al., 1993; Engel et al., 1993), require a soils hydrologic group index (A,B,C,D) determined for a particular mapping unit, and an antecedent moisture condition. Hydrologic/NPS models incorporating physical-based infiltration equations (Vieux et al., 1993; Saghafian, 1993; Gao et al., 1993) utilize percent sand, silt, clay and organic matter for the soil mapping unit as determined from the SOILS-5 records. These GIS coverages are applied to empirical models (Rawls et al., 1983) for determining the required soil parameter values; saturated hydraulic conductivity, capillary suction, bulk density and porosity.

Soil coverages also supply the required data for estimating erosion. The soils mapping unit USLE K (soil erodibility) value is used in the USLE, MUSLE and RUSLE calculations. Physical-based soil erosion equations require information on soil particle size, which can be derived from the percent sand, silt, clay.

2.2.7.2 Topographic Coverages

Topographic information is a key input parameter required in hydrologic models. The influences of elevation change and the rate of change are crucial in representing water erosion and sediment transport processes (Moore and Nieber, 1989). The most common source of digital elevation data is the USGS DEM (digital elevation module). 7.5 minute DEMs are lattice representation of elevation heights based upon a 30-meter interval. Speight (1980) and Moore et al. (1991) have identified a number of topographic parameters that can be computed from DEM data,

with many of them required as input parameters to hydrologic/NPS models, including; aspect, slope, upslope slope, upslope area, upslope length, profile curvature, flow path length and catchment area.

Caution must be practiced in using DEMs for certain landscape topographies (Panuska et al., 1991). DEMs are generated utilizing interpolation methods with inherent levels of error. Panuska et al. (1991, p. 63) note "the accuracy with which a DEM represents the land surface depends on the accuracy and resolution, both horizontally and vertically, of the original survey data". Error in DEMs generated from interpolation of digitized contour lines can range from a maximum root mean square of one-half a contour interval to an absolute error no greater than two contour intervals (USGS, 1987). For a contour map with a 10-meter interval, the potential error ranges from 5-20 meters.

The complexity of erosion processes occurring in a variable micro-terrain of a hillside cannot be represented by DEMs at the resolution presently available. The developers of the RUSLE LS Factor (McCool et al., 1991, p. 4) state: "Slope may be estimated from contour maps having 2-ft contour intervals if considerable care is used". However, the minimum possible error contained in a DEM is several times larger than 2 feet. They further emphasize that: " Slope lengths estimated from contour maps are usually too long because most maps do not have the detail to indicate all concentrated flow areas". The limited resolution of available DEMs presents practical problems in generating physically representative hydrologic and erosion parameters for upland areas. Freezor's et al. (1989) integration of AGNPS

and ARC/INFO determined slope and slope length without enlisting DEMs. The dominant soil mapping unit was determined for each cell, and the associated percent slope reported in the SOILS-5 file was assigned to that cell. Slope lengths were determined from established look-up tables relating slope to a given slope length. Otterby and Onstad (1978) have developed these relationships for Minnesota.

2.2.7.3 Land Use / Land Cover Coverages

Most research into GIS/model linkage for hydrologic/NPS modeling has been carried out in research watersheds, where land cover information is generated from detailed surveys. However, delineation of watershed land use and cover and the determination of surface hydraulic parameters can be obtained from a number of sources. Olivieri et al. (1991) and Hamed and Engel (1993) incorporated Thematic Mapper (TM) satellite imagery, low level aerial photography was utilized in the study by Needham and Vieux (1988), and 1:100,000 scale USGS Land Use / Land Coverage digital coverages have been used by Hamed and Engel (1993) and Engel (1993). Event-driven hydrology/NPS models can use the information interpreted from "snapshot" images from satellites or photographs representing a given ground condition. Continuous simulation modeling requires information on changes in land cover and soils resulting from agricultural management practices and plant growth, including type and timing of cultivation and rates of chemical application. For NPS pollution modeling the timing and type of practice is crucial for accurately estimating the loading of NPS pollutants (Young et al., 1992).

2.2.7.4 Channel Coverages

Information on channel characteristics is required in modeling routing of runoff through a watershed. Channel length data in digital format can be obtained from the USGS DLG (Digital Line Graph) files at 1:24,000 scale. These stream lines, however, do not capture first order concentrated flow paths that can become critical sources of sediments during a rainstorm event (Moore et al., 1993). Terrain analysis procedures can process DEM data generating flow path networks as well as other topography-related parameters.

O'Callaghan and Marks (1984) established a set of techniques (D8) for determining topographic parameters such as drainage areas and flow path networks. Band (1986) and Jenson and Domingue (1988) have improved the techniques, making them more efficient. These DEM techniques are based upon determining a flow path direction by locating one of the eight neighboring lattice values with the largest elevation difference. A second weighting matrix is used to keep track of flow accumulations, assigning a weight of 1 to a receiving position and 0 to a non-receiving position. An accumulation matrix is derived from the weight matrix, summing up the weights of all elements draining into a given element. A streamline is represented by flow directions for those cells with upslope accumulated cell numbers greater than a user-selected threshold value. This terrain analysis procedure is incorporated into most GISs including ARC/INFO (ESRI, 1991).

In long, non-undulating and constant slope hillsides and flat, minimally sloped areas, the above technique tends to create parallel streamlines. A further limitation of

this technique is that it cannot represent convergence or dispersion in streamlines (Moore, 1993). A number of alternative terrain analysis procedures are used to overcome the limitation of the D8 method. Fairfield and Leymaire (1991) introduce a random variable to avoid the formation of parallel streamlines. In flat areas and constant sloping hillsides, streams will begin to converge, eventually forming one stream rather than multiple parallel streams. This method, however, does not account for flow divergence in upper slopes. Moore (1993) has modified the D8 and Fairfield and Leymaire method to account for catchment spreading. The branching from a single flow direction to multiple downslope lattice points and the partitioning of upslope contributing areas is achieved by a slope weighting procedure as forwarded by Freeman (1991) and Quinn et al. (1991).

Runoff routing modeling requires additional channel information beyond areal dimension of watershed and length of channels. Channel slope, cross-sectional area of the channel and hydraulic radius are needed in physical-based models. Channel slope can be approximated by overlaying a coverage of channel paths onto a DEM-generated land slope coverage. This method has been applied by most GIS/model linkages, including Needham and Vieux (1989), Olivieri et al. (1991) and Panuska et al. (1991). Caution must be practiced in using DEM-generated slope values for determining channel slope. The cross-width dimension of the narrow valley in which the small order streams flow may be less than the 30-meter resolution of the DEM. Channel dimension cannot be resolved by a DEM.

2.2.7.5 Grid Cell Representation

Distributed-parameter models require that the watershed be delineated into areas representing homogeneous physical properties. The previous section presented a description of different types of spatial delineation that have been applied in hydrologic and NPS modeling. A GIS can facilitate the process of computational unit delineation and the determination of a representative physical property (Vieux et al., 1989). The following discussion will pertain to one particular unit delineation; a grid cell. The grid-cell unit is the method of delineation used in the ANN-AGNPS model and is the most common representation in those models linked to GIS (Engel, 1993).

Reducing the computational unit's cell size will reduce the variability of physical features within the boundaries of the cell and better represent the spatial variability of features across a watershed. Less internal variability ensures a more representative parameter value from the computational unit and a truer representation of relative feature location throughout a watershed. A truer representation of actual features in the model input parameters is assumed to lead to better model results. There are, however, tradeoffs in decreasing cell size. A smaller cell size requires additional data be collected, manipulated, stored and processed. Selecting a grid-cell size for generating input parameters requires carefully weighing needed accuracy in result output against the amount of data compilation and computer processing (Vieux and Needham, 1993).

Panuska et al. (1991) found that grid-cell size will influence the determination of several key parameters used in hydrologic/NPS modeling, including upslope

contributing areas and maximum flow path length. They concluded that the small cell size generally characterizes terrain variability best, therefore application of a smaller grid-cell size is desirable when representing a crucial hydrologic parameter such as flow path length. Vieux and Needham (1993) reiterated these findings by demonstrating the influence of cell size and related flow path length on sediment loading for the AGNPS model. By varying cell size, they determined that of all the hydrologic parameters, sediment loading was most sensitive to flow path length. Freezor et al. (1989) compared cell size changes for 4, 16, 64 and 256 acres against a one-acre base cell size also utilizing the AGNPS model. They found that the four-acre cell best approximated the values generated with the base one-acre cell, and that an increasing cell size increased the difference between the various output results.

CHAPTER 3

WATERSHED DESCRIPTION

The USDA-Agricultural Research Service (ARS) supported research watershed (Moyer watershed) is located 19 miles south of Morris and 15 miles west of Benson, Minnesota within Swift County (Figure 1.1). The watershed includes parts of sections 33, 34, 35 of Fairfield Township as well as parts of sections 2, 3, 4 of Moyer Township. The watershed is comprised of 1076 acres of private farm land, with 8 different operators farming 22 separate fields.

The 8 operators were first contacted during the winter and spring of 1992. Permission was obtained for setting up gauging and sampling equipment, and for surveying hillside topography and channels. Most of the operators were willing participants in the study, freely providing field management information. A few, however, were more reluctant, and did not provide field management information. A further constraint of working on private lands was the inability to place weir structures within the concentrated flow channels. Alternative and less accurate channel measurements were made to be used in channel flow calculations.

The physiogeographic characteristics of West-Central Minnesota and of Moyer watershed, which include topography, soils, and drainage networks, are a product of its glacial history. The Mankato Substage of the Wisconsin Glaciation covered the region during the last glacial episode. 8,000 years ago, the glaciers began receding,

leaving behind a thick mantle of glacial drift. Melt waters flowing from the glaciers modified drift into lacustrine and outwash deposits. Terminal moraines are found scattered across the landscape creating the region's only form of local relief.

The Moyer watershed is an amphitheater-shaped impression cut by erosional processes into the south side of the Bigstone Moraine. Overland flow concentrates into a number of natural channel flow depressions and artificial drainage networks running through fields and along road embankments. The overall topography of the watershed is represented by gradual overland flow slopes intersected by steeper short slopes descending into concentrated flow paths. Overall watershed slopes decrease from upland portions of the watershed towards the watershed outlet, where the land is nearly level. Also, interspersed throughout the watershed are local areas of low-slope to flat land.

Slopes within the watershed range from 0 to 6.8% with a weighted average slope of 1.9%. A breakdown of the slope classes, as determined from a GIS-generated 30-meter DEM elevation lattice, is as follows: 0-1% 285 acres, 1-2% 318 acres, 2-3% 256 acres, 3-4% 138 acres, 4-5% 63 acres, 5-6% 15 acres and 6-7% 2 acres. Figure 3.1a displays the spatial distribution of slope classes. Figure 3.1b displays the concentrated flow paths for both natural and artificial channels, dividing channels into grass and soil-based. Also shown are contour lines from the 7.5 minute USGS topographic quad. sheet.

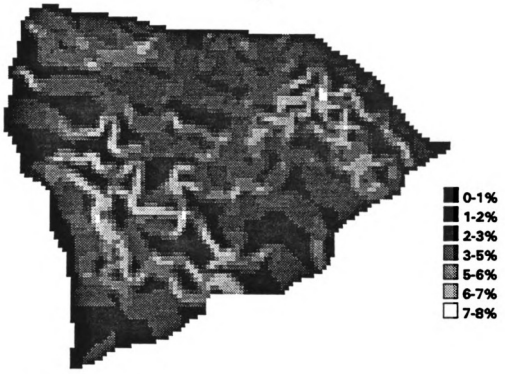

Figure 3.1a Percent Slope

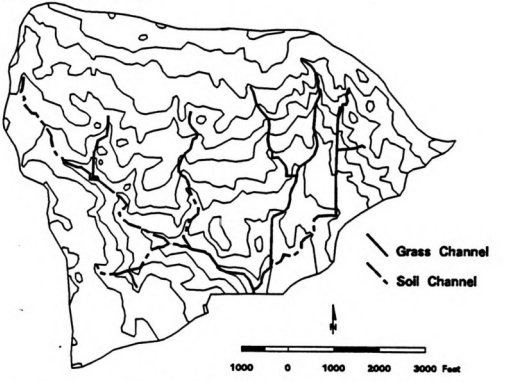

Figure 3.1b Concentrated Flow Paths and Contour Elevation Lines

Soils within the Moyer watershed are a direct product of the glacial till, forming the fundamental parent material comprising the terminal moraine. These soils represent a range of textures based upon topographic location and parent material. The vast majority of soils are a Barnes-Buse series complex derived directly from calcareous loam glacial till. Barnes-Buse complexes are located throughout the upper reaches as well as interior ridges and knolls. Porosity of this complex is relatively high in these larger textured loam soils. Erosive potential for these soils is also relatively high. Continuous farming practices have caused erosion resulting in exposure of parent calcareous materials on small-scale ridges and knolls. Soils forming within the flatter depressional areas along-side concentrated flow channels are primarily Parnell series soil. These soils are derived from materials transported from upland Barnes-Buse complexes. Parnell soils are comprised of small silts and clays with very low porosity. Topographically and structurally between the Barnes-Buse and Parnell soils are the Tara and Hamerly soils series. These soils have been formed from eroded silted materials deposited on top of flatter areas of glacial till. Porosity characteristics are intermediate between Barnes-Buse and Parnell. Table 3.1 lists the soils mapping units and acreage as found in the Moyer watershed. Figure 3.2a displays the spatial distribution of the soil mapping units. Appendix A contains the detailed descriptive soils data derived from SCS's SOILS-5 data base.

The weather of West-Central Minnesota is representative of a Northern Plains Continental climate. Non-growing season winter temperatures for Morris, MN range from an average high of 31 degrees F to an average low of 11 degrees F between the

months of November and March. A 50 percent probability exists that a frost will occur in spring later than May 15 and a 50 percent probability that a frost will occur in the fall earlier than September 25. Snow accumulations vary significantly from year to year, with an average accumulated snowfall of 29 inches and maximum snowfall occurring in March. The average number of days with more than 1 inch of snow on the ground is 98.

Table 3.1 Soil Mapping Units in Moyer Watershed

Map Symbol	Mapping Unit	Acres
BaA	Barnes loam, 0-2%	11
BbB2	Barnes-Buse loams,2-6%	661
BbC2	Barnes-Buse loams, 6-12%	2
BuB2	Buse-Barnes loams, 2-6%	26
D1B	Doland silt loam, 2-6%	9
HdA	Hamerly loam, 0-3%	27
HhA	Hantho silt loam, 0-2%	1
Pa	Parnell silty clay loam	9
Pf	Parnell and Flom soils	150
SuA	Svea loam, 0-2%	60
SuB	Svea loam, 2-4%	3
TaA	Tara silt loam, 0-2%	111
Va	Vallers-Winger silty clay loams	6

Growing season months experience warm temperatures and humid conditions. During this period maximum average temperatures are 73 degrees F and minimum average temperatures are 48 degrees F. The length of the growing season is 138 days given the 50 percent probability level of spring and fall frost. Seventy-five percent

of the precipitation falls during the growing period. The early summer months of May and June receive a large percentage of rainfall from thunderstorms. The percentage of rain attributed to thunderstorms declines in July and again in August. Table 3.2 provides the average monthly and average annual temperatures and precipitation for Swift County (USDA-SCS, 1973).

Table 3.2 Climate Summaries for Morris, MN

Month	Ave Max Temp (F)	Ave Min Temp (F)	Ave Total Precipitation (in)
January	23	2	0.7
February	27	5	0.8
March	38	18	1.3
April	56	33	2.2
May	70	45	2.8
June	79	55	4.1
July	86	60	2.8
August	83	58	3.6
September	74	48	2.0
October	62	36	1.4
November	41	21	1.1
December	28	8	0.8

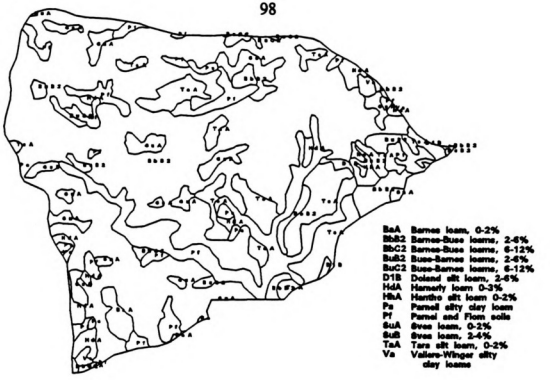

Figure 3.2a Soil Mapping Units

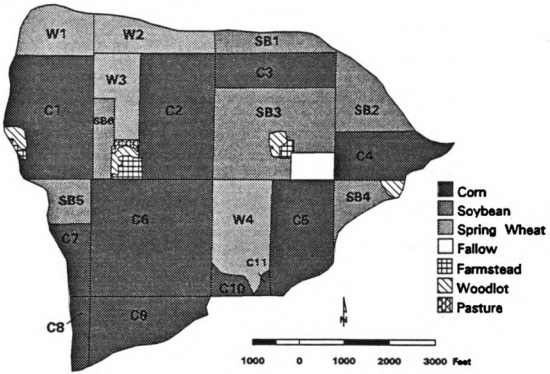

Figure 3.2b 1992 Crops

The major crops grown in West-Central Minnesota are corn, soybeans and small grains which include spring wheat, barley and rye. The Moyer watershed reflects this regional cropping pattern. Within the watershed, 634 acres of corn, 232 acres of soybeans and 173 acres of spring wheat were planted during the 1992 growing season. Also included in the watershed are 15 acres of tree shelters, 10 acres of fallow fields, 10 acres of homestead/barnyard area, and 3 acres of pastures. The spatial distribution of 1992 crops is presented in Figure 3.2b.

Agronomic and conservation practices vary greatly based on the preference of the individual farmer. Normally, fall tilling follows harvest for incorporating plant residues into the soil as a method to protect soils from wind and water erosion as wellas increase infiltration for recharging soil moisture levels. Fall tilling is also preferable on less permeable soils in low-lying areas. Spring tillage in these areas is difficult due to wet soil conditions from snow melt and heavy rains. In areas with increased slopes, fall tillage is sometimes skipped to avoid runoff and soil erosion occurring in the early spring months from snow melt and heavy rains.

The research watershed reflects the diversity of farming techniques practiced throughout the region. For the 1992 season, certain fields were fall tilled while others were first tilled in the spring. The selection of tillage implements also varied. Some farmers used disk tills while others tilled with cultivators. The implementation of most operations, including tillage, planting, fertilizer and pesticide application, however, occurred approximately during the same weeks of the year. Appendix B contains the description and timing of management practices for 1992 as well as for

the previous year.

CHAPTER 4

RESEARCH METHODS

The research is divided into two separate but connected phases for testing the stated research hypotheses. The first phase investigates the two methods of generating data input parameters for the ANN-AGNPS model. These methods are: (1) map interpretation and reconnaissance field surveying, and (2) GIS techniques, as developed for this research. The second phase of the research is concerned with testing the predictive capabilities of the ANN-AGNPS model utilizing the map interpretation- and field surveying-generated parameters. Model-generated results for runoff volume, peak runoff flow, sediment loading and soluble Total-Nitrogen loading will be compared to data collected from the watershed for two storm events.

This chapter is split into four main sections. The first section will detail the two techniques for model parameter collection and generation, and present the derived information. The second section will describe the experimental design and techniques for collecting model verification data, and present the collected data. The third section provides a detailed mathematical description of processes modeled by the ANN-AGNPS model not covered within the literature review chapter. The final section of this chapter will describe the analytic techniques employed for testing the two research hypotheses.

4.1 Model Parameter Data Collection and Generation

Generating parameter input data for ANN-AGNPS is a two-step process. The first step requires delineation of the watershed into grid cell-based computational units. The grid sizes chosen for this study are 40 and 10 acres. The second step is to identify a single parameter value to represent the "on-the-ground" physical and agronomic characteristics. Both steps are required by the two parameter generation methods assessed in this study, map interpretation and reconnaissance field surveying, and GIS techniques.

4.1.1 Map Interpretation and Reconnaissance Field Surveying

Map interpretation and reconnaissance field surveying represent the conventional method of gathering parameter input data for NPS water pollution modeling and are usually employed by conservation planners. Readily available topographic and soils maps together with aerial photography are interpreted for determining a base-line set of model parameter values. Follow-up reconnaissance field surveys are then undertaken to verify and adjust the map-generated parameters. Map interpretation and field surveying carried out for this research are representative of the effort a conservation planner could give to one project. The survey undertaken for this research, therefore, does not represent a scientific data gathering effort. Rather it was a cursory check relating map-generated parameters to the landscape's physical characteristics. If considerable divergence was found between map interpretations and field survey, map interpreted parameter values were changed to observed recordings.

Field surveying consisted of measuring slopes and slope length for only topographically steeper areas in the watershed that were assumed to be more highly erodible. Map-generated parameters for channel length, channel slope and channel side slope were field-checked by walking the major channels identified on the USGS quad. sheet and recording lengths and slope by pacing and surveying. Field management information was obtained through informal interviews with the farmers and/or observation of practices in the fields. The field management information required by the ANN-AGNPS model includes type and timing of field operations. Field management practices are presented in Appendix B.

Manually delineating a grid cell framework is accomplished with the use of a USGS 7.5 minute quad. sheet. For the Upper Midwest, a large-scale grid delineation exists on these maps in the form of roads and field boundaries conforming to the 640 acre-section. Sections can be quartered until the desired size cell is achieved. Using the existing public survey boundaries as a framework for grid delineation is advantageous because grid cells line up with field boundaries, thus enabling better ground representation. Once the area encompassing and surrounding the watershed is gridded, only watershed grid cells are retained for parameter data collection. The AGNPS Users' Guide (Young et al. 1989) suggests that grid cells with one-half or more of their area within the watershed should be retained. Figures 4.1a-b display the grid cell representation of the watershed for 40 and 10 acre grid cells.

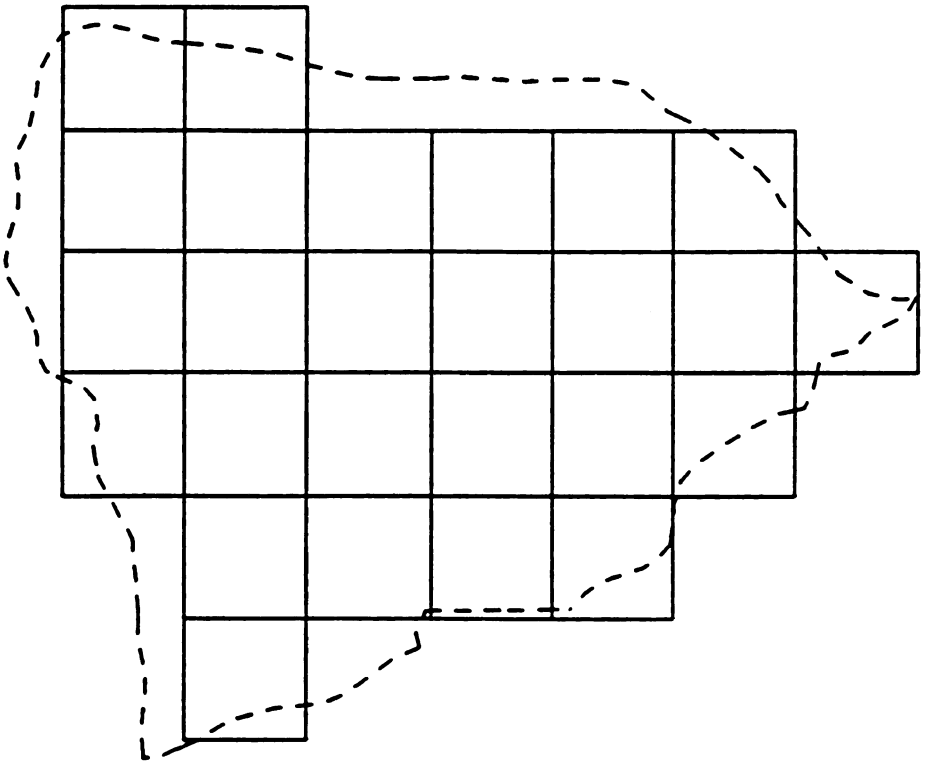

Figure 4.1a 40 Acre Interpreted Watershed Grids

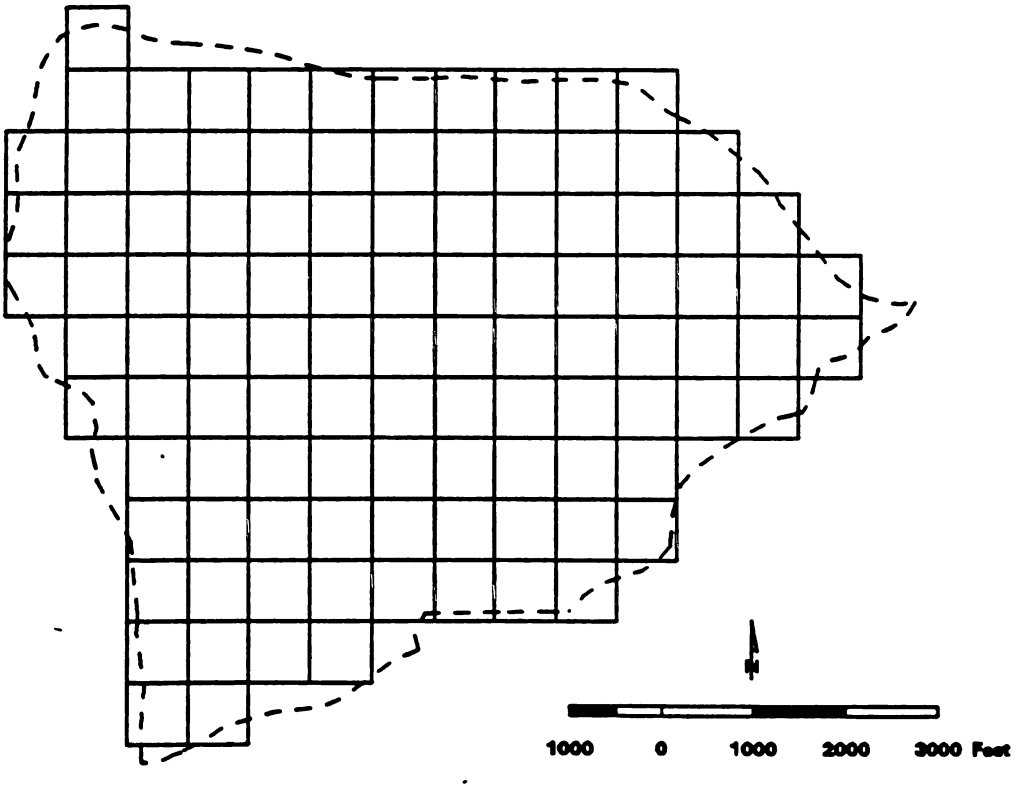

Figure 4.1b 10 Acre Interpreted Watershed Grids

The physical and agronomic information required as parameter data input into the ANN-AGNPS model can be divided into four basic feature classes: (1) land cover/land use, (2) soils, (3) topography, and (4) channels. These four classes of information can be determined from three basic sources of available data as well as field surveys. The sources used in this project include: (1) aerial photography; 1:40,000 scale National Aerial Photography Program (NAPP) (April 28, 1991), (2) USDA-SCS 1:16,000 Soil Survey of Swift County (1973), and (3) USGS 7.5 minute 1:24,000 scale Hancock SW topographic quadrangle (1968).

These maps represent a primary source of information for generating model parameters. The follow-up field survey is a needed second level of parameter verification. The information source of ANN-AGNPS parameter values associated with each feature is given in Table 4.1. As can be noted from the table, most map-derived parameter values required a field survey validation.

The four feature classes represented in the three data sources can be defined as either area-based or linear-based geographic elements. The two elements require different techniques for extracting parameter data from the map sources. Soils and land use maps are representative of parameters derived from area-based elements, and channel and hillside slope information is representative of linear-based element data.

Table 4.1 Information Sources for ANN-AGNPS Parameters

	Aerial Photo.	County Soils Survey	USGS 7.5 min. Quad. Sheet	Field Survey
Receiving Cell			X	
Flow Direction			X	
Land Cover/Use	X			X
Hillside Slope			X	X
Hillside Slope Length			X	X
Soils Mapping Unit		X		
Channel Slope			X	X
Channel Side Slope				X
Channel Length			X	X
Manning Coeff.	X			X

For area-based features, the dominant map characteristic within the cell becomes the single parameter value used as input into the model. A simple "dot-counting" method was enlisted to determine attribute dominance when a large degree of spatial variability existed. The dominant field or soil mapping unit was chosen for a cell by superimposing a lattice of points onto the land cover/land use and soils maps, then selecting the field or soil mapping unit with the largest number of points. Figures 4.2a-b and 4.3a-b show 40 and 10 acre cell size superimposed onto soil maps and aerial photographs. Once a soils mapping unit is identified for the cell, soil descriptive information is required as input to the model. Soil descriptive data can be located in either the USDA-SCS Soils 5 sheets available at the county SCS office or

from the county soil survey. Field management information must also be obtained for each of the identified cells. This type of descriptive information can be obtained through observation, farmer interview or questionnaires, or through the use of locally representative practices.

Linear attributes are determined by first identifying the spatial extent of the feature, then measuring the vertical distance and horizontal difference between the established end points. Information required in linear measurements is derived from the USGS quad. sheet as shown in Figures 4.4a-b for 40 and 10 acre cells.

Estimating a representative hillsides' percent slope requires interpreting contour line crenulation to determine the ridgetop beginning of the slope and its termination in a gully depression. The horizontal distance between the beginning and ending point is divided into an estimated elevation difference. An elevation contour interval of 10 feet does not provide sufficient vertical resolution to determine an accurate elevation. Considerable interpretation is thus required, and error of up to 10 feet in the vertical direction is possible.

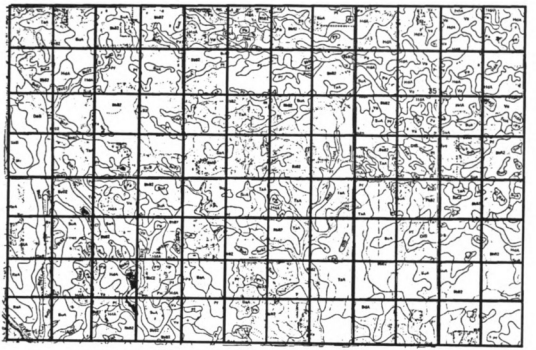

Figure 4.2a 40 Acre Grid and Soil Mapping Units

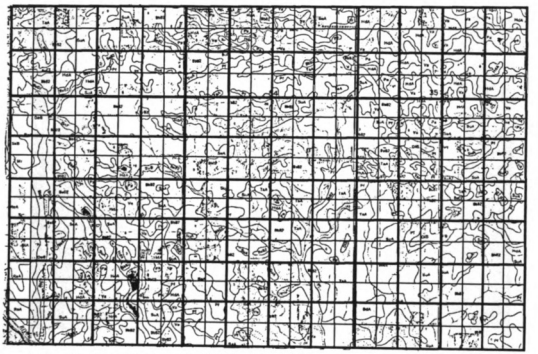

Figure 4.2b 10 Acre Grid and Soil Mapping Units

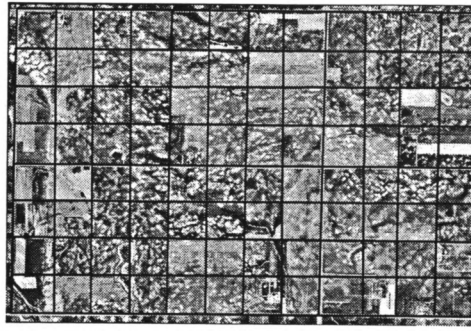

Figure 4.3a 40 Acre Grid and Aerial Photograph

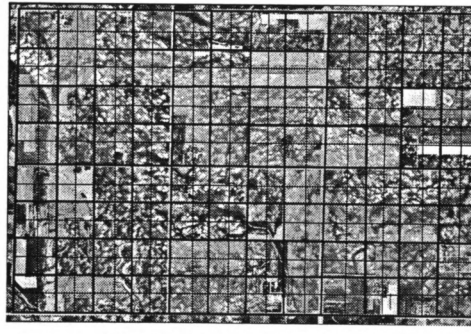

Figure 4.3b 10 Acre Grid and Aerial Photograph

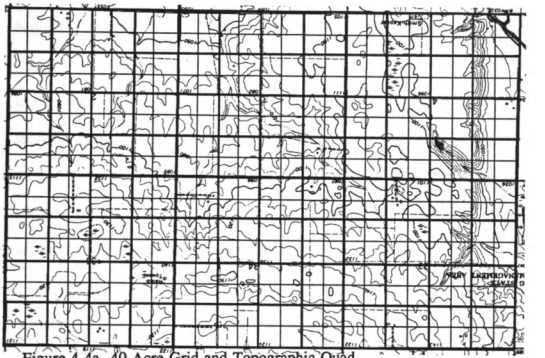

Figure 4.4a 40 Acre Grid and Topographic Quad.

Figure 4.4b 10 Acre Grid and Topographic Quad.

Channel lengths are measured directly off the topographic map with the beginning and ending measurement points located at the grid cell edge. Channel slopes are calculated by dividing the difference in elevation from one end of the cell to the other by the channel length. For those cells without a mapped channel, channel length is calculated as a straight-line distance across the cell based upon the flow direction into and the flow direction out of the cell. This is the channel length method enlisted in the AGNPS model (Young et al., 1989). Channel slope is assigned a value of one-half the hillside slope.

Flow direction and receiving cell parameter data are also generated using contour and channel lines off the quad. sheets. Channel network lines determine the direction of flow and the receiving cell. However, if a cell does not contain a channel, elevation contour lines must be evaluated to determine the dominant flow direction as well as the cell which receives the flow. Multiple channels may exist within a cell. The primary flow direction and receiving cell are represented by the channel with the largest drainage area.

The final input parameter values developed through map interpretation and reconnaissance field surveying are presented in Appendix C Table C1 for 40 acre cell size and Table C2 for 10 acre cell size.

4.1.2 GIS-Interface Program

A GIS-interface to the ANN-AGNPS model was developed for this research project. It allows resource planners with no previous GIS experience to interact with available digital coverages in generating input parameters to the ANN-AGNPS model.

The GIS-interface consists of a set of base menus, data specific "pop-up" menus, and a graphical display window, that lead the user in entering descriptive parameter input data, running GIS processes, and editing GIS-generated parameter results. The interface program was written in ARC/INFO's Automated Macro Language (AML). AML is a high-level script language which integrates ARC/INFO command line routines with the UNIX graphical user interface.

The GIS-interface program processes the same base maps as utilized in map interpretation procedures, however, in a spatial digital format. The digital coverages used in the GIS-interface program include: (1) a 10 ft resolution scanned NAPP photograph, scanned at 300 dots per inch, (2) a digital coverage of the USDA-SCS soils mapping units from the county soil survey, (3) a digital coverage of elevation contour lines, (4) a digital coverage of USGS intermittent streamlines, and (5) a digital coverage of section lines.

Pre-processing of the digital elevation contour lines was needed to convert the digital line format data into raster format data whereby the GIS capabilities were used to delineate the watershed boundary. The contour lines were first converted to an intermediate TIN (Triangulated Irregular Network) coverage, the TIN coverage was then converted to a lattice of elevation heights (DEM) with a 90 ft resolution. As a DEM, the topographic information was processed with raster-based techniques for calculating flow directions and flow accumulation. This information was in turn used to delineate the watershed boundary. The spatial resolution of the DEM in horizontal and vertical dimensions determines the shape the watershed boundary assumes. Major

differences in both the shape and area occur between the GIS-generated and the visually interpreted boundaries. Tables 4.2, 4.3, 4.4 list the differences in area for feature classes of crops, soils and slopes between the visually interpreted and the GIS-generated watershed boundaries. Figures 4.5a, 4.5b, 4.6a and 4.6b demonstrate the basic map features clipped to the GIS-generated watershed boundary for percent slope, flow paths, soils and crops respectively.

Table 4.2 Soils Acreage Difference

Map Symbol	Acres in interpreted watershed boundary	Acres in GIS-generated watershed boundary	Acre difference
BbB2	660.2	651.6	8.6
SuA	58.8	63.0	4.2
Pf	150.4	137.6	12.8
BuC2	4.2	3.7	0.5
TaA	110.3	99.8	10.5
HdA	27.1	26.3	0.8
Pa	7.7	6.4	1.3
Va	5.6	3.2	2.4
BuB2	25.5	21.8	3.7
D1B	9.6	3.1	6.5
SuB	3.1	2.7	0.4
HhA	0.9	0.9	0
BbC2	1.6	1.6	0
BaA	11.0	10.6	0.4
Total	1076.0	1032.3	43.7

Table 4.3 Crop Acreage Difference

Crop	Acres in interpreted watershed boundary	Acres in GIS-generated watershed boundary	Acre difference
Corn	632.9	575.1	57.8
Soybeans	231.2	256.4	25.2
Wheat	171.6	162.6	9.0
Fallow	13.4	13.4	0
Farmlot	9.8	10.1	0.3
Woodlot	14.3	12.0	2.3
Pasture	2.6	1.6	1.0
Total	1076.0	1032.2	43.8

Table 4.4 Percent Slope Acreage Difference

Percent slope	Acres in interpreted watershed boundary	Acres in GIS-generated watershed boundary	Acre difference
0-1	274.4	251.8	22.6
1-2	316.6	294.4	22.2
2-3	254.3	262.3	8.0
3-4	138.6	140.4	1.8
4-5	64.2	65.0	0.8
5-6	16.0	16.1	0.1
6-7	11.9	2.3	9.6
total	1076.0	1032.3	43.8

Figure 4.5a Percent Slope

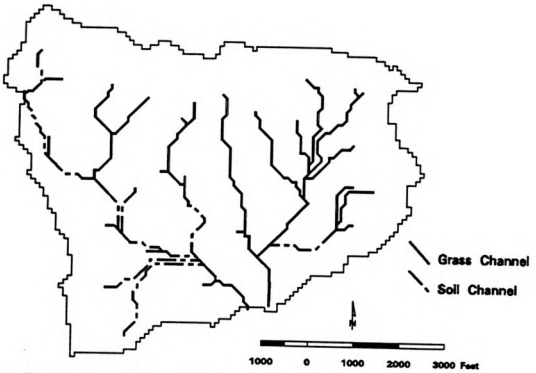

Figure 4.5b Concentrated Flow Paths

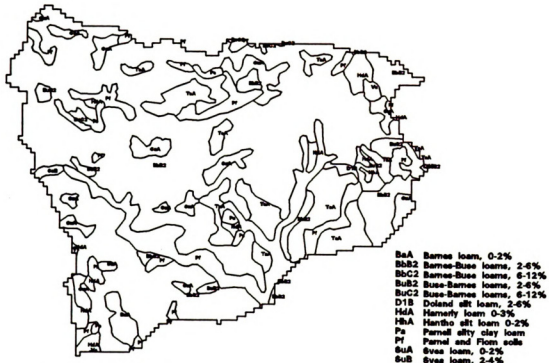

Figure 4.6a Soil Mapping Units

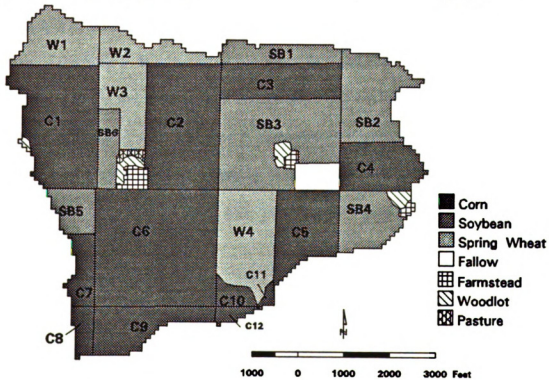

Figure 4.6b 1992 Crops

The GIS-interface program creates a grid structure in the same way it would be done by hand. The program identifies a section corner south and west of the watershed and then generates a grid structure based upon the selected cell size. Quartered derivatives of the 640 acre cell size will best represent ground information, as mentioned above. The GIS then determines which cells have one-half or more of their area within the watershed. Figures 4.7a-b show the grid configuration for the GIS-generated watershed boundary.

Based upon the chosen grid cell size and spatial placement of the cell within the watershed, the GIS-interface program determines a single parameter value for the area-based fields and soils digital coverages by converting the polygon (arc-node) format coverages into a raster-based format. The GIS operation utilizes the same basic principle of dominant area attribute in assigning a single value to the grid cell. A portion of the Soils-5 tabular digital file was subset and entered into the INFO data base. After a single soil mapping unit is determined for a grid cell, a relational link between the grid and the soils data base is automatically created by the program. The GIS-interface program provides the capacity to update soil data. Figure 4.8 shows the interface program screen for selecting and updating soils data on a cell-by-cell basis.

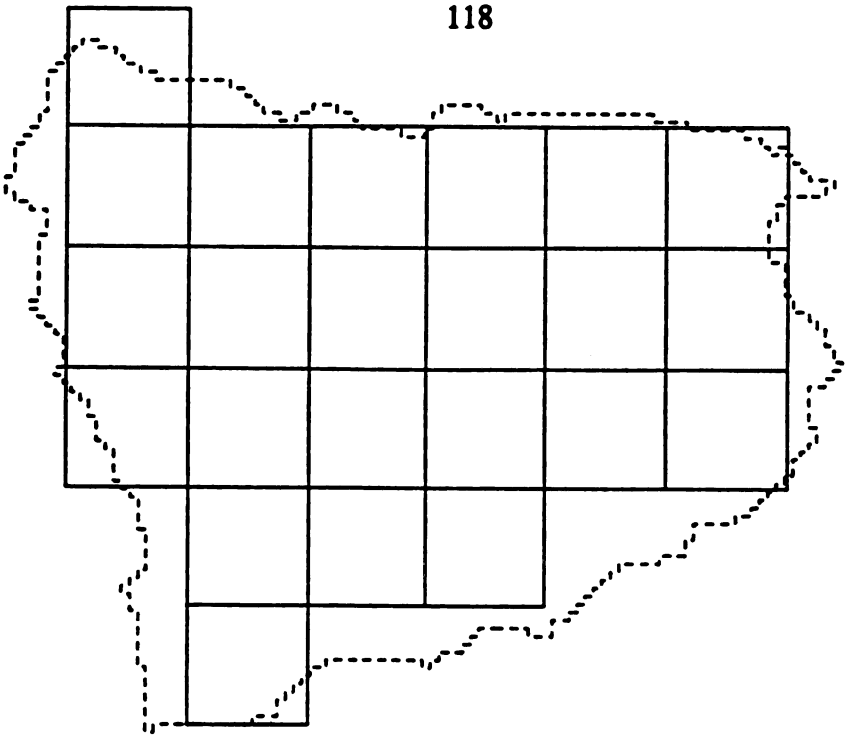

Figure 4.7a 40 Acre GIS-Delineated Watershed Grids

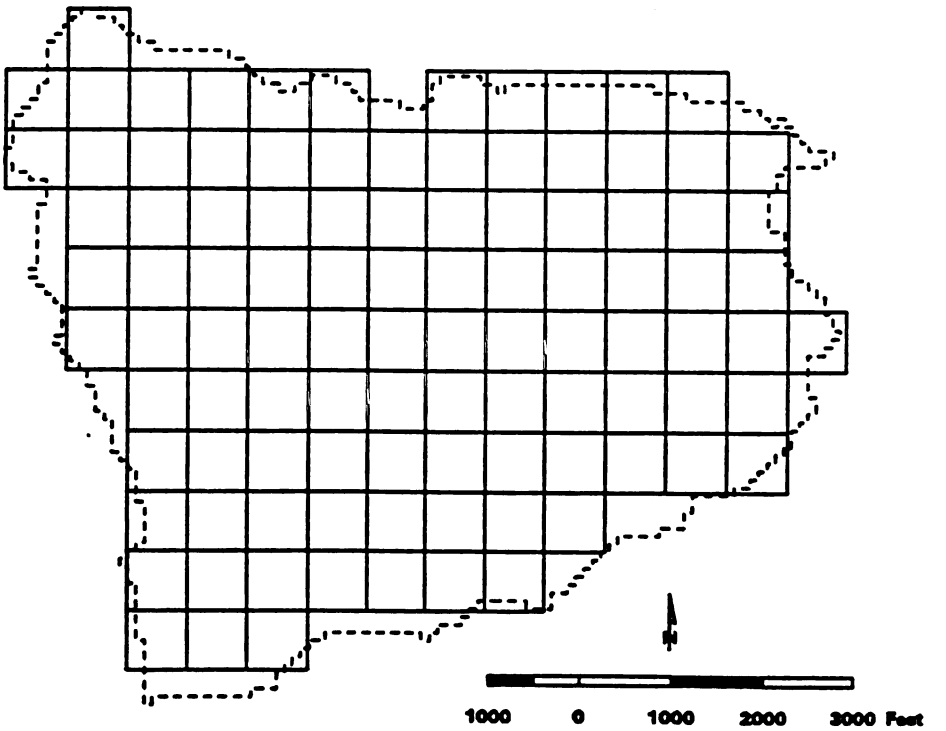

Figure 4.7b 10 Acre GIS-Delineated Watershed Grids

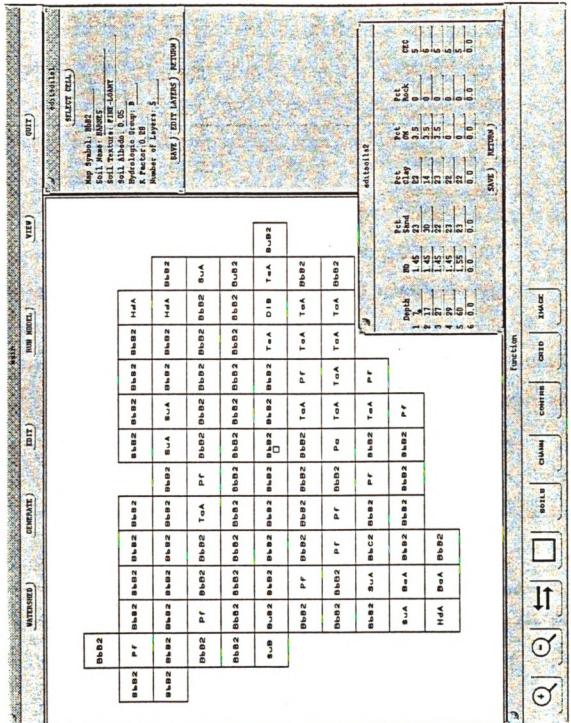

Figure 4.8 Soils Mapping Unit Parameter Input and Edit Screen

The most extensive parameter input requirements of the ANN-AGNPS model are with the description of type and timing of field implements. The GIS-interface enables the model user to input this information on a field-by-field basis by providing menu interfaces for selecting a field and entering the field operations. Figures 4.9 through 4.15 display the menu interfaces which guide the user in developing field management scenarios.

Field management input begins by selecting a field for entering field operation data (Figure 4.9) and allowing the user to input owner/operator names associated with the particular field. The user then has the options of creating a new field management scenario, assigning an existing scenario to the field, editing an existing scenario for the field, or viewing the scenario. If a field management scenario is to be created or edited, a new set of menus are displayed which lead the user in entering the required parameter data describing field practices. Figure 4.10 displays the information required for determining the conservation practice used and the crop grown within the present growing season. Presently, the GIS-interface does not support the entry of conservation practice parameters. Further, the number of crops that can be entered into the program is limited to one. These limitations reflect the fact that in the research watershed no contour plowing or terracing occurs, and the model is being run for only one growing season.

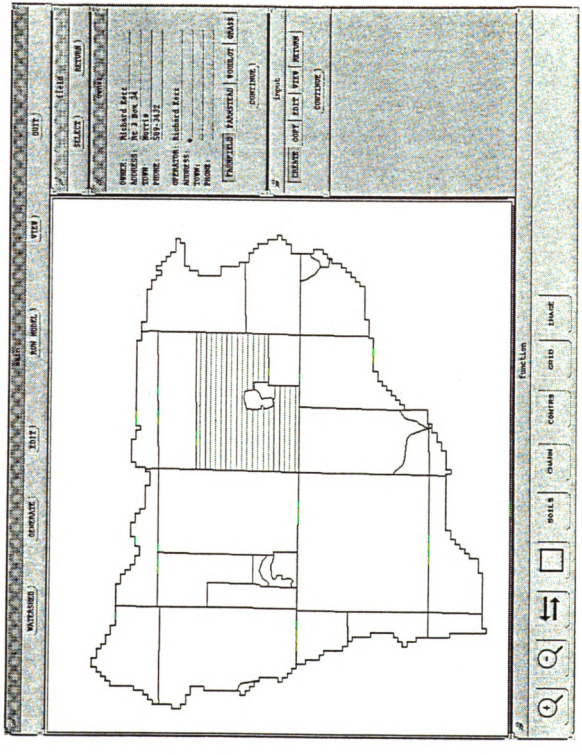

Figure 4.9 Field Selection and Identification Screen

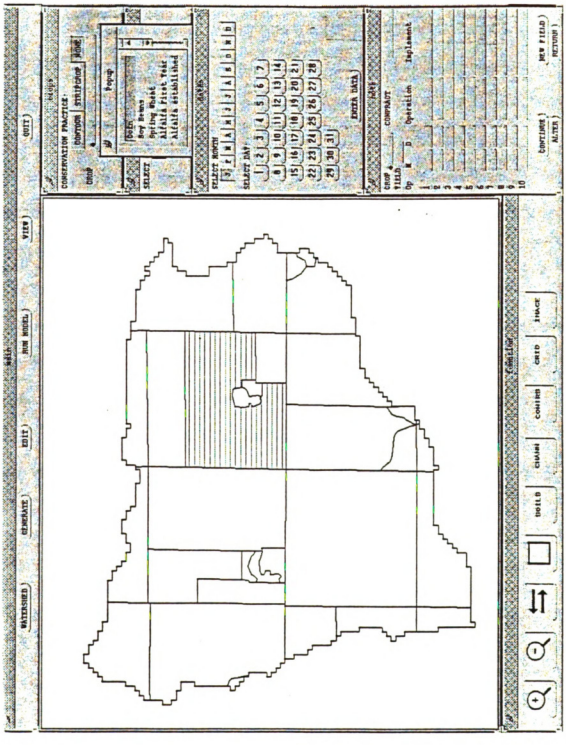

Figure 4.10 Conservation Practice and Crop Selection Screen

The next computer screen displayed by the GIS-interface is for selecting a particular field operation (Figure 4.11). A user begins building a field management scenario with the first practice after the last harvest. For most of the fields in the watershed this is a fall tillage practice. After selecting the operation type and implement, the user enters the date on which the practice occurred. Figure 4.12 presents the calendar for selecting a month and a day. In addition to tillage operations, planting, fertilizing (Figure 4.13) and harvesting (Figure 4.14) operations can be selected, and the associated implement, application rate and yield can be entered. The last operation of a scenario is a harvest. After it has been selected, the field management scenario is saved for the current field. The newly created field operation scenario can also be saved as an independent scenario, which can then be copied to any selected field. Independent scenarios as well as field-specific scenarios can be edited. The program allows the user to select a particular operation and change the implement, date or operation type. Further, a new operation can be added to the scenario (Figure 4.15).

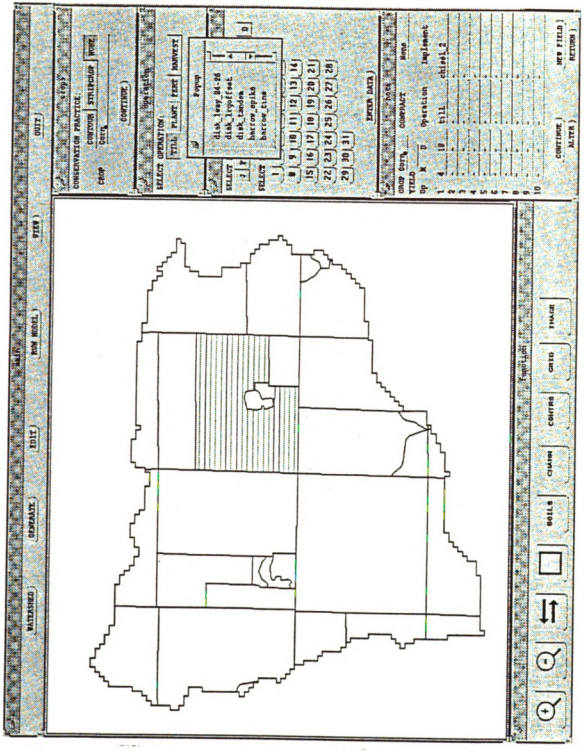

Figure 4.11 Tillage Implement Selection Screen

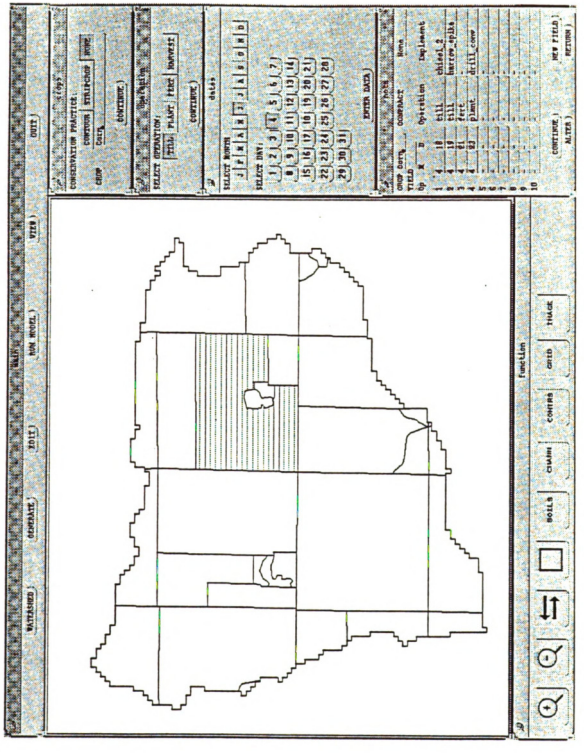

Figure 4.12 Calendar Dates Selection Screen

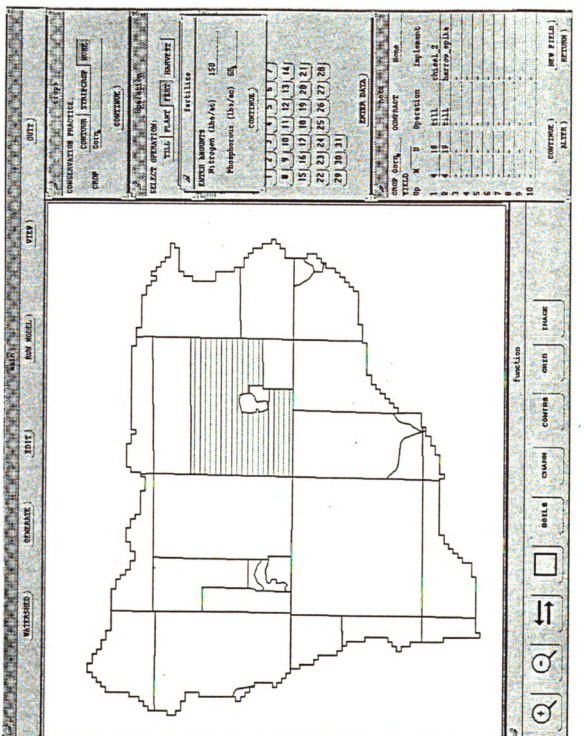

Figure 4.13 Fertilizer Selection Screen

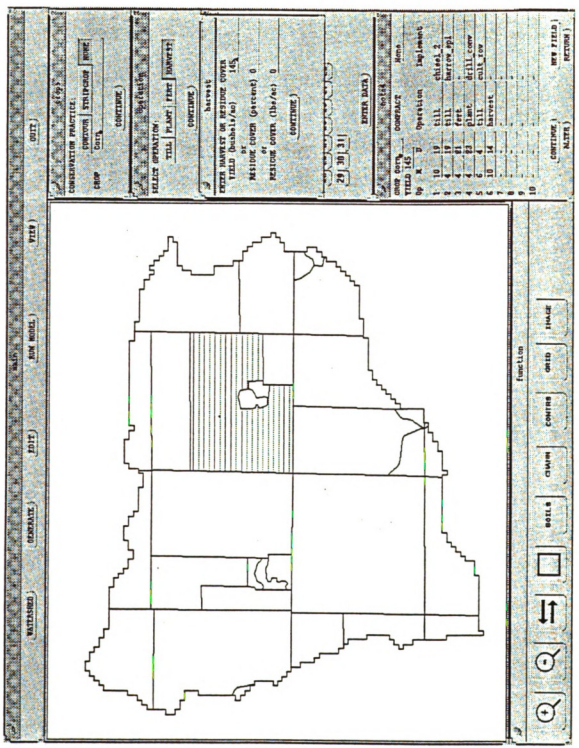

Figure 4.14 Harvest Yield Selection Screen

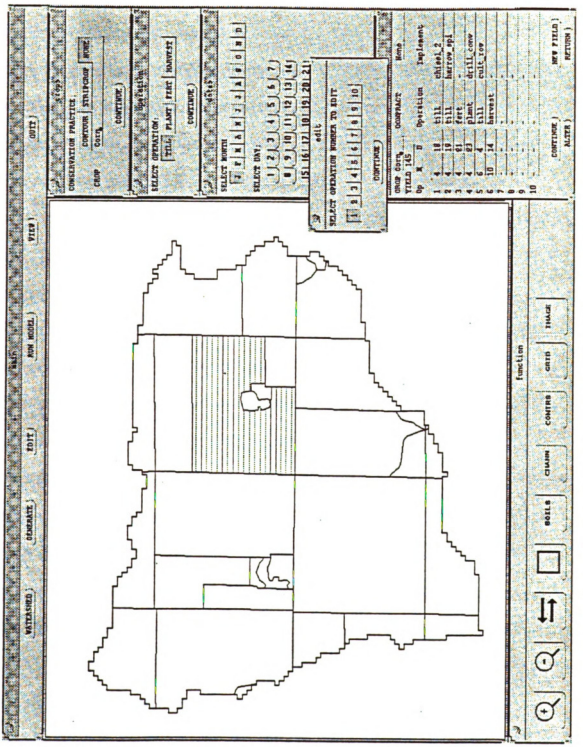

4.15 Operation Edit Selection Screen

Three separate program subroutines calculate model parameters for linear-based features of hillsides and channels as well as flow directions and receiving cells. Slope calculations are performed on the generated DEM utilizing ARC/INFO's grid routines. The slope routine determines a slope value for each of the 90-foot grid cells by identifying the largest elevation difference between a cell and its eight neighbors. The vertical difference is then divided by the length of one cell; 90 feet.

The 90-foot resolution slope grid is resampled to the selected grid cell size, 40 and 10 acres. The resampling technique employed is a bilinear interpolation which determines the value of the new cell, based upon a weighed distance average of the four nearest input cell centers. The resampling process is iterative until the desired cell size is reached. A routine for determining a slope length appropriate for input into the RUSLE erosion model was not developed due to the lack of horizontal and vertical resolution of the 90 ft. DEM. Slope lengths were determined based upon the percent slope/slope length association tables developed for Minnesota by Otterby and Onstad (1978). Figure 4.16 shows the GIS-interface screen for editing slopes and slope lengths after they have been generated. GIS-generated hillside parameters will not be edited, in order to compare GIS-generated parameters with the map interpretation/field survey parameters.

Channel parameter data is generated with the GIS-interface program by enlisting several different types of raster-based manipulation routines. The watershed's cells are first divided into three separate surface flow regimes; permanent channel flow, ephemeral gully flow and overland rill flow. Permanent channel flow

areas are represented by those grid cells that are intersected by a streamline represented in the USGS 7.5 minute quad. sheet. These channels are assumed to be permanent and relatively stable features within the watershed landscape, not altered by tillage operations. The ephemeral gully flow is represented by those grid cells where concentrated flow is likely to occur in non-permanent gullies. These are gullies created throughout the year through erosional processes. However, they are obliterated by tillage practices. In order to determine the extent and location of these ephemeral gullies, a stream network was generated using terrain analysis procedures as outlined by Jensen and Domingue (1988) and incorporated into ARC/INFO's GRID routines. The upland cumulative contributing area size selected was 5 acres. This represents the overland flow area required before concentrated ephemeral channel formation occurs. Overland rill flow areas are represented by the remaining cells after permanent and ephemeral cells have been identified. These are the most elevated areas in the watershed, located at the watershed boundary and on ridges separating sub-watersheds.

After assigning cells to one of the three flow categories, channel slope, channel length, and Mannings coefficient are determined. Channel slope for permanent flow channels and ephemeral gully flow channels is determined by first converting the USGS streamlines and terrain analysis-generated streamlines into grid cell format at a comparable 90 ft cell resolution. The channel grid coverage is superimposed onto the slope grid coverage to identify which slope cells to use in determining a channel slope. An average channel slope is then calculated for the 40

and 10 acre computational unit grid cell using the identified channel slope grids. The channel slope assigned to overland rill flow is equal to the determined hillside slope value.

Channel length input parameter values were determined for each permanent flow and ephemeral gully flow channel cell by using the 40 and 10 acre grid boundaries to intersect the channel coverage. A channel length can now be determined for each cell with a channel. For cells with multiple channels, the longest continuous channel length was selected as the ANN-AGNPS parameter value. If a cell's channel length was less than half the cell length, an alternative channel length was determined. This method is the same as is used in calculating length in overland rill flow cells. Overland rill flow lengths were determined based upon the direction of flow both entering and exiting the cell. The method used is the same as incorporated by the AGNPS model as outlined in the Users' Guide (1989).

A Mannings N value was assigned to cells according to the type of concentrated flow taking place. For this research, cells with permanent channel flow or ephemeral gully flow were assigned a Mannings value of 0.033, representing flow on bare smoothed soils. Cells with overland rill flow were assigned N values equal to 0.045, representing flow on bare soils with roughness generated by tillage practices. Figure 4.17 shows the GIS-interface program window for selecting, displaying and editing channel parameters. GIS-generated channel parameters were not edited, in order to allow comparison with map interpreted-parameters.

The direction of flow out of a cell to one of the cell's eight neighbors as well as the identification of the cell receiving flow are required input parameters of the ANN-AGNPS model. These parameter values are also determined by the terrain-analysis procedures provided by ARC/INFO. The 90 ft DEM lattice coverage is processed to determine which of the eight neighbor cells has the greatest slope. The neighbor cell with the largest downhill slope thus becomes the flow direction.

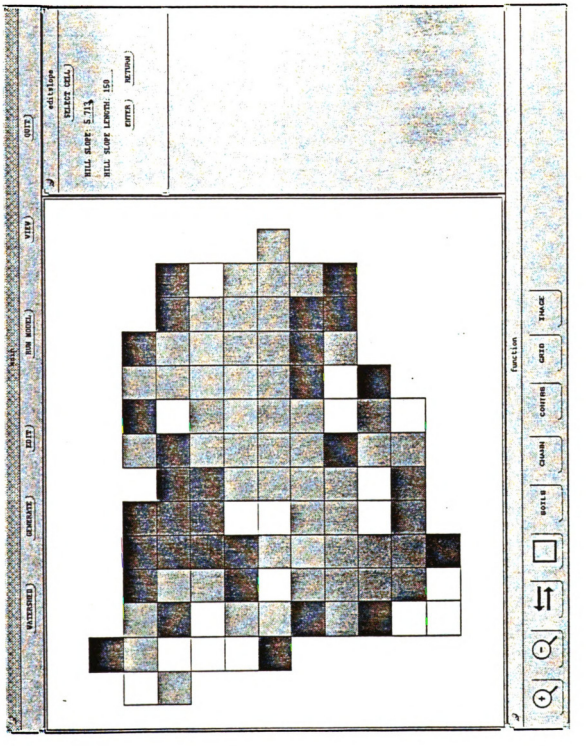

Figure 4.16 Hill Slope Display and Edit Screen

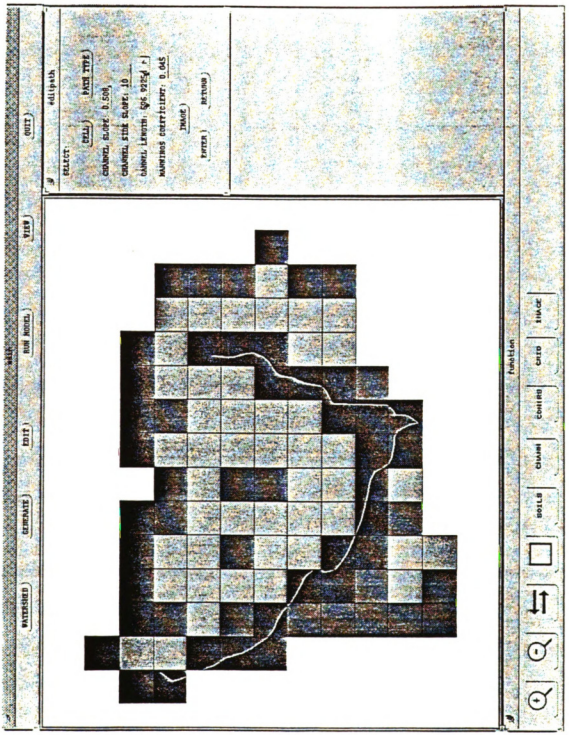

Figure 4.17 Channel Display and Edit Screen

Direction of flow is represented for a cell by a value from 1 to 8, where 1 represents a flow direction to the north, 2 is a flow direction to the northeast, etc. This labeling process continues for all 8 directions, assigning a number to each of a cell's 8 neighbors. The 90 ft resolution grids are then resampled to 40 and 10 acre grid sizes where the dominant flow direction is selected for the larger resampled cell size.

The process of generalizing flow direction detail from a small resolution grid (90 ft) to a coarse resolution grid (40 or 10 acres) will result in the omission of information describing actual flow directions. That is to say, the dominant flow direction represented within the 40 or 10 acre grid cell may not be the actual flow direction. This is due in part to the placement of the 40 and 10 acre cell relative to the watershed topography and the inability of the 90 ft grid to capture information determining flow direction at smaller scales. The flow direction errors that result include; grid cells whose flow direction is out of the watershed, grid cells that have crossing flow paths and grid cells that have circular flow directions between two or more cells. Figure 4.18 represents the GIS-interface program's window for editing flow direction. The program allows the user to select grid cells and change their flow direction based upon interpretation of contour lines and concentrated flow channels. Receiving cells are determined based upon flow direction and grid cell topology. Receiving cell parameters are automatically updated when flow directions are altered in the editing program.

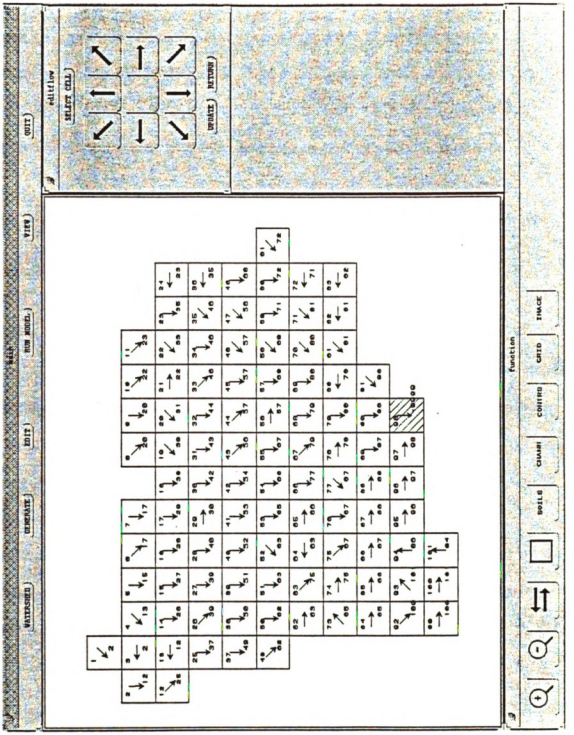

Figure 4.18 Flow Direction/Receiving Cell Display and Edit Screen

In this research project, a number of cells' flow directions for both 40 and 10 acre grids required editing because of errors generated when the automated GIS flow direction routine was implemented. The flow direction errors must be corrected for the ANN-AGNPS model to simulate channel routing. Cells with incorrect flow directions were replaced with flow directions created by map interpretation.

The final input parameter values developed with the GIS-interface are presented in Appendix C, Table C3 for 40 acre cell size and Table C4 for 10 acre cell size.

4.2 Observation Data for Model Verification

4.2.1 Sub-Watershed Delineation

Testing the predictive capabilities of ANN-AGNPS, as specified in the second hypothesis, requires delineation of runoff, sediment and nutrient contributing areas throughout the watershed. To achieve this, the watershed was divided into five sub-watershed areas represented in a nested hierarchy configuration. This configuration enables determination of sediment and nutrient loading from each of the sub-watershed areas as well as loading for one internal intermediate position, and for the watershed outlet. Figures 4.19a-b show the configuration of sub-watersheds as developed by two different delineation methods.

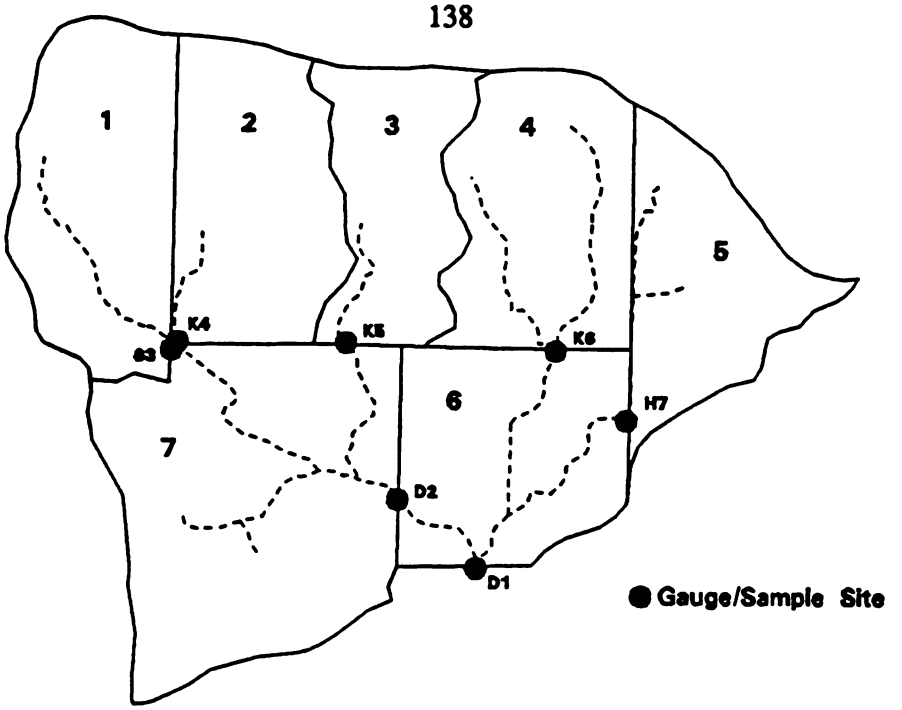

Figure 4.19a Interpreted Sub-Watershed Delineation

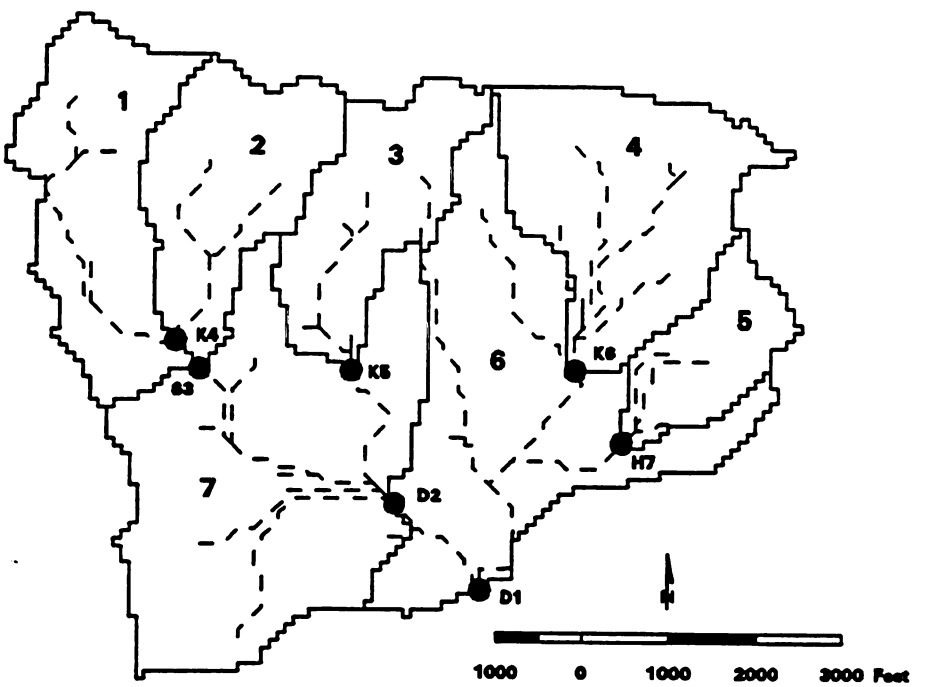

Figure 4.19b DEM-based Sub-Watershed Delineation

The sub-watersheds in Figure 4.14a were delineated by interpreting contours and streamlines from the USGS 7.5 minute quad. sheet, color-infrared photography and field checking. The straight-line boundaries are due to flow barriers caused by elevated roads, and fence lines dividing fields. The sub-watersheds in Figure 4.14b were delineated utilizing the GIS terrain analysis on a 90 ft resolution DEM. Differences are due to lack of vertical resolution in the DEM. DEMs are not capable of capturing elevation detail for micro-level relief which can create flow boundaries in minimal sloping watersheds. Further, preferential flow paths such as culverts and canals found in a restructured landscape are not represented in a 90 ft resolution DEM. Table 4.5 provides the acreage of each sub-watershed using the two delineation methods.

Table 4.5 Sub-Watershed Acreage

Sub-watersheds	Interpreted (Acres)	GIS-Generated (Acres)	Acre difference
1	153.7	129.6	24.1
2	142.8	109.0	33.8
3	106.7	95.0	11.7
4	147.8	152.5	4.7
5	116.8	56.7	60.1
6	145.5	219.2	73.7
7	262.7	270.3	7.6
Total	1076.0	1032.3	43.7

4.2.2 Recording Equipment and Channel Dimensions

At each of the outlets of the five sub-watersheds, at the intermediate and the watershed outlet position, a stage recorder and water sampler were positioned (Figures 4.19a-b). The beginning letter in gage/sample site label scheme is based upon the last name of the owner on whose land the equipment is stationed. The equipment consisted of Belfort Instruments (5-FW-1) liquid level stage recorders positioned atop a PVC stilling well and an automated ISCO 2900 water sampler for collecting water samples of suspended sediments and dissolved nutrients. As previously mentioned, due to the fact that the watershed was entirely on private lands, flow weirs were not installed. Rather, channel dimensions were recorded (Appendix D, Table D1 and Figure D1) and a computer program was written to relate discrete-time stage heights to a flow volume. Mannings Equation was then used to calculate a flow velocity for converting discrete-time flow volume to a flow rate. The flow rate was accumulated to provide a total runoff volume. Mannings Equation is represented as:

(4.1) $$Q = \frac{1.49}{n} \frac{A^{1.66}}{WP^{0.66}} S^{0.5}$$

where:

Q = flow rate

n = Manning roughness coefficient for channel

A = flow cross-sectional area

WP = wetted perimeter

S = slope of the channel

4.2.3 Rainfall Records

Rainfall - runoff recording in the watershed began on April 6, 1992 and continued to October 16, 1992. A tipping bucket automatic rain recorder was used to collect rainfall. The gauge is calibrated to record a tip after every 0.25 mm of precipitation. The rain recorder was placed at the outlet of the Moyer watershed, at the D1 position. Precipitation occurred on 69 of the 194 recording days. Of the 69 days of rain, 30.4% had rainfall greater than 0.25 inches, 14.5% had rainfall greater than 0.5 inches, and 4.3%, or 3 rain-days, had precipitation greater than 1.0 inch. For the entire growing season, only two storm events generated channel flow through all seven of the gauging stations. Both of these storm events extended over a period of several days (Table 4.6 and Table 4.7). Under these conditions channel flow never completely returned to base levels at the watershed outlet. The entire period is thus treated as a single event.

Table 4.6 Storm Event 1

Day	Month	Year	Precip (in)
14	6	92	0.09
15	6	92	0.44
16	6	92	2.04
17	6	92	0.49
18	6	92	0.16
Total			3.22

Table 4.7 Storm Event 2

Day	Month	Year	Precip (in)
30	7	92	1.24
1	7	92	0.0
2	7	92	0.53
Total			1.77

A complication to complete watershed data collection was the malfunction of sub-watershed 5 recording equipment for the two storm periods. Therefore, only 12 observations were recorded for the two storm events.

The ANN-AGNPS model requires weather input in addition to daily rainfall. These parameters include; daily minimum and maximum temperature and solar radiation. Weather data from the University of Minnesota's West-Central Experiment Station in Morris were enlisted as model input parameter values. It was assumed that temperature and solar radiation would not vary considerably between the Moyer watershed and Morris, located 19 miles north. Appendix E contains the weather parameters for the entire growing season.

A final weather parameter input required by the model is a daily RUSLE energy intensity (EI) factor value. The EI factor value was calculated using the energy intensity information generated from the tipping bucket rain gauge and the following equations, which utilize maximum 30-minute rainfall intensity and a total rainstorm intensity value (SCS, 1978):

(4.2) $$EI = I_{30} E$$

(4.3) $E = 916 + \log_{10}$ $i \leq 3.0$ in/hr

(4.4) $E = 1074$ $i > 3.0$ in/hr

where:

I_{30} = 30-minute maximum rainfall intensity

E = total storm energy

4.2.4 Overland Runoff

Runoff recorded at the six gauging stations for the two storm events are provided in Tables 4.8 and 4.9 for total runoff volume and peak flow rate. The histograms recorded for the two storm events are also presented in Figures 4.20 and 4.21.

Table 4.8 Runoff Storm 1

Sub-Watersheds	Total Runoff Volume (in)	Peak Flow Rate (cfs)
D1	0.42	42.4
D2	0.12	19.5
S3	0.09	23.4
K4	0.01	5.2
K5	0.01	2.0
K6	0.12	37.5

Table 4.9 Runoff Storm 2

Sub-Watersheds	Total Runoff Volume (in)	Peak Flow Rate (cfs)
D1	0.11	9.4
D2	0..03	3.9
S3	0..001	0.04
K4	0.0002	0.1
K5	0.002	0.5
K6	0.02	2.3

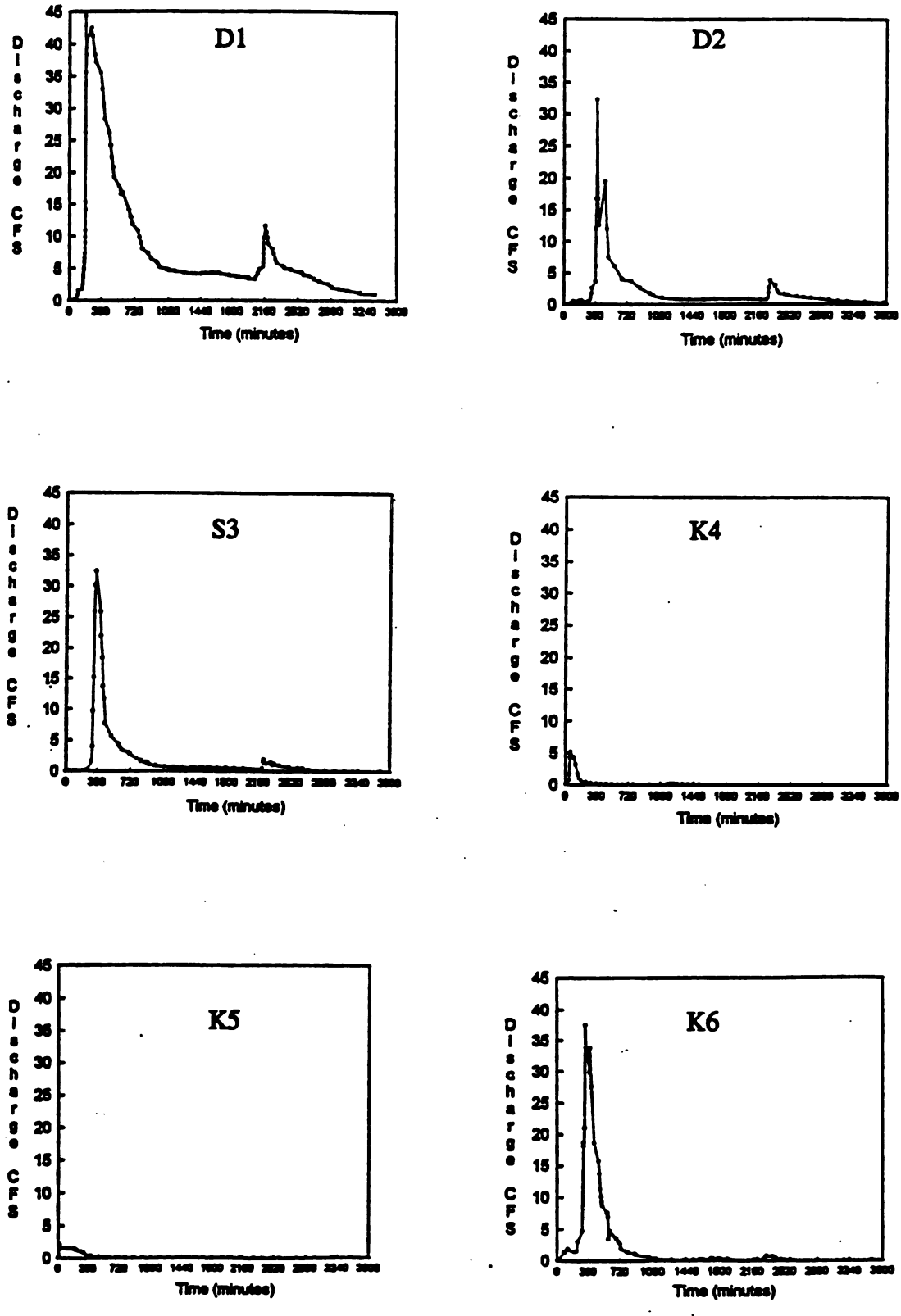

Figure 4.20 Storm 1 Hydrographs

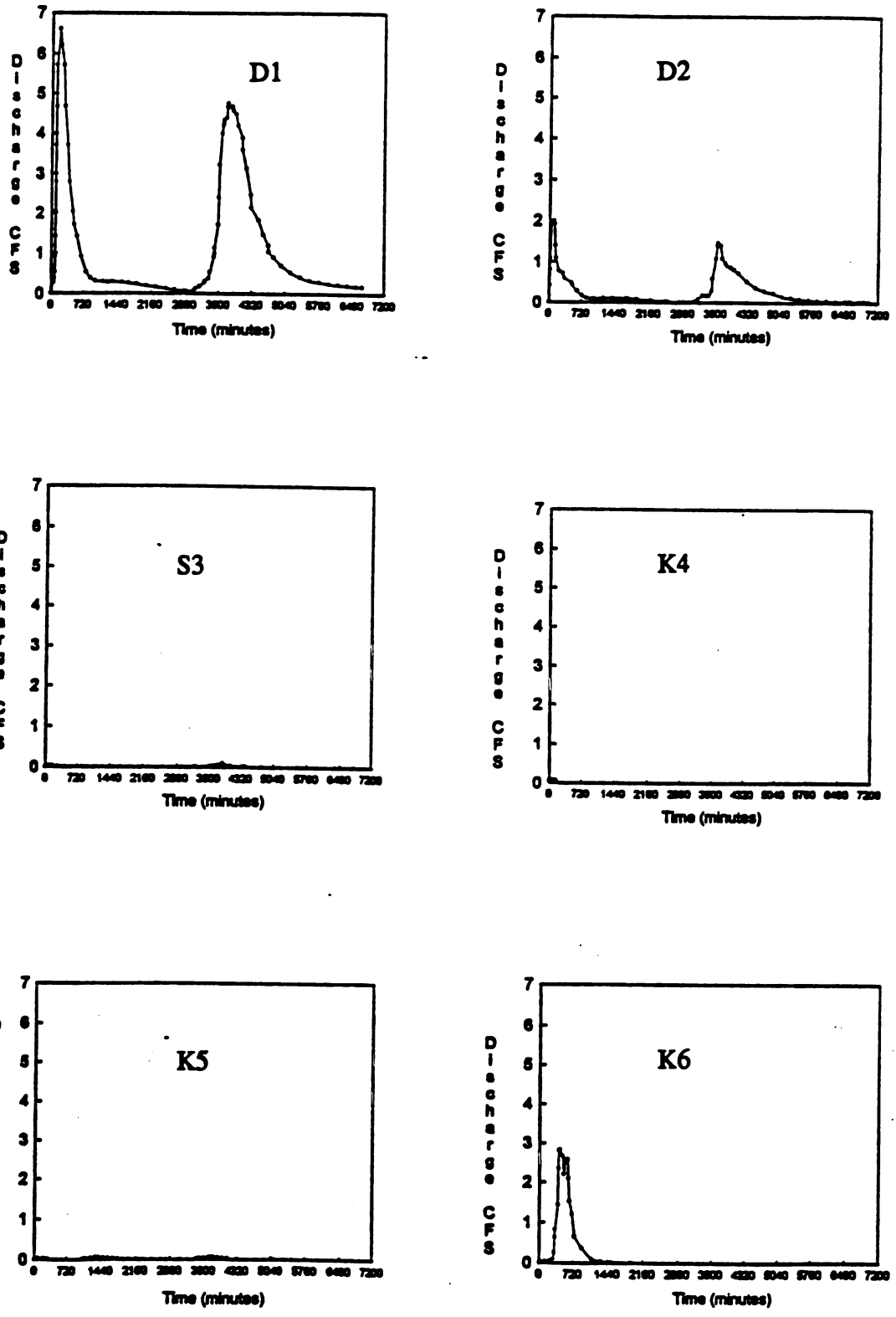

Figure 4.21 Storm 2 Hydrographs

4.2.5 Sediment Loading

Sediment loads for the two runoff events were collected at the six gauging stations. Water sample collection began when a rise in channel levels occurred, and continued every hour through the duration of the storm. Samples were allowed to settle, and a portion of the water was siphoned off to be used in chemical analysis. Water from the remaining particulate-laden samples was evaporated. The sediments were then weighed and a sediment mass determined for the liter volume sample bottle. The sediment mass values for each sample was extrapolated up to the total flow volume for the hour period between sampling times in order to determine a mass weight of sediment moving with the runoff. The hourly sediment weights were then added for the entire storm to give a total sediment loading in tons. The sediment loading results are provided in Tables 4.10 and 4.11 for total tons of sediment.

Table 4.10 Sediment Loading Storm 1

Sub-Watershed	Sediment Loading (tons)
D1	15.6
D2	12.5
S3	26.1
K4	0.8
K5	1.2
K6	27.2

Table 4.11 Sediment Loading Storm 2

Sub-Watershed	Sediment Loading (tons)
D1	4.3
D2	1.7
S3	0.4
K4	0.0
K5	0.1
K6	2.5

4.2.6 Nutrient Loading

Total Kjeldahl Nitrogen (TKN) and Nitrate Nitrogen (NO_3) were tested for with the RFA method as implemented in the automated ALPKEM testing kit. A mass of Total-Nitrogen was related to the liter volume sample. Total-Nitrogen mass was then extrapolated to relate to a total flow volume, similar to the procedure used for suspended sediments. The Total-Nitrogen loading results are provided in Tables 4.12 and 4.13 in pounds of N.

Table 4.12 Total-Nitrogen Loading Storm 1

Sub-Watershed	Total-Nitrogen (lbs)
D1	1349
D2	14
S3	7
K4	24
K5	2
K6	10

Table 4.13 Total-Nitrogen Loading Storm 2

sub-watershed	Total-Nitrogen (lbs)
D1	284
D2	2
S3	0.5
K4	0.14
K5	0.18
K6	1.14

4.3 The ANN-AGNPS Model

The basic hydrologic, erosion and NPS transport processes represented in the ANN-AGNPS model were previously discussed in the literature review chapter. These basic processes are supported by a number of sub-processes which modify the physical environment of the basic processes. This section of the methods chapter will detail those sub-processes incorporated in ANN-AGNPS influencing the major processes identified above. These sub-processes include percolation, plant growth, evapotranspiration, residue decay, soil temperature and soil surface roughness. An additional set of algorithms presented in this section are soil approximation equations. These algorithms are used in the model to calculate required model soil parameter values, including; bulk density, saturated hydraulic conductivity, field capacity, wilting point, and upper limit soil moisture holding capacity.

The ANN-AGNPS model is divided into two basic sets of routines. The first simulates overland runoff, erosion and nutrient loading for each runoff-generating rain

event and for each grid cell. The second set of routines simulates the routing of water, sediment and nutrients through the watershed's channel network. For each cell soil moisture balancing, plant growth and residue decay are calculated on a daily basis for the modeling period. Whenever a rain event occurs, runoff, erosion and nutrient losses associated with runoff and sediment loading are calculated for the day and the results are output to a temporary transfer file. Once the overland simulation is finished for all cells in the watershed, flow routing through the watershed's channels begins. Runoff, erosion and nutrient loss output for each cell are copied from the temporary transfer file. Channel flow calculations are first made for cells that originate a channel flow path (primary cells). Peak flow rate, flow duration, sediment and nutrient loads are calculated for the exit point of the cell. Once all the channel flows for the primary cells have been calculated, the model routes water flow, sediment and nutrient loading from the primary cells to the watershed outlet. Figure 4.22 outlines the separate subroutines for the grid cell overland processes and Figure 4.23 for the channel routing processes included in the ANN-AGNPS model program.

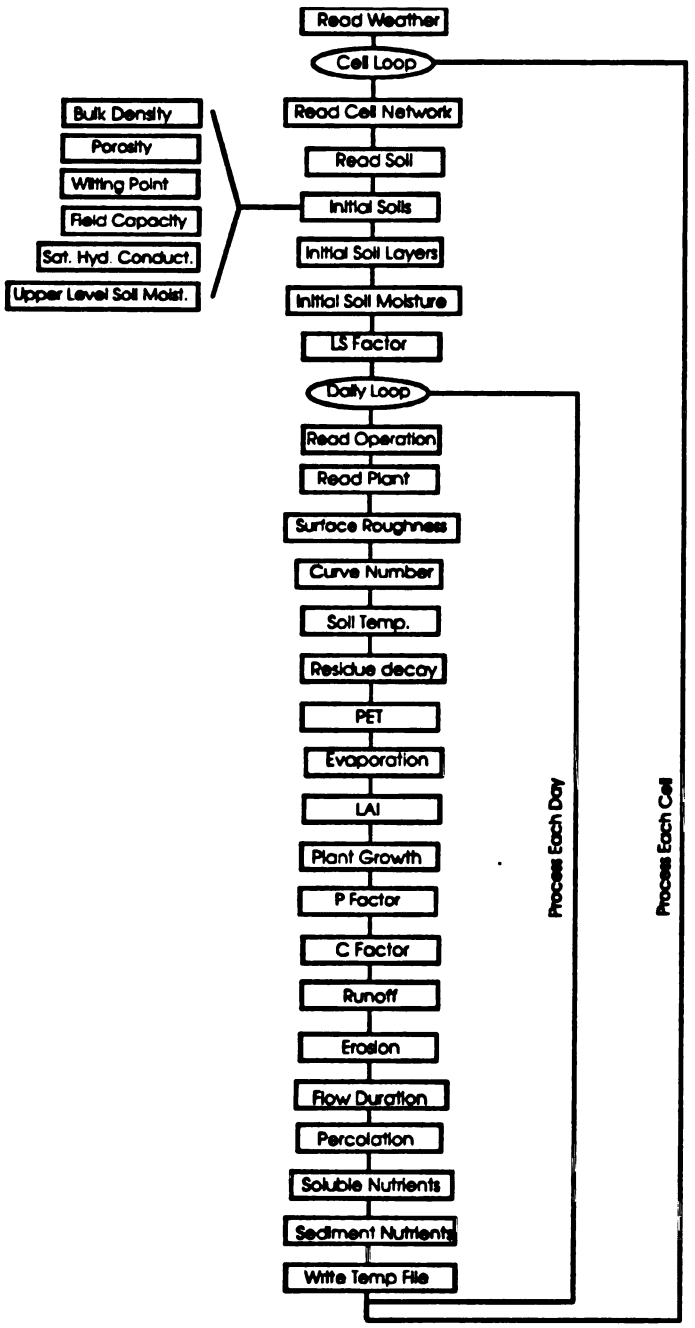

Figure 4.22 Overland Grid Cell Routines

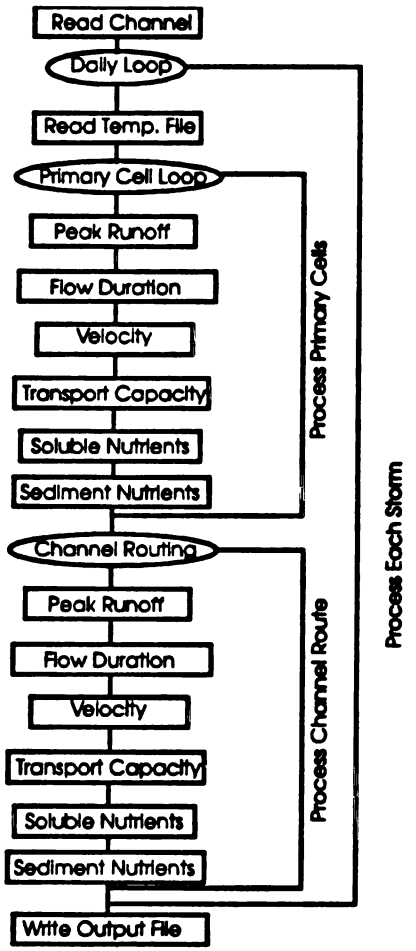

Figure 4.23 Channel Routines

4.3.1 Plant Growth

The plant growth routines within ANN-AGNPS are not used for estimating biomass and grain production based on soil-water and nutrient availability, such as in the CERES-Maize (Ritchie et al., 1989), SOYGRO (Jones et al., 1989) or BEANGRO (Hoogenboom et al., 1990). Rather, the growth model calculates daily biomass accumulation based upon an upper growth boundary and a harvest date. Updated crop characteristics are needed as parameter inputs to modify hydrologic and soil erosion processes, such as providing cover to soils, binding soil with root mass and causing obstruction to overland flow. ANN-AGNPS uses the crop growth model forwarded by Ghebreiyessus and Gregory (1987). Their model simulates the accumulation of plant biomass based upon the ratio of cumulative growing degree days to a growing degree day value at plant maturity. Daily biomass accumulation is determined with the following equation:

(4.5)
$$B_m = \left[\frac{\sum G_d}{G_{dm}} \right]^{\omega} B_{mx}$$

where:

B_m = vegetative biomass

G_d = cumulative growing degree days from planting

G_{dm} = growing degree days at physiological maturity

ω = plant-dependent growth parameters

B_{mx} = vegetative biomass at maturity ($B_{mx} = Y_g\ Y_c$)

Y_g = plant grain yield

$Y_t =$

(4.6

wh

T_m

T_m

T_b

ca

co

co

(4.

wh

C_t

β_t

(4.

wh

R_b

Y_e = residue mass produced per unit of grain

Growing degree days are calculated as follows:

(4.6) $$G_d = \frac{T_{mx} + T_{mn}}{2} - T_b$$

where:

T_{mx} = daily maximum air temperature

T_{mn} = daily minimum air temperature

T_b = base daily air temperature of a given plant

Given the daily biomass value, several additional plant characteristics are calculated, including; the partitioning of above and below ground biomass, canopy cover and canopy height, senescence, root depth, and leaf area index (LAI). Canopy cover is estimated using the following exponential function (Alberts et al., 1989):

(4.7) $$C_c = 1 - e^{-\beta_c B_a}$$

where:

C_c = fraction of ground covered by crop (0-1)

β_c = crop row dependent parameter, determined with the following equation:

(4.8) $$\beta_c = \frac{-\beta_1}{\ln\left[1 - \frac{R_w}{\beta_2}\right]}$$

where:

R_w = row width

β_1 = plant dependent constant

β_2 = maximum canopy width at maturity

Canopy height calculations also implement an exponential function relating a daily height to a maximum height and the daily plant biomass (Alberts et al., 1989):

(4.9) $$H_c=\left[1-e^{-\beta_h B_m}\right]H_{cm}$$

where:

H_c = canopy height

H_{cm} = maximum canopy height

β_h = plant dependent constant

Cumulative daily biomass is partitioned into above ground and below ground biomass based upon a "root-to-shoot" coefficient (Alberts et al., 1989). Below ground biomass is calculated by:

(4.10) $$B_r = R_{wt}\, B_m$$

where:

B_r = below ground (root) biomass

R_{wt} = "root-to-shoot" coefficient; where $R_{wt} = 0.4\text{-}0.2\ G_d$

Above ground biomass (B_a) is the difference between overall biomass and root biomass:

(4.11) $$B_a = B_m - B_r$$

Decrease in plant canopy coverage due to senescence must be considered because of the reduction in ground cover protection from rainfall. A decrease in canopy cover once senescence begins is represented with the following equation (Alberts et al., 1989):

(4.12) $$\Delta C_{cm} = C_{cm}\left[\frac{1-C_{cs}}{S_p}\right]$$

where:

ΔC_c = daily loss of canopy cover (0-1)

C_{cm} = canopy cover at maturity (0-1)

S_p = number of days between the beginning and end of leaf drop

C_{cs} = fraction of canopy cover remaining after senescence. C_{cs} is updated daily by subtracting ΔC_c from the previous day's canopy fraction $C_{cs(t-1)}$

Plant root growth is required on a daily basis to drive the plant transpiration model. Further, the depth of roots is used to indicate at what point infiltrated water becomes deep percolation and thus potentially available to groundwater recharge. The equation used to describe root growth was developed by Borg et al. (1986). The empirical equation modifies a known maximum root depth.

(4.13) $$R_d = R_{dx}\left[0.5+0.5\sin\left[3.03\left[\frac{D_p}{D_m}\right]-1.47\right]\right]$$

where:

R_d = daily root depth

R_{dx} = maximum root depth

D_p = number of days after planting

D_m = number of days to reach maturity

Leaf area index (LAI) is an important parameter used in plant transpiration calculations. It is calculated with two different equations representing plant growth up to senescence and then after senescence. The equations used in ANN-AGNPS were derived by Williams et al. (1984). The plant growth period before senescence is related to the time senescence begins by comparing F_{gs} to LAI_{max}. F_{gs} is the running account of the fraction of the growing period which has passed, calculated from user input of planting and harvest date. LAI_{max} is a plant constant parameter for the fraction of growing season when LAI begins to decline.

When $F_{gs} < LAI_{max}$

(4.14)
$$LAI = \frac{LAI_{max} B_m}{B_m + 0.552 e^{-6.8 B_m}}$$

and $F_{gs} \geq LAI_{max}$

(4.15)
$$LAI = LAI_d \left[\frac{1 - F_{gs}}{1 - F_{lai}} \right]^2$$

where:

LAI = daily leaf area index value

LAI_{max} = plant dependent maximum leaf area index potential

LAI_d = plant dependent leaf area index value when the leaf area index begins declining

4.3.2 Percolation

The redistribution of infiltrated water through the soil profile is calculated on a daily basis. The distribution of water through the soil profile is required parameter input data for a number of processes including overland runoff and plant transpiration. A percolation rate for redistributing the infiltrated water is calculated using a storage routing technique forwarded in the WEPP model (Savabi et al., 1989). When soil moisture (θ) in the top soil layer is greater than the field capacity (FC), a percolation rate is calculated and water is moved to the next lower soil layer. ANN-AGNPS divides the soil matrix into seven different soil layers of equal depth based on the maximum root depth for a selected crop. The percolation rate is calculated with the following equation:

when $\theta_i > FC_i$

(4.16)

$$d_i = (\theta_i - FC_i)\left[1 - e\left[\frac{-\Delta t}{t_i}\right]\right]$$

and $\theta_i \leq FC_i$

(4.17)

$$d_i = 0$$

where:

d_i = percolation rate

FC_i = field capacity water content

i = soil layer

Δt = travel interval

t_i = travel time through layer i. $t_i = \theta_i\text{-}FC_i/K_i$

K_i = hydraulic conductivity

Hydraulic conductivity is adjusted based upon the level of soil moisture within a soil layer. Conductivity ranges from a saturated conductivity rate when soil moisture is at the upper limit of soil moisture holding capacity, to zero when soil moisture is at field capacity. The adjustment to conductivity is given in the following equation:

$$K_i = K_{si}\left[\frac{\theta_i}{UL_i}\right]^{B_i} \tag{4.18}$$

where:

K_{si} = saturated hydraulic conductivity

UL_i = upper limit of soil's water holding capacity

B_i = parameter causing K_s to approach 0 as θ_i approaches FC_i

4.3.3 Residue Decay

The mass of crop residue and its location within the soil profile or on top of the soil surface influence infiltration, overland runoff and subsequently soil erosion. The decomposition model incorporated in ANN-AGNPS was developed by Stroo et al. (1985), who forward a decomposition day concept analogous to the growing degree day. A decomposition index is accumulated on a daily basis based upon the environmental conditions of soil moisture and temperature. Under optimal conditions, the daily added value is equal to 1. Under less than optimal conditions, a value less than one is determined from calculated temperature and water coefficients. The form

of the decomposition day index is as follows:

(4.19) $\text{ENVIND}_t = min(\text{TCF}, \text{WCF}) + \text{ENVIND}_{t-1}$

where:

ENVIND_t = cumulative environmental index

ENVIND_{t-1} = cumulative environmental index from previous day

TCF = temperature coefficient

WCF = water coefficient

min = specifies that the minimum value coefficient be selected

A water- and temperature-related environmental index is determined for both surface and buried residue. The water-related surface residue index is determined with the equation:

(4.20) $$WCF_{s(t)} = \frac{RAIN}{4}$$

and the buried residue index with the equation:

(4.21) $$WCF_{b(t)} = \frac{\theta_t}{\theta_{opt}}$$

where:

WCF_s = water-related surface residue index

WCF_b = water-related buried residue index

RAIN = daily rainfall

θ_t = soil moisture content in top layer

θ_{opt} = optimum soil moisture for residue decay

For either equation, if WCF is greater than one, then optimal conditions exist and the WCF index equals 1.

The temperature-related index is calculated using an equation developed to describe photosynthetic activity as a function of temperature (Taylor and Sexton, 1972). The same equation is used for both surface and buried residue, except that the average daily temperature needed to calculate buried residue is a soil rather than an air temperature.

(4.22) $$TCF = \frac{2(T_{avg}+A)^2(T_m+A)^2 - (T_{avg}+A)^4}{(T_m+A)^4}$$

where:

T_{avg} = average daily temperature

T_m = optimum decomposition temperature

A = constant

Daily decomposition of surface and buried residue is determined with an exponential function utilizing the cumulated decomposition days as a power variable.

(4.23) $$M_t = M_1 e^{(ENVIND)(ORATE)}$$

where:

M_t = current residue mass

M_1 = initial residue mass

Orate = decomposition constant

4.3.4 Soil Surface Roughness

Soil surface roughness plays an important role in both overland runoff and erosion. Rougher surfaces created through tillage operations create barriers to overland flow and sediment transport, and increase soil porosity and resulting infiltration. The roughness of the soil changes throughout the year resulting from field implement use, rainfall, freeze thaw and soil settling. Certain tillage practices, such as moldboard plows, offset disks, and chisel plows can create considerable roughness, whereas other implements such as field cultivators or listers smooth the soil surface. Rainfall also modifies surface roughness by smoothing out the soil through both rainsplash and surface flow. The roughness values assigned to a particular tillage implement used in ANN-AGNPS are the same as those used in WEPP (Lane and Nearing, 1989). The random roughness value is calculated immediately after a tillage practice with the equation:

(4.24) $$R_{ri}=R_{ro}T_i+R_{r(t-1)}\,[1-T_i]$$

where:

R_{ri} = random roughness immediately after tillage

R_{ro} = random roughness created by a tillage implement

T_i = tillage intensity

$R_{r(t-1)}$ = random roughness prior to tillage

The decay of random roughness resulting from rainfall is represented with the following exponential function:

(4.25) $$R_{r(t)} = R_{ri} e^{\alpha_r R_e}$$

where:

α_r = random roughness parameter base on soils silt content

R_e = cumulative rainfall since a tillage operation

4.3.5 Soil Approximation

A number of quantitative descriptive soil characteristics are required in various sub-process calculations. The ANN-AGNPS model uses soil approximation calculations to convert available soil information from data describing percentages of textural soil classes to the needed parameter input value. The soil parameters required in the model include; bulk density, saturated hydraulic conductivity, gravimetric soil water content at 0.033 MPa (field capacity), gravimetric soil water content at 1.5 MPa (wilting point), and upper limit water holding capacity.

Bulk density is required as an intermediate parameter value needed to calculate several soil characteristics including soil temperature, soil water field capacity and wilting point values, porosity and saturated hydraulic conductivity. A baseline bulk density value is calculated from soil texture input values as follows (Alberts et al., 1989):

(4.26) $$\rho = [1.524 + 0.25 S_a - 13.0 S_a O_m - 6.0 C_l 0_m - 0.48 C_l CEC_r] 10^3$$

where:

ρ = consolidated soil bulk density at 0.033

S_a = sand content (0-1)

O_m = organic matter (0-1)

C_l = clay content (0-1)

CEC_r = ratio of the cation exchange capacity of the clay (CEC_c) to the clay content of the soil: CEC_c/C_l

(4.27) $$CEC_c = CEC - O_m[142 + 170D_g]$$

where:

CEC = cation exchange of soil, model input parameter

D_g = average depth of the horizon of interest

3.3.5.2 Wilting Point and Field Capacity

Volumetric water content at 1.5 MPa is calculated using the following equation (Alberts et al., 1989):

(4.28)

$$\theta_d = 0.0022 + 0.383C_l - 0.5C_l^2S_a^2 - 0.265C_lCEC_r^2 - [0.06C_l^2 + 0.108C_l]\left[\frac{P_{(t)}}{1000}\right]$$

where:

θ_d = volumetric water content at 1.5 MPa

Volumetric water content at 0.033 MPa is calculated as follows (Alberts et al., 1989):

(4.29) $$\theta_{fc}=0.2391-0.19S_a+2.1O_m+0.72\theta_d$$

where θ_{fc} = volumetric water content at 0.033 MPa

Saturated hydraulic conductivity is utilized to calculate redistribution of soil water within the percolation equations. It is calculated with the following equation (Alberts et al., 1989):

(4.30) $$K_s=\frac{\phi_e^3}{[1-\phi_t F_a]^2\left[\frac{0.001\rho_{(t)}}{\theta_r}\right]^2 0.0002C^2}$$

where:

K_s = saturated hydraulic conductivity

ϕ_e = effective porosity

ϕ_t = total porosity

F_a = volume of entrapped air in soil

θ_r = residual soil water content

C = soil texture parameter

The porosity parameter required to calculate saturated hydraulic conductivity is determined first by calculating a baseline porosity value.

(4.31) $$\phi_t=1-\frac{\rho_{(t)}}{2650}$$

where:

ϕ_t = total porosity

A value for entrapped air within the soil is required to calculate the effective porosity. Baumer (1989) forwarded the following empirical equation:

(4.32)

$$F_a = 1.0 - \frac{3.8 + 1.9C_l^2 - 3.4S_a + 12.6CEC_rC_l + 100O_m\left[\frac{S_a}{2}\right]^4}{100}$$

where:

F_a = volume of entrapped air, represented as a fraction (0-1)

A residual water content is also required in the effective porosity calculation. An empirical-based equation (Baumer, 1989) is used which incorporates obtainable parameters:

(4.33) $$\theta_r = [0.000002 + 0.0001O_m + 0.00025C_lCEC_r^{0.45}]\,\rho_{(t)}$$

where:

θ_r = residual volumetric water content of the soil

Effective porosity used in calculating saturated hydraulic conductivity is given as:

(4.34) $$\phi_e = [\phi_t F_a] - \theta_r$$

where:

ϕ_e = effective porosity of soil

4.3.6 Soil Temperature

Soil temperature is calculated on a daily basis and then provided as parameter input in the calculation of residue decay and soil evaporation. The soil temperature calculations used in ANN-AGNPS are the same as developed for SWRBB (Arnold et al., 1990). The SWRBB soil temperature routines incorporate a number of factors influencing soil temperature, including: (1) the soil profile influence on temperature distribution, which considers bulk density, soil moisture and profile depth, (2) a temperature lag due to the presence of surface residues, and (3) temporal influence which considers the present day's temperature relative to those within the month. The equations used to determine soil temperature are as follows:

(4.35) $$T_s = T_{ave} + T_t T_d$$

(4.36) $$T_t = (T_{amp}/2) + BS_{adj} - BS_{t2}$$

(4.37) $$T_d = \cos((2.0\ \pi/365)(D-200)-(S_1/D_{dpth})e^{S1/Ddpth}$$

(4.38) $$BS_{adj} = (RES_{lag}\ BS_{t1})+((1-RES_{lag})\ BS_{t2})$$

(4.39) $$BS_{t2} = (T_{wt}\ T_{max})+ ((1- T_{wt})\ T_{min}$$

(4.40) $$T_{wt} = (([T_{mave}\ (D_{mp} + D_{md})]-[T_{mmin}\ D_p])/D_d)- T_{mmin}/(T_{mmax}-T_{mmin})$$

(4.41) $$RES_{lag} = B_a / B_a + e^{(7.563-0.00012\ Ba)}$$

(4.42) $$D_{dpth} = D_{dpthmax}\ e^{\log(500/Ddpthmax)(1-\theta sp)/((1+\theta sp)\ (1+\theta sp))}$$

(4.43) $$\theta_{sp} = \theta_1/(0.356-0.144\ \rho)R_{dx}$$

(4.44) $$D_{dpthmax} = \rho/\rho+e^{-5.63\rho}$$

where:

T_s = daily soil temperature

T_{ave} = average annual soil temperature

T_t = base soil temperature

T_d = temperature dampening coefficient

T_{amp} = average annual temperature amplitude

BS_{adj} = base soil adjustment coefficient

BS_{t2} = base soil temperature for present day

D = present julien date

S_1 = depth of first soil layer

D_{dpth} = soil depth dampening coefficient

RES_{lag} = crop residue lag factor coefficient

BS_{t1} = yesterday's base soil temperature

T_{wt} = surface weight factor coefficient

T_{max} = maximum daily temperature

T_{min} = minimum daily temperature

T_{mave} = average monthly temperature

D_{mp} = number of days in month with rain

D_{md} = number of days in month without rain

T_{mmin} = average monthly minimum temperature

T_{mmax} = average monthly maximum temperature

B_a = mass of surface residue

D_{optmax} = maximum soil depth dampening coefficient

θ_{sp} = soil moisture scaling parameter

θ_1 = soil moisture of first soil layer

ρ = soil bulk density

R_{dx} = maximum root depth

4.3.7 Evapotranspiration

Evapotranspiration is the accumulative water loss through both soil evaporation and plant transpiration. Evapotranspiration reduces the amount of soil moisture, which in turn can impact infiltration and runoff as well as erosion. ANN-AGNPS utilizes Ritchie's ET model (1972) for calculating potential evapotranspiration:

(4.45) $$E_u = 0.00128 \frac{R(1-A)}{58.3} \frac{\delta}{\delta + 0.68}$$

where:

E_u = daily potential evapotranspiration

R = daily solar radiation

A = ground surface albedo

δ = slope of the saturated vapor pressure curve at mean air temperature

Ground surface albedo is calculated as follows:

(4.46) $$A = A_p (1.0 - C_f) + (A_s) C_f$$

where:

A_p = plant albedo, equal to 0.23

C_f = vegetative soil cover index. $C_f = e^{(-0.000029C)}$

C = sum of above ground biomass and plant residue

A_s = soil albedo

The slope of the saturated vapor pressure curve can be determined with the following equation:

(4.47) $$\delta = \frac{5304}{T_k^2} e^{\left[21.25 - \frac{5304}{T_k}\right]}$$

where:

T_k = daily average air temperature, degrees Kelvin

Evaporation takes place as a two-stage soil drying processes (Ritchie, 1972). Stage one soil evaporation occurs at the potential soil evaporation rate, defined as:

(4.48) $$E_{sp} = E_u e^{(-0.4LAI)}$$

where:

E_{sp} = potential soil evaporation

The upper limit of stage one evaporation is defined as:

(4.49) $$E_{su} = 0.009\,(T_r - 3.0)^{0.42}$$

where:

T_r = soil transmissivity, which can be calculated with the following empirical equation utilizing soil texture characteristics:

(4.50) $$T_r = 4.165 + 0.02456 S_a - 0.01703 C_l - 0.0004 S_a^2$$

Once accumulated moisture evaporation exceeds the stage one upper limit, evaporation takes place at a stage two rate, defined as:

(4.51) $$S_2 = 0.001 T_R [d_2^{.5} - (d_2 - 1)^{.5}]$$

where:

S_2 = stage two soil evaporation

d_2 = days since stage two soil evaporation began

If rainfall occurs during stage two evaporation and its volume is greater than the accumulated stage two soil evaporation, stage one evaporation will be reassumed. Soil evaporation can also be modified by the presence of surface cover residue. The WEPP model (1989) uses the following exponential function:

(4.52) $$E_s = E_{sb} e^{-0.000064 C_r}$$

where:

E_s = adjusted soil evaporation rate

E_{sb} = bar soil evaporation rate

C_r = surface plant residue

A potential plant transpiration rate is calculated for the PET value. It is accomplished with the following equation:

(4.53) $$E_{tp} = \frac{E_u LAI}{3}$$

where:

E_{tp} = daily plant transpiration rate

The above equation will calculate transpiration when the LAI is less than a value of 3; when LAI is greater than 3, the daily transpiration rate (E_{tp}) is equal to the daily potential rate (E_u).

The removal of water by plant transpiration throughout the soil profile is dependent upon the depth of the plant's roots. The following WEPP equation (Lane and Nearing, 1989) is used in the ANN-AGNPS model:

(4.54) $$U_p = \frac{E_{tp}}{1 - e^{(-V)}}\left[1 - e^{\left[-V\frac{h_i}{RZ}\right]}\right] - \sum_{j=1}^{i-1} U_j$$

where:

U_p = potential water use rate for layer i

V = use rate-depth parameter (3.065)

h_i = depth of soil layer

RZ = root zone depth

U = actual use of water from above soil layer

4.3.8 Nutrients

The continuous daily time-step of ANN-AGNPS requires that adjustments in the nutrient pool be made to account for additions and depletions. Additions to the nutrient pool include fertilizer application, mineralization of organic N to nitrate, and rainfall, while deletions include plant uptake, leaching and nutrient losses from water runoff and soil erosion. Based upon the availability of nutrients for a given day, the extraction coefficient, as discussed above in the literature review, removes a portion of the available soluble N and P, and the enrichment ratio/sediment loss removes the sediment-attached nutrients.

The ANN-AGNPS model incorporates the nutrient routines as implemented in CREAMS (Knisel, 1980). The mean concentration of soluble N and P in runoff subject to transport through overland flow is calculated as follows:

(4.55)
$$\overline{C_2} = \left[\frac{C_1 - C_r}{K_2 Q} 1 - e^{-K_2} \right] + C_r$$

where:

C_2 = mean concentration during runoff

C_2 = final concentration after runoff

C_1 = concentration at the end of infiltration and start of runoff

C_r = concentration in rainfall

K_2 = rate constant for movement of nutrients into runoff (N=0.05, P=0.025)

Q = total runoff

(4.56) $$C_1 = (C_1 - C_r)\, e^{-K_1 F} + C_r$$

(4.57) $$C_2 = (C_1 - C_r)\, e^{-K_2 Q} + C_r$$

C_o = initial nutrient concentration

F = total infiltration for storm

K_1 = rate constant for movement of nutrients down into soil (N=0.25, P=0.25)

The extraction coefficient is then applied to the mean concentration in estimating the amount of nutrients removed. The removal of both N and P is calculated in similar manner except that rainfall does not supply P to the initial P concentration. The amount of nutrients transported away through runoff is then subtracted from the original initial concentration to give an updated nutrient amount. This above process describes losses of nutrients through overland flow and leaching, as well as addition in rainfall. The N nutrients pool is also reduced through plant uptake and added to through mineralization.

Plant uptake as calculated in ANN-AGNPS is based upon the relationship of plant growth through biomass accumulation and accumulated plant N concentrations as forwarded in the CREAMS model (Knisel, 1980). The N concentration in the plant is determined as follows:

(4.58) $$C_i = \min \left[b1\,(DM_i/TDM)^{b2} \text{ (or) } b3\,(DM_i/TDM)^{b4} \right]$$

where:

C_i = N concentration in plant on day i

TDM = total dry matter production for growing season

DM_i = accumulated dry matter production

The actual N uptake from the available pool of soluble N within the soil is calculated with the equation:

(4.59) $$UN_i = C_i DM_i$$

where:

UN_i = accumulated N uptake for day i

Mineralization adds to the N pool through the transformation of organic N to nitrates. This process as represented in the CREAMS model is dependent upon both temperature and moisture levels within the soil. The following equations calculate the amount of mineralized N taking place between rainfall days.

(4.60) $$MN = POTM\ WK\ \ 1\text{-}e^{-TK\ DAYS}$$

where:

MN = mineralized N for the period between rainfall days

POTM = potentially mineralizable N in the soil

WK = water coefficient

TK = temperature coefficient

(4.61) $$WK = \theta/FC$$

(4.62) $$TK = e^{15.1\text{-}6350/TA}$$

where:

θ = soil moisture content

FC = soil moisture content at field capacity

TA = soil temperature in degrees Kelvin

Soluble P removal from the available source of P is accounted for with only the extraction coefficient. The binding nature of P to soil particles and the loss of P through sediment transport is a much more important source of P. Unlike soluble sources of nutrients, soil-attached N and P forms are not reduced. The ANN-AGNPS model uses a constant enrichment ratio which relates nutrient concentration to eroded soil mass. The enrichment ratios used in ANN-AGNPS were discussed in the literature review section.

4.3.9 CN Modification

The ANN-AGNPS model incorporates two modifications to the original SCS CN method reported in the literature review. The first modification adjusts the CN value based upon field residue mass, the second modification accounts for unevenly distributed antecedent moisture conditions through the soil profile.

The method for adjusting CN values due to field residue has been forwarded by Rawl et al. (1980). They utilized data from 531 simulated and natural rainfall events on a large residue crop (corn) and medium residue crops (wheat, oats, barley, rye, sorghum, soybeans) with differing residue amounts to create graphs that serve as guidelines for developing curve number reduction tables.

Smith and Williams (1980) developed a weighting factor to account for uneven distribution of water through the soil profile on generating runoff/infiltration. When

using the curve number method it was found that soils which were wet near the surface tended to under-predict runoff and over-predict infiltration, while the opposite was true for drier soils. The weight values of the soil layers decrease with depth reflecting the importance of soil moisture, or lack of it, in the upper soil layers.

$$W_i = 1.016\left[e^{-4.16\left(\frac{D_{i-1}}{RD}\right)} - e^{-4.16\left(\frac{D_i}{RD}\right)}\right] \tag{4.63}$$

where:

W_i = weight factor

D_i = depth to the bottom of a soil layer

RD = total soil layer depth

i = soil layer

The weighting factor is applied to the retention parameter to adjust the final runoff/infiltration value.

$$S = S_{max}\left[1.0 - \sum_{i=1}^{NN_i}\left(\frac{SM_i}{UL_i}\right)\right] \tag{4.64}$$

where:

SM_i = soil moisture

UL_i = upper limit of soil moisture capacity

4.4 Analytic Techniques

Two hypotheses were forwarded in the introduction to formally guide the research process in the investigation of two parallel research questions. The first line

of research is to assess the capability of GIS to provide input data to a distributed parameter watershed model. The second line of research is to evaluate the model's predictive accuracy and determine a level at which the model can best describe the contribution of NPS pollution loading from sub-watersheds inside a larger watershed.

4.4.1 Testing Hypothesis 1

GIS-generated parameter data will be compared and contrasted to parameter input values as determined through map interpretation and reconnaissance level field surveys. Data comparison will occur at two different input scales, a 40 acre and a 10 acre grid cell resolution. A "Matched Pair" T test will be enlisted to determine if a statistically significant difference exists between parameters generated using GIS and map interpretation/field surveys. Also to be tested for differences will be two sets of output results from the ANN-AGNPS model. Results to be assessed include cell-level output for overland runoff volume, erosion and Total-Nitrogen loading, as well as results for routed output generated at the sub-watershed outlets; including runoff volume, peak flow rate, suspended sediment and Total-Nitrogen loading.

The null hypothesis is presented as: Ho: $\mu_D = \mu_1 - \mu_2 = 0$, where μ_D is the mean difference between the two input parameters and output results, μ_1 is the mean of the GIS-generated input parameter and output results and μ_2 is the mean of the map interpretation/reconnaissance input parameters and output results. The test statistic is given as:

(4.65) $$t = \frac{\bar{D}}{S_D/\sqrt{n}}$$

where the level of significance established is $\alpha = 0.05$.

and

(4.66)
$$S_D = \sqrt{\frac{\sum_{i=1}^{n} D_i^2 - \frac{(\sum_{i=1}^{n} D_i)^2}{n}}{n-1}}$$

where:

S_D = standard deviation

D_i = difference between parameter input values utilizing two methods

n = number of observations, equal to the number of cells in the watershed at the 40 and 10 acre size

4.4.2 Testing Hypothesis 2

The predictive capabilities of the ANN-AGNPS model, including: quantitative predictions, contributing sub-watershed ranking predictions, and significant sub-watershed identification predictions, will be assessed by comparing observed recordings of total runoff volume, peak flow rate, sediment loading and soluble Total-Nitrogen loading to model simulated values.

Quantitative comparisons will be evaluated for each of the sub-watersheds, the intermediate watershed number 7, as well as the entire watershed. Quantitative predictions for peak runoff, volume, sediment loading, and soluble total-Nitrogen loading will first be plotted against observations to graphically display correlation. Next a simple linear regression model will be incorporated to estimate the linear

correlation coefficient (r). Testing the hypothesis, as to whether or not correlation exists at a given confidence level, is achieved by testing the linear regression coefficient: Ho: $\beta_1 = 0$. The T-statistic is given as:

(4.67)
$$t = \frac{r\sqrt{n-2}}{\sqrt{1-r^2}}$$

Based upon both the observed and the simulated quantitative values for sediment and Nitrogen loading from the sub-watersheds, a ranking of sediment and nitrogen loading will be generated. The two rankings will be compared to determine whether the model can correctly match the ranking of observed contribution.

Testing the capacity of the model to determine which sub-watersheds contribute significant sediment and nutrient loading requires selecting an arbitrary cut-off value for defining contribution significance. For this research, 25% of the total sediment and nutrient load will be used: a sub-watershed that generates more than 25% of the total sediment or nutrient load to the outlet of the watershed is considered a significant contribution of NPS pollution. The significant by contributing sub-watersheds, as determined from the recorded data, will be compared to the simulated results to evaluate the ability of the model to identify significant contributing areas.

CHAPTER 5

RESULTS

5.1 Introduction

The hypotheses forwarded in the introductory chapter will be tested utilizing statistical and comparative tests on both model input parameter data as well as collected watershed observational and model-generated results. A discussion of the significance of the results and how they are reflected in the acceptance or rejection of the hypotheses will also be provided.

Hypothesis 1 was formulated to guide the research in assessing GIS's ability to generate model input parameters and to evaluate the impact of GIS-generated parameters on model output results, as compared to a standard set of input values generated by more conventional map interpretation and field surveying methods.

Hypothesis 1: The input parameter error introduced using GIS-based spatial data manipulation methods is insignificant as compared to model input data values generated from conventional map interpretation and reconnaissance field surveys. Thus the simulation results utilizing the two sets of model input parameters will be comparable.

A Matched Pair T test was used to test the validity of the hypothesis by determining if the input parameter means from the two different data generation methods are

significantly different. Further, model results generated with the two different input parameter generation methods are also assessed to determine if significant similarities or differences exist when utilizing different input data.

Hypothesis 2 was articulated to guide the research in testing the ANN-AGNPS model's predictive capabilities and determine at what level of specificity the model is capable of generating results describing the sub-area contribution of NPS pollutants within a watershed. This test is carried out specifically for suspended sediments and soluble Total-Nitrogen.

Hypothesis 2: The ANN-AGNPS model cannot accurately predict quantitative contributions of NPS pollutants from sub-watersheds within a larger agricultural watershed. The model is only capable of providing identification and ranking description.

Six stage recorders and water samplers were set up in the watershed. Data was collected from four sub-watersheds, the watershed outlet and an intermediate position between the watershed outlet and the upper sub-watersheds. Watershed observational data is compared to ANN-AGNPS model-generated results. A 10 acre grid cell size is used to delineate the watershed, and map interpretation / field surveying methods were used to determine input parameter data. A correlation coefficient derived from linear regression analysis is used for testing the hypothesis. A basic comparative analysis is also incorporated to compare output results.

5.2 Hypothesis 1

The map interpretation / field surveying and GIS-based input parameters will be statistically evaluated for two different cell sizes; 40 acres and 10 acres. The input parameters used in testing the hypothesis are topography-related and field practice-related. They were either generated through elevation contour-line interpretation, field surveying, or GIS-based terrain and overlay analysis methods. These data values are representative of quantitative rather than descriptive data types. They include; hillside slope, hillside length, channel slope, channel side slope, channel length and Mannings coefficient. Quantitative parameter values associated with the soils mapping unit and farm fields, such as SCS curve number and RUSLE K-Factor, were not included for parameter comparison. The two parameter generation methods resulted in the assignment of the same soil mapping unit and farm field for each grid cell comprising the watershed. Therefore, parameter values such as the curve number and RUSLE K-Factor are the same between the two methods.

The Matched Pair T test employed in testing Hypothesis 1 assesses whether the means for the GIS-generated input parameters are statistically similar, or different, from the map-interpreted input parameter means. Table 5.1 provides the T statistic for 40-acre grid cell size parameters. At the 95% confidence level ($p = 1.711$), only the channel slope input parameter's mean can be considered statistically similar for both data generation methods. Table 5.2 provides the T statistic for a 10 acre grid cell size. At the 95% confidence level ($p = 1.658$), the hillside slope and hillside length means can be considered statistically the same. Thus for these three

parameters, one cannot reject the null hypothesis: $\mu_D = \mu_1 - \mu_2 = 0$, and it must therefore be assumed that for these three input parameters, the two parameter generation methods will result in statistically similar input data values.

Table 5.1 40 Acre Grid Cell. Input Parameter. T Statistic

Input Parameters	T Statistic
Hillside Slope	1.718
Hillside Length	2.021
Channel Slope	-1.262 *
Channel Side Slope	-2.509
Channel Length	2.833
Mannings Coefficient	3.579

Level of Significance $\alpha = 0.05$. $p = 1.711$. $n = 23$

Table 5.2 10 Acre Grid Cell. Input Parameter. T Statistic

Input Parameters	T Statistic
Hillside Slope	-1.048 *
Hillside Length	-1.619 *
Channel Slope	-4.334
Channel Side Slope	-2.442
Channel Length	3.595
Mannings Coefficient	5.248

Level of Significance $\alpha = 0.05$. $p = 1.658$. $n = 97$

For the remaining 40 acre parameters, hillside slope, hillside length, channel slide slope, channel length and Mannings coefficient, the Matched Pair T test statistic is greater than the 95% significant probability level, and thus the null hypothesis is

rejected. The null hypothesis must also be rejected for the 10 acre input parameters of channel slope, channel side slope, channel length and Mannings coefficient. For these parameters, there is a statistically significant difference between the means for the two parameter generation methods.

The second half of hypothesis 1 evaluates the model output results for the two different parameter generation methods. A statistical comparison using the Matched Pair T test was carried out for output values generated for each cell. These results included overland runoff, overland erosion and overland Total-Nitrogen loading. The cell-based output results represent the generation of water and constituents flowing from a cell's overland area and into the cell's channel. A statistical evaluation was also carried out for channel hydrologic descriptions, including runoff volume and peak flow rate, as well as sediment and Total-Nitrogen loading at the six gauge sites for the two storms.

The Matched Pair T statistic used for determining statistical significance for the 40 acre cell size hydrology, sediment and Total-Nitrogen generation is given in Table 5.3. At the 95% probability level ($p=1.671$) only the mean for Total-Nitrogen loading is less than the T statistic. Therefore the null hypothesis cannot be rejected; Total-Nitrogen loading means are significantly similar for the two parameter generation methods. The T statistic value for overland runoff and sediment loading, however, is greater than the 95% probability value. The null hypothesis is rejected, and the means for the runoff and sediment loading parameters for the two methods are considered significantly different. Table 5.4 demonstrates that for the 10 acre cell

size hydrology, sediment and Total-Nitrogen model output results are less than the 95% probability level (p=1.645). Thus the null hypothesis cannot be rejected; at the 95% confidence level, the mean output result values for the two different methods are significantly the same.

Table 5.3 40 Acre Grid Cell. Storm 1 & 2 Output Results. T Statistic

Output Results	T Statistic
Overland Runoff	2.419
Sediment Loading	1.689
Total-Nitrogen Loading	0.371 *

Level of Significance $\alpha = 0.05$. P = 1.671. n = 46

Table 5.4 10 Acre Grid Cell. Storm 1 & 2 Output Results. T Statistic

Output Results	T Statistic
Overland Runoff	0.012 *
Sediment Loading	0.035 *
Total-Nitrogen Loading	0.192 *

Level of Significance $\alpha = 0.05$. P = 1.645. n = 194

Table 5.5 and 5.6 provide the Matched Pair T statistic for determining significance between map interpretation/field surveying and GIS-based parameters for channel hydrology, sediment loading and Total-Nitrogen loading output at the six gauge sites for the two storms. Table 5.5 represents the 40 acre cell size and Table 5.6 the 10 acre cell size.

Table 5.5 40 acre Grid Cell Gauge Sites. Storm 1 & 2 Output Results. T Statistic

Input Parameters	T Statistic
Channel Runoff	3.883
Channel Peak Flow	1.861
Channel Sediment Loading	0.685
Channel Total-Nitrogen Loading	2.348

Level of Significance $\alpha = 0.05$. $P = 1.702$. $n = 12$

Table 5.6 10 acre Grid Cell Gauge Sites. Storm 1 & 2 Output Results. T Statistic

Input Parameters	T Statistic
Channel Runoff	-1.431
Channel Peak Flow	-1.103
Channel Sediment Loading	0.042
Channel Total-Nitrogen Loading	-0.197

Level of Significance $\alpha = 0.05$. $P = 1.702$. $n = 12$

The Matched Pair T statistic for determining statistical significant similarity between the means of map interpretation/field surveying and GIS-based methods model output were assessed at the 95% probability level. At the 40 acre grid cell size only the channel sediment loading T statistic was less than the probability value. Therefore the null hypothesis cannot be rejected and it supports the argument that channel sediment loading means for the two parameter generation methods are significantly similar. The T statistic value for channel runoff, channel sediment loading and channel Total-Nitrogen loading is greater than the 95% probability value.

The null hypothesis is rejected, and the means for the runoff and sediment loading parameters for the two methods are significantly different. Table 5.6 shows that the T statistic for all results is less than the 95% probability level. Thus the null hypothesis cannot be rejected for channel runoff, peak flow, sediment and Total-Nitrogen loading. The output value means for the two different methods at the 10 acre cell size are significantly the same.

5.2.1 Discussion

Tables 5.1 and 5.2 demonstrate that most of the input parameters for the two generation methods at the 40 acre and 10 acre grid cell size are statistically different. There are, however, exceptions for each cell size. At the 40 acre cell size, the channel slope parameter is statistically similar for the two input methods, and the hillside slope and hillside length are statistically similar at the 10 acre grid cell size.

It is interesting to note that the similar parameters at the two cell sizes represent different landscape characteristics. The parameter that is statistically similar at the 40 acre grid cell is related to a channel characteristic, whereas the parameters similar at the 10 acre grid cell are related to overland flow characteristics.

5.2.1.1 Channel Parameter Generation

It can be seen from the T statistic values in Tables 5.1 and 5.2 that the mean difference between channel parameter input data for the two methods is less in the 40-acre cell size than in the 10 acre cell size. One reason the 40 acre cell size has channel input parameter values with a higher degree of similarity is that in both map interpretation/field surveying and GIS-based parameter generation methods a larger

percentage of the watershed is covered by cells containing a channel for generating channel parameter values. As described in the methods chapter, a cell must have a channel length that is greater than one-half the length of a cell side in order to be assigned that length, otherwise the default value is assigned. Therefore at the 40 acre cell size, there are fewer cells without channels that require a default channel parameter value than at the 10 acre cell size. The default channel slope is equal to one-half the land slope for the 40 acre cell size, the default channel side slope is equal to 10%, and the default Mannings coefficient is based upon dominant tillage practice for the cell. At the 10 acre cell size for both map interpretation / field surveying and GIS-based parameter generation methods, a larger percentage of the cells in the watershed do not have channels. Thus more default channel values must be generated. Figure 5.1a demonstrates that at the 40-acre cell size, 8 out of 23 cells do not have a channel for the map interpreted/field survey method, and Figure 5.1b shows 3 out of 23 cells in the GIS-based method without channels. Figure 5.2a demonstrates that at the 10 acre cell size, 55 out of 98 cells do not have a channel for the map interpreted/field survey method, and Figure 5.2b shows 44 out of 98 cells in the GIS-based method without channels.

A number of additional reasons explain why there is significant dissimilarity between map interpretation/field surveying and GIS-based parameter generation methods. The first explanation relates to the above-discussed differences in cells with and without channels. For each cell size, the two different parameter generation methods result in a different combination of cells that contain channel-derived data

rather than default channel information. At the 40 acre cell size 6 cells are misidentified between methods, and at the 10-acre cell size 19 cells are misidentified. The 10 acre cell size with greater channel misidentification between parameter generation methods thus results in lower correlation values than the 40 acre cell size with fewer channel misidentifications.

Second, the terrain analysis procedures carried out by the GIS-method can result in a different channel network pattern and a different density of channels than map interpretation methods. GIS-methods will generate straight line flow paths in topographically flat areas whereas map-interpreted flow paths follow the landscape topography better and thus represent actual flow paths more accurately (Figures 5.1 and 5.2). Conversely, map-interpreted flow paths may conform to straight line artificial channels, where the GIS-generated flow paths do not. Because of the differences in channel delineation between the two methods, channel lengths within a cell can be different. Further, because the two channel delineation methods can result in different placement of a channel within a cell, different elevation values will be selected in calculating a channel slope; thus channel slope values for a cell will be different.

Third, default channel lengths can be different due to the configuration of cell flow directions. If a particular cell has different inflow and outflow directions for the two methods, then the default channel lengths will be different. Finally, channel side slope and Mannings coefficient values are different between the two methods because of the use of field checking versus the identification of several common values and

their extrapolation throughout the watershed.

5.2.1.2 Overland Parameter Generation

From Tables 5.1 and 5.2 it can be seen that at the 10 acre cell size the two overland parameters, hillside slope and hillside slope length, are significantly similar for the two parameter generation methods, whereas they are dissimilar at the 40 acre cell size. GIS-generation of a hillside slope parameter requires that the 90-foot slope lattice be re-sampled to either a 10 acre or 40 acre resolution. The larger 40 acre grid cell size will contain a greater diversity of 90-foot resolution slope values than the 10 acre cell size, thus the loss of slope information through the aggregation process is greater at the 40 acre grid cell size. Aggregation at the 10 acre cell size will also result in a loss of information, however because of the cell's smaller size a better approximation of slope can be achieved relative to the measurements made by map interpretation and field surveying. The smaller 10 acre grid cell size also limits the area for determining a representative hillside slope to measure using the map interpretation/field surveying methods. Therefore, there are fewer hillsides to choose for measuring slope. Further, the hillside that is chosen is more likely to be a dominant hillside slope. A dominant or reoccurring hillslope value is more likely to be retained in the GIS aggregation process. Hillside length for both methods was defaulted to the hillside slope value based upon Otterby and Onstad (1978) tables for Minnesota. Thus if the hillside slope is similar between methods, so is the hillside length.

5.2.1.3 Output Results

The significant similarity in Total-Nitrogen cell loading from cells for both methods at 40 and 10 acres was to be expected. Both parameter input methods resulted in the exact same cell selection of field management practices and soil types. Thus the parameters generated from field management and soils information for calculating a cell's Total-Nitrogen loading will be the same.

At the 40 acre cell size, overland runoff and sediment loading were determined significantly different (Table 5.3). This can be attributed to the 40-acre assessment of input parameters for hillside slope and length. Both these input parameters were determined to be significantly different. These two parameters, together with field practices and soils, are used to calculate both cell runoff and sediment loading. Thus significant differences in cell-based input parameter data resulted in significant differences in cell-based output results. The 10 acre grid cell (Table 5.4) demonstrates that when hillside input parameters for slope and length are significantly the same, then the output results which use these input values in their calculation will also be significantly similar.

Tables 5.5 and 5.6 relate to the cumulative effects of cell-based calculations for runoff, sediment and Total-Nitrogen loading, plus the influence of channel characteristics on water flow and the transport of sediments and Total-Nitrogen. Model results for the six gauge sites are also a factor of sub-watershed size as well as channel network configuration. The two methods employed in sub-watershed delineation, map interpretation/field surveying and the GIS-based method, resulted in

different size sub-watersheds and differently shaped sub-watersheds with different channel network configurations.

At the 40 acre grid cell size only the channel sediment loading results are significantly similar at the six gauge sites for the two storms. Runoff volume, peak flow and Total-Nitrogen loading results are significantly different. An inconsistency exists between the cell-level output results and the cumulative channel output results. Sediment loading at the cell-level was shown to be significantly different for the two parameter generation methods and Total-Nitrogen was significantly similar. At the six gauge sites the results were reversed. The ability to predict similar total-Nitrogen values was influenced by the different size of the sub-watersheds above the gauges. The ANN-AGNPS model does not calculate depletion of soluble nutrient concentrations once nutrient concentrations are calculated for the cell. Because map interpretation/field survey and GIS-based parameter generation methods resulted in sub-watersheds of different size and cell number, concentration values at the outlet of a sub-watershed, representing the Total-Nitrogen loading from cells, are different.

The reason why sediment loading values were significantly different at the cell level and significantly the same at the gauge sites may be related more to offsetting errors and the limited number of observational data used in the analysis. Significant similarities in gauge results may be explained by compensating sediment deposition or scouring within the channels. A significant difference for overland runoff results at the cell level was carried through with significant differences in calculations of flow volume and peak flow rate at the gauge sites.

At the 10 acre cell size, significantly similar cell-level results for overland runoff, sediment and Total-Nitrogen loading may have influenced the results obtained at the gauge sites. Table 5.6 shows that all output results are significantly similar. The ability of the smaller 10 acre cell to produce similar output results may be due to the capability of GIS-based methods to more closely match actual sub-watershed drainage areas. For the 40-acre cell, the total sub-watershed area difference between parameter input methods is 360 acres, representing 17.0 %, whereas the 10 acre grid cell difference is 220 acres, representing 9.7%. Further, the fact that the channel-related input parameters for the two methods were determined significantly different did not cause the results at the gauge sites to significantly differ.

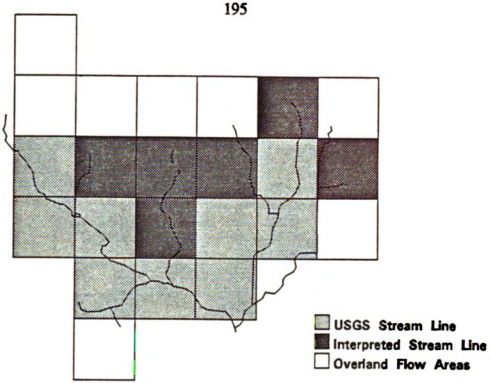

Figure 5.1a 40 Acre Channel Cells: Interpretation Method

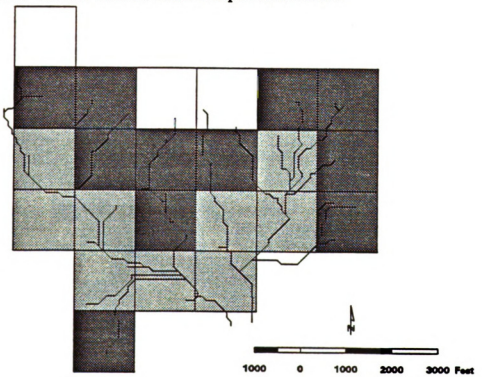

Figure 5.1b 40 Acre Channel Cells: GIS Method

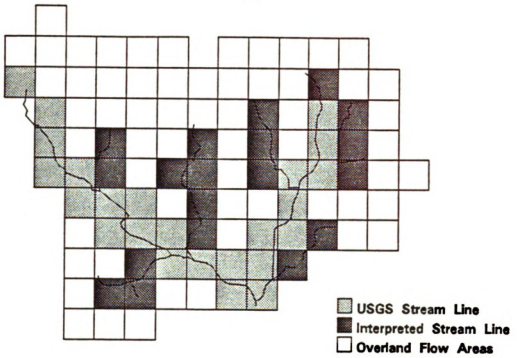

Figure 5.2a 10 Acre Channel Cells: Interpretation Method

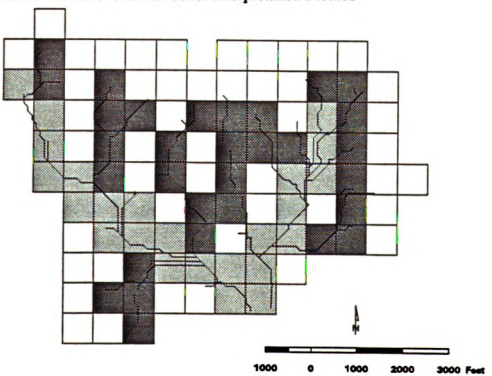

Figure 5.2b 10 Acre Channel Cells: GIS Method

5.3 Hypothesis 2

Hypothesis 2 is concerned with how well the ANN-AGNPS model is capable of describing the contribution of NPS pollutants from sub-areas within a watershed. In this research two NPS pollutants are studied, suspended sediments, measured in tons, and soluble Total-Nitrogen, measured in pounds. The research has identified three descriptive levels for testing the model's predictive capabilities. The first level is a quantitative description for NPS sediment and Total-Nitrogen loading, the second level is a ranking description based upon NPS pollutant contribution from the sub-watersheds, and the third level is an identification description. Sediment and Total-Nitrogen loading from a sub-watershed greater than 25% of total watershed loading is used to determine whether or not a sub-watershed is considered significantly contributing.

Testing the ability of the model to quantitatively describe loading is achieved with the use of a statistical test. A simple linear regression model is used for generating the correlation coefficient. The "r" value indicates a "goodness-of-fit" between observed and simulated results. The correlation coefficient is also evaluated at the 95% probability level to determine if the correlation coefficient is significantly greater than 0. The descriptions for ranking and identification are compared and contrasted.

5.3.1 Quantitative Description

Data collected at the six sub-watershed sites for the two storm events were statistically evaluated against the ANN-AGNPS model's simulated results. A 10 acre

grid cell size and map interpretation/field survey methods were used to generate input parameters. Model output results were compared to observational data for runoff volume, peak flow rate, sediment and Total-Nitrogen loading. Runoff and peak flow values are included in the assessment because they are important input data used in the calculations of sediment and nutrient loading. Tables 5.7a-b display observed and simulated runoff values for each of the six recording sites for the two rainstorms, Tables 5.8a-b present peak flow rate, Tables 5.9a-b sediment loading, and Tables 5.10a-b Total-Nitrogen loading. Figures 5.3 a-d display the plotted data for each of the output results. It must be noted that station D1 observed runoff volume and peak flow rate values for storm 1 were used to calibrate the geomorphic peak flow rate and curve number soil moisture adjustment equations.

The statistical evaluation of observed and simulated data was carried out by developing a simple linear regression model for each output result and calculating the linear correlation coefficient (r). The correlation coefficient value ranges from 0 to 1, with 0 representing a random scattering of points around the regression line and indicating the absence of correlation between observed and simulated output values. A value of 1 represents perfect correlation, with all points falling exactly on the regression line. The square of r (r^2) is the coefficient of determination. It represents the proportion of total variation explained by the regression line. $1-r^2$ is the portion of variability which cannot be explained. Correlation statistics for each of the observed and simulated results are presented in Table 5.11. Also given in Table 5.11 is the T-statistic for testing whether or not the correlation coefficient is significantly

different from 0. The formal hypothesis is presented as: H_o: $\rho = 0$. At the 95% confidence level p is equal to 1.812.

Table 5.7a Runoff (in). Storm 1

	Observed	Simulated: 10 Acre
D1	0.42	0.37
D2	0.12	0.34
S3	0.09	0.29
K4	0.01	0.32
K5	0.01	0.31
K6	0.12	0.42

Table 5.7b Runoff (in). Storm 2

	Observed	Simulated: 10 Acre
D1	0.11	0.04
D2	0.03	0.03
S3	0.001	0.01
K4	0.0002	0.02
K5	0.002	0.02
K6	0.02	0.05

Table 5.8a Peak Flow (cfs). Storm 1

	Observed	Simulated: 10 Acre
D1	42.4	48.5
D2	32.3	34.1
S3	32.4	14.4
K4	5.2	10.6
K5	2.0	10.5
K6	37.5	9.5

Table 5.8b Peak Flow (cfs). Storm 2

	Observed	Simulated 10 Acre
D1	6.6	5.7
D2	1.9	3.2
S3	0.03	0.8
K4	0.08	1.1
K5	0.04	0.8
K6	2.8	3.2

Table 5.9a Sediment Load (tons). Storm 1

	Observed	Simulated: 10 Acre
D1	15.6	14.6
D2	12.5	42.6
S3	26.1	7.45
K4	0.8	14.7
K5	1.2	1.8
K6	27.2	20.7

Table 5.9b Sediment Load (tons). Storm 2

	Observed	Simulated: 10 Acre
D1	4.3	3.7
D2	1.7	10.9
S3	0.05	0.8
K4	0.0009	1.8
K5	0.1	0.3
K6	2.5	2.3

Table 5.10a Total-Nitrogen Load (lbs). Storm 1

	Observed	Simulated: 10 Acre
D1	1349.6	104
D2	14.1	48
S3	7.4	18
K4	24.4	7
K5	1.9	7
K6	9.8	30

Table 5.10b Total-Nitrogen Load (lbs). Storm 2

	Observed	Simulated: 10 Acre
D1	284.0	11
D2	2.4	0
S3	0.5	0
K4	0.14	0
K5	0.18	0
K6	1.14	6

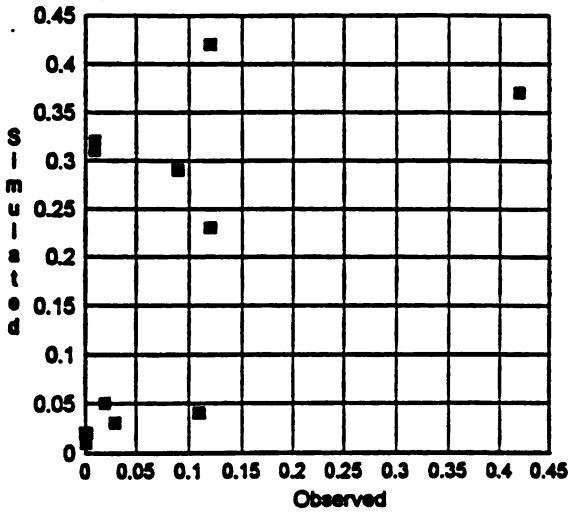

Figure 5.3a Runoff (in)

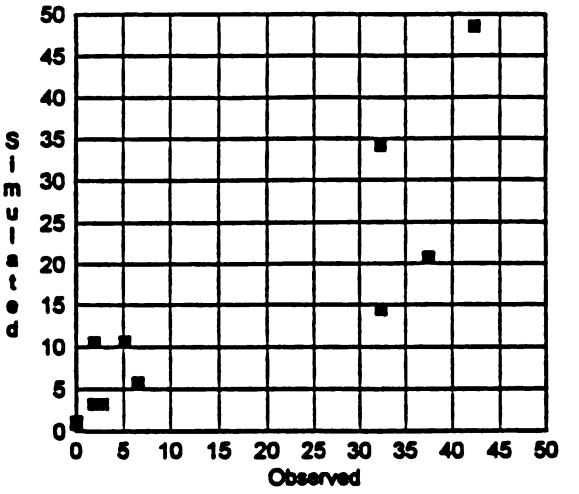

Figure 5.3b Peak Flow (cfs)

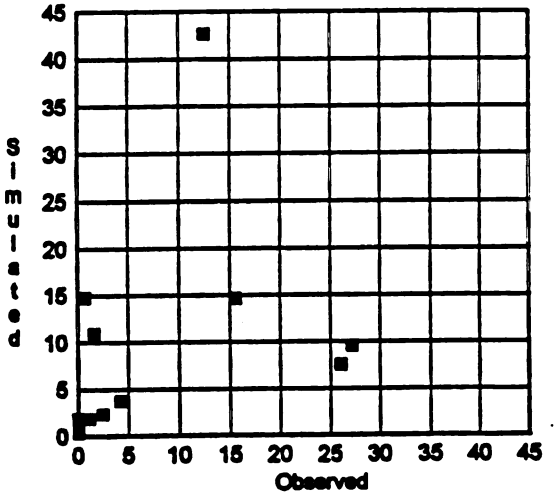

Figure 5.3c Sediment Loading (tons)

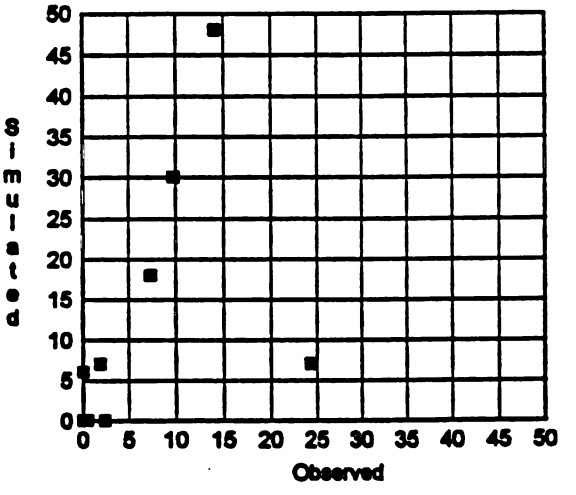

Figure 5.3d Total-Nitrogen Loading (lbs)

Table 5.11 Correlation Statistics

	r	r^2	$1-r^2$	T-statistic
Runoff	0.522	0.272	0.728	1.935
Peak Flow	0.903	0.853	0.185	6.640
Sediment	0.346	0.120	0.880	1.166
Total-Nitrogen	0.503	0.253	0.747	1.841

The T-statistic value for sediment loading (1.166) is demonstrated to be less than the probability value at 95% confidence level. Thus the null hypothesis fails to be rejected for sediment loading. The correlation coefficient is not statistically different from 0, therefore at the 95% confidence interval, correlation between the observed and simulated sediment loading values does not exist. Correlation between the remaining observed and predicted results was determined to be significantly different from 0 with the rejection of the null hypothesis. Therefore, there is some level of correlation evident between the observed and predicted output values. The degree of correlation, however, is extremely weak for runoff and Total-Nitrogen loading as measured by $1-r^2$. $1-r^2$ is equal to 0.728 for runoff volume, and 0.747 for Total-Nitrogen loading. Peak flow runoff is the only output value where the model's simulated results are strongly correlated to the observed values. The correlation coefficient for peak flow is 0.903. This compares to an average correlation coefficient for runoff, sediment and Total-Nitrogen equal to 0.457.

5.3.2 Ranking Description

Ranking of sub-watershed contribution is carried out for the four uppermost sub-watersheds, S3, K4, K5, and K6. Tables 5.12 - 5.13 list both observed and simulated results in order of largest contribution to smallest contribution of sediment and Total-Nitrogen for storms 1 and 2.

Table 5.12a Sediment Loading Ranking. Storm 1

Ranking	1	2	3	4
Sub-Watershed	K6	S3	K5	K4
Observed Sediment Loading	27.2	26.1	1.2	0.8
Sub-Watershed	K4	K6	S3	K5
Simulated Sediment Loading	14.7	9.5	7.5	1.8

Table 5.12b Sediment Loading Ranking. Storm 2

Ranking	1	2	3	4
Sub-Watershed	K6	K5	S3	K4
Observed Sediment Loading	2.5	0.1	0.05	0.001
Sub-Watershed	K6	K4	S3	K5
Simulated Sediment Loading	2.3	1.8	0.8	0.3

Table 5.13a Total-Nitrogen Loading Ranking. Storm 1

Ranking	1	2	3	4
Sub-Watershed	K4	K6	S3	K5
Observed Nitrogen Loading	24.4	9.8	7.4	1.9
Sub-Watershed	K6	S3	K4	K5
Simulated Nitrogen Loading	30	18	7	7

Table 5.13b Total-Nitrogen Loading Ranking. Storm 2

Ranking	1	2	3	4
Sub-Watershed	K6	S3	K5	K4
Observed Nitrogen Loading	1.1	0.5	0.2	0.1
Sub-Watershed	K6	S3	K5	K4
Simulated Nitrogen Loading	6	0	0	0

It can be observed in Tables 5.12 - 5.13 that ranking of sediment loading from the sub-watersheds is similar between observed and predicted values. There is, however, one sub-watershed that nullifies a near perfect matching of rankings. The over-prediction of sediment loading from K4 places it at the beginning of the simulated ranking order for storm 1 sediment loading and second in the ranking order for storm 2. Based upon observational data, K4 sediment loading is ranked last for both storms. Nutrient ranking comparison for all four sub-watersheds can only be carried out for storm 1 because of the model's inability to calculate fraction of a pound for Total-Nitrogen loading. Sub-watershed K4 ranks highest for observational

Total-Nitrogen data, however, in model simulation results it is ranked third. For storm 1 the model was able to select K6 as the second ranked watershed followed by S3. This ranking order is reflected in the observed data, however K6 is the highest ranked sub-watershed. For storm 2 K6 was the only watershed for which Total-Nitrogen loading was predicted, therefore it received the highest ranking. This number one ranking is confirmed in the observed Total-Nitrogen loading.

5.3.3 Identification Description

Sediment and Total-Nitrogen loading results were evaluated to determine which of the four upper-most sub-watersheds; S3, K4, K5, or K6, generated loading greater than 25% of total loading at the watershed outlet. 25% of total loading represents a cut-off value whereby a sub-watershed is considered a significant contributor of sediment and Total-Nitrogen. Tables 5.14 - 5.15 list the contributions from the sub-watershed for observed and simulated records and identify those significantly contributing sub-watersheds for storms 1 and 2.

Table 5.14a Sediment Loading Contribution Identification. Storm 1

Ranking	1	2	3	4	Loading at Watershed Outlet
Sub-Watershed	*K6*	*S3*	K5	K4	
Observed Sediment Loading	*27.2*	*26.1*	1.2	0.8	15.6
Sub-Watershed	*K4*	*K6*	*S3*	K5	
Simulated Sediment Loading	*14.7*	*9.5*	*7.5*	1.8	14.6

Table 5.14b Sediment Loading Contribution Identification. Storm 2

Ranking	1	2	3	4	Loading at Watershed Outlet
Sub-Watershed	K6	K5	S3	K4	
Observed Sediment Loading	2.5	0.1	0.05	0.001	4.3
Sub-Watershed	K6	K4	S3	K5	
Simulated Sediment Loading	2.3	1.8	0.8	0.3	3.7

Table 5.15a Total-Nitrogen Loading Contribution Identification. Storm 1

Ranking	1	2	3	4	Loading at Watershed Outlet
Sub-Watershed	K4	K6	S3	K5	
Observed Nitrogen Loading	24.4	9.8	7.4	1.9	1349.6
Sub-Watershed	K6	S3	K4	K5	
Simulated Nitrogen Loading	30	18	7	7	104

Table 5.15b Total-Nitrogen Loading Contribution Identification. Storm 2

Ranking	1	2	3	4	Loading at Watershed Outlet
Sub-Watershed	K6	S3	K5	K4	
Observed Nitrogen Loading	1.1	0.5	0.2	0.1	284
Sub-Watershed	K6	S3	K5	K4	
Simulated Nitrogen Loading	6	0	0	0	11

The model is capable of identifying significant sub-watershed contributions for storm 1 sediment loading. However, for storm 1 the ANN-AGNPS model includes sub-watershed K4 as a significant sediment contributor, when the observed data demonstrates that is not a significant contributor. The observed sub-watershed sediment loading values for storm 2 are all extremely low except for sub-watershed K6, which is identified as generating greater than 25% of total sediment load. Simulated results selected sub-watersheds K6 and K4 as significant contributors. These sub-watersheds are the same two selected for storm 1.

An extremely high observed Total-Nitrogen loading value at the watershed outlet prohibited any of the sub-watersheds from being classified as a contributing sub-watershed for both storms. If the Total-Nitrogen value observed at station D2 is substituted as the watershed outlet value for those sub-watersheds draining through that station, K4 and S3 become significant contributors. Sub-watershed S3 is the only significant contributor of simulated Total-Nitrogen when D2 is considered the watershed outlet. If the same procedure is carried out for storm 2, none of the sub-watersheds draining through D2 are identified as a contributing sub-watershed for the observed data. The model-simulated results also demonstrate that none of the sub-watersheds are significant contributors.

5.3.4 Discussion

5.3.4.1 Quantitative Description

The ANN-AGNPS model generally over-predicts runoff throughout the watershed. Results from station D1 for storm 1 are not included in the statistical

analysis because the model was calibrated to the first storm's observed runoff volume and peak flow rate. All other predictions for storm 1 are over-predicted. The same over-prediction is true for storm 2, except for station D1 which under-predicts runoff.

The largest over-prediction errors occur for sub-watersheds K4 and K5, where predicted runoff volume is 32 and 31 times greater than observed runoff, respectively. This compares to an average error between observed and simulated runoff of 2.3 times. A possible explanation for such a large degree of over-prediction is that the fields in sub-watersheds K4 and K5 received a different sequences of field tillage practices from the rest of the fields in the watershed. The fields in sub-watersheds K4 and K5 were not fall-tilled, whereas all the other fields, except for fields in K6, were fall-tilled after harvest.

Over-prediction results because the model is incapable of properly accounting for the infiltration and percolation enhancing effects of residue and surface roughness in these fields. The residue-based curve number adjustment procedure adopted by the ANN-AGNPS model did not reduce the curve number significantly enough, thus resulting in greater simulated runoff than observed. Another source of error that affects curve number adjustment relative to residue volume is the inability of the model to properly decay the residue. A larger curve number relates to less residue mass, thus too much residue decay may have taken place between harvest and the growing season's rain storms. A further source of error relates to the curve number model's extraction coefficient adjustment. Soil moisture build-up in the top soil layers will decrease the extraction coefficient value, thus increasing the amount of

runoff. Soil moisture build-up results because the percolation rate between soil layers is under-predicted. The increased mass of surface and incorporated residue and the resulting infiltration and percolation facilitating influences were not properly incorporated in the model's percolation routines. The effects of residue-increasing percolation may even be greater for the quick-draining Barnes-Buse soil type, which comprises the majority of sub-watersheds K4 and K5.

Sub-watershed K6 did not experience the large over-prediction of K4 and K5 because of a wet, low-lying area directly above the K6 recording site. The soils here are comprised mainly of slow-draining clay soils. It is this area which probably generates the majority of runoff recorded at K6. The simulation of K6 sub-watershed over-predicted runoff in the upland low-till portions of the fields above this low-lying area, however, the model under-predicted runoff from this low-lying area. Offsetting errors may have occurred which resulted in a simulated value that more closely approximates the observed runoff values.

Under-prediction of runoff volume at the watershed outlet for storm 2 is a result of under-prediction for areas between the upper sub-watersheds and the watershed outlet. Similar to the case for sub-watershed K6 much of the low-lying areas of the watershed near the watershed outlet consist of less permeable soils. The model was not able to properly account for antecedent soil moisture conditions and greater runoff through the extraction coefficient adjustment. This inability is due in part to the limitations in the percolation calculations as well as the soil characterization algorithms which define quantitative values for; saturated hydraulic

conductivity, porosity, soil wilting point and field capacity.

The inaccuracy in runoff predictions can also relate to the inability of the SCS curve number runoff model. The SCS curve number method has been proven to be most accurate when calculating runoff from "design" size storms (Rawls et al., 1993), consisting of larger rainfall amounts occurring over a relatively short time period. Storm 1 was a protracted storm event lasting five days and totalling 3.22 inches. In one 24-hour period 2.04 inches of rain fell. Storm 2 was one of the larger events of the season. It amounted to 1.77 inches over two days, with 1.24 inches falling in one 24-hour period. A 5-year 24-hour "design" typical of West Central Minnesota will produce 3.3 inches of rainfall (US Weather Bureau, 1961). Some of the over-prediction may be a result of the inability of the curve number model to calculate an accurate runoff value for such low rainfall amounts.

As previously indicated, simulated peak flow rate best correlated to observed flow rate. Peak flow rate estimations both over-predicted and under-predicted observed values. Over-prediction occurs at D2, K4 and K5 for storm 1 and D2, S3, K4, K5 and K6 for storm 2. Under-prediction occurs at S3 and K6 for storm 1, and D1 for storm 2. Over-predictions were most significant for sub-watersheds K4 and K5. These over-predictions can be related back to the above discussions on over-predictions of runoff volume. Runoff volume is an input parameter into the peak runoff equation. In the peak runoff equation, runoff volume positively correlated with peak flow, thus a smaller runoff volume will produce a smaller peak flow rate.

The relatively high correlation between observed and simulated peak flow rates relative to the other output results is in part due to the success of calibrating the geomorphic-based peak runoff model to observed data. The use of the relatively uncorrelated input parameter runoff volume in the peak runoff equation indicates that runoff volume is not a sensitive parameter, whereas other parameters relating to watershed length and width dimensions, as well as channel slope are more sensitive. There is, however, a positive correlation in the predictive capabilities of the model to estimate peak flow rate when using runoff volume. Nine out of the eleven results demonstrate that an over- or under-prediction in runoff gives a similar over- or under-prediction in peak flow.

Sediment simulation as compared to observed data is both over- and under-predicted. The model over-predicts at D2, K4, K5 for storm 1 and D2, S3, K4, and K5 for storm 2. It under-predicts at D1, S3, K5 for storm 1 and D1 and K6 for storm 2. Sediment loading at the outlet of a sub-watershed is the result of two processes. The first process is overland erosion which includes sediment entrainment and deposition in interrill and rill areas. The second process is channel erosion including the transport of overland sediments, the entrainment of channel materials and their deposition within the channel. Over-prediction for K4 and K5 can be traced to smaller volumes of overland and channel flow from increased infiltration, and the inability of channel flow to transport sediment loads. Sediment loading may also be due to the model's inability to account for the sediment deposition capability of residue in both overland and channel erosion processes.

Sediment over-prediction at D2 for storm 1 and 2 may be due to the model's inability to account for sediment deposition from a decreasing channel slope gradient. Station D2 is located directly below a conventional fall-tilled field. Approximately 100 yards from the D2 sampler, the channel gradient slope decreases. In the field, a considerable amount of sediment deposition was observed. The model, however, does not reflect this deposition. In fact, the model simulates additional entrainment of sediments from within the channel. The slope of the channel through the cell directly upslope from station D2 was identified as 0.5% and the channel length through the cell was estimated at 818 feet. The section of the channel where channel slope flattens out is considerably smaller than the entire cell. Thus the information required to represent the depositional processes within the cell is a smaller scale than that of the grid-cell size used to delineate watershed characteristics. The inability to represent the smaller scale landscape information resulted in the model simulating entrainment rather than the actual deposition.

Considerable under-prediction of sediment loading at S3 and K6 occurs for storm 1. The model calculates a total of 41 tons eroded from sub-watershed S3 and 384 tons of sediment from K6 in overland processes. This sediment was subsequently transported overland to the sub-watershed's channel system. However, the model predicted 7.5 tons passing out of watershed S3 and 9.5 tons for K6. This represents channel deposition of 82% for sub-watershed S3 and 98% for sub-watershed K6. Observed sediment loadings of 26.1 and 27.2 tons at stations S3 and K6 demonstrate that not as much deposition occurred as was predicted by the model. A potential

source of error explaining the discrepancy between simulated and observed results is that the transport capacity calculated by the model was less than actual. The model calculated more sediment deposition along the sub-watershed's channels. Channel slopes which are not sufficiently steep will result in sediment deposition. A large percentage of the grid cells in sub-watersheds S3 and K6 did not contain a delineated channel, thus the default channel slope value - one half of the determined land slope - was used. In reality, concentrated flow channels are steeper for these cells, resulting in less deposition. A second potential source of error, particular to K6, is in the selection of a channel Mannings coefficient for fields experiencing low-till management practices. A large Mannings coefficient represents a flow path with residues obstructing the flow. Thus a large Mannings flow value, as assigned to the cells in sub-watersheds K4, K5 and K6, will result in slower flow velocities and less sediment transport capacity.

In general, the model over-predicts the amount of soluble Nitrogen. One sampling site for both storms however greatly under-predicts soluble Nitrogen. Total-Nitrogen loading at D1 for storm 1 was 1349.6 lbs, 13 times greater than predicted, and for storm 2 it was 284 lbs, 25 times greater than predicted. Over- and under-prediction also occurs at the other sampling sites. The average simulation error for the other stations is 3.2 times greater than observed data. A possible explanation for the large discrepancy in error related to D1 and the other sample sites is, that after establishing the sample sites within the Moyer watershed, it was noticed that the farmer who owned the field upstream from station D1 was depositing dead cattle

carcasses 20 to 30 yards away from the channel. Out-of-channel flow took place, potentially displacing decaying parts into the runoff flow. It is not known if this site has been a dump for a long period of time, creating a nutrient-rich point source.

Accuracy in nutrient predictions is extremely difficult due not only to the complex nature of the constituents within the natural environment, but also because of the inability to correctly determine application rates across a given field. Unfortunately not all the farmers in the watershed were willing to disclose Nitrogen application rates. Therefore the study had to assume a level of application that was consistent with neighboring farmers, and matched locally recommended fertilizer application rates.

5.3.4.2 Ranking Description

An ordinal ranking is achieved by a comparison of quantitative output results for sediment and Total-Nitrogen loading for each of the sub-watersheds. Although quantitative values were used to generate the ranking of watersheds, the ranking itself doesn't indicate more than the relative contribution of each of the sub-watersheds. In ranking sediment and Total-Nitrogen loading, the overestimation of loading from sub-watershed K4 created a ranking mismatch between observed and simulated results. As can be seen from the quantitative result output, a relatively large difference exists for sub-watershed K4 between observed and simulated output for both sediment and Total-Nitrogen loading. This difference between observed and simulated loading output for K4 is large enough to create a mismatch in the results order. Differences between the other sub-watersheds were not of the same magnitude, thus the ranking of

these sub-watersheds is the same for the two output results.

5.3.4.3 Selection Description

Identification of a sub-watershed as a contributing area is dependent upon the cut-off value used. The 25% value chosen for this study is arbitrary. Selecting a larger or smaller value will add or drop sub-watersheds from the list of contributing areas. A large difference between observed and simulated output values can result in the identification of different sub-watersheds as significant contributors. Such is the case for sub-watershed K4. Because of model overestimation for sediments and Total-Nitrogen, sub-watershed K4 was identified as a contributing watershed. However, from the observed results, sub-watershed K4 was not identified as a significant contributor of sediments and Total-Nitrogen.

CHAPTER 6

CONCLUSIONS

Geographic Information Systems and simulation models have been identified as integral tools for supporting the development of agricultural resource conservation and water quality management plans. It is anticipated that by enlisting these technologies, local conservation planners will operate more efficiently within the newly restructured farm services agency. It is further anticipated that by extending the management strategies developed with the aid of computer tools, effective, efficient and equitable reductions in NPS pollution can be achieved.

The basic goal of this research was to asses the capabilities of the GIS/simulation model integrated computer technology prior to its adoption into mainstream agricultural NPS pollution water quality planning and management. Development of this type of integrated technology is rapidly advancing in both academic and government research institutions. However, very little attention has been paid to the accuracy and the applied utility of this particular technological approach.

This research was divided into two separate parts, with each part addressing one half of the identified integrated technology: GIS, and the NPS pollution simulation model ANN-AGNPS. The first half of the research focused on the capabilities of the GIS to generate input parameters for the NPS pollution simulation

model from identified available digital data sources as compared to typically used map interpretation/field survey methods. The capabilities of GIS parameter generation were further tested by assessing model output results for the two parameter generation methods. The GIS used in this research was ESRI's ARC/INFO version 6.1 running on a UNIX workstation. The second half of the research focused on the predictive capabilities of the ANN-AGNPS water quality simulation model. The research was aimed at determining which type of NPS pollution contribution description the model is best capable of providing.

6.1 Hypothesis 1

Hypothesis 1 was divided into two sub-hypotheses. The first sub-hypothesis focused on assessing the similarities and differences of parameter input values from map interpretation/field surveying and GIS-based generation methods. It was concluded that the input parameter values are significantly different for the two methods when considering both 40- and 10-acre cell sizes. Thus the stated hypothesis: "... the error introduced with GIS-generated parameters will be insignificant" must be rejected.

The input parameters tested in the first sub-hypothesis were limited to topographically-derived inputs. Soil and field practice-derived parameters were not included in the analysis because the two input parameter generation methods resulted in the exact same selection for each cell throughout the watershed. The significant difference observed in the input parameter generation methods was thus due to the limitations of the GIS-based terrain analysis and slope determination procedures

together with the automated aggregation process of transferring data at a 30-meter resolution scale to 40- and 10-acre resolution scales. The terrain analysis procedures utilized in the research were those provided by the ARC/INFO software. The Jensen and Domingue (1988) method for generating concentrated flow networks, as mentioned in the literature review, has limitations particularly in flat or constant sloping landscapes. Other methods identified may provide more accurate location of concentrated flow channels as compared to map interpretation and field surveying. However, these alternative terrain analysis methods are primarily research procedures, and have not been integrated into commercially available GIS software. Development of spatial data bases more accurate than what can be provided by GIS processing of available digital data thus requires additional field surveying and measurements, including measurements of channel length and channel slope

The second sub-hypothesis addressed the propagation of error from the GIS-generated parameters to the output results. The hypothesis was tested by statistically comparing output results at individual grid cells as well as for the sub-watershed outlet points for the map interpretation/field survey and GIS-based parameter generation methods. The second sub-hypothesis assumed that model output results would be statistically similar because input values were significantly the same. The research has shown that the output results for both 40- and 10-acre cell size are in fact significantly similar. The second sub-hypothesis can be accepted. However, hypothesis acceptance is not due to statistically similar input parameter values.

The second sub-hypothesis demonstrates that even though the topographically-based parameters generated from the GIS routines are not well correlated with map interpretation/field survey methods, the final model output results, using the GIS parameters, are significantly the same as the results using map interpretation/field surveying methods. These results indicate that the ANN-AGNPS model output values are less sensitive to topographically-related input parameters and more sensitive to field practice and soil-related parameters. The observations from this research support the identification of model sensitive parameters made by Young et al. (1987). Three of the four most sensitive parameters they identified were related to soils and field practices: soil erodibility (K Factor), cropping practice (C Factor) and Curve Number. The fourth sensitive parameter was the topography-related hillside slope.

6.1.1 Implications of Hypothesis 1

By testing the hypotheses, this research has demonstrated that an agricultural NPS pollution water quality model will perform as well as more accurate and costly conventional methods of parameter generation when using GIS-generated input parameters. The results of this research support the direction of current technology-supportive policies. Federal and state government development of natural resource digital data will enable cost efficiencies in natural resource management when integrated with environmental simulation models through Geographic Information Systems. In light of this research, the Soils Conservation Services' current programs in developing integrated GIS/water quality simulation modeling tools are heading in a logical direction. Further, the efficiencies achieved with this technology will be

greatly needed in the anticipated restructured USDA farm service agency.

However, it is critical that limitations in the developed spatial data, due to collection error, scale and spatial resolution, as well as the short-comings in the geographical processing of spatial data not be forgotten. This research addressed the applicability of one tool widely used in NPS pollution water quality planning and management: AGNPS. There are many other water quality simulation models available to conservation resource planners. Some of the models are more analytically rigorous and sophisticated than AGNPS, others are not. It is not known whether the same conclusions about the sensitivity of the model to the inaccuracies in GIS-generated data can be extended to these modeling tools.

6.2 Hypothesis 2

Hypothesis 2 concentrated on testing the predictive capabilities of the ANN-AGNPS distributed-parameter agricultural NPS water pollution model. Model capabilities were assessed based upon the model's ability to describe sediment and Total-Nitrogen loading from sub-watersheds within the larger experimental watershed. The predictive descriptions to be tested included a quantitative description, a ranking description, and an identification description defined by a pre-determined cut-off range of greater than 25% of total loading. It was concluded through statistical analysis that the ANN-AGNPS model is incapable of estimating loading values when comparing simulated results to collected records. Thus Hypothesis 2: "The model cannot accurately predict quantitative contributions of NPS pollutants" is accepted. A qualitative comparative assessment of ranking and identification descriptions

determined that although the rankings and sub-watershed identifications did not match perfectly between model-simulated and observed values, there was a general correlation and alignment in the results. Thus, "the ANN-AGNPS model is only capable of providing identification and ranking description to contributing land", as stated in Hypothesis 2.

The ANN-AGNPS model's inability to accurately predict observed recordings was expected. Distributed-parameter process-based hydrologic and NPS pollution research models have been shown not to be accurate predictors of observed physical characteristics (Beven, 1989; 1993; Grayson et al., 1993; Loague and Freeze, 1985; 1993). Research models applied outside the experimental environment demonstrate even less predictive capabilities (Mitchell et al., 1993; Binger et al., 1989). Beven (1989, p. 159) identifies a number of reasons why distributed-parameter quasi-physical-based models are incapable of replicating the physical processes taking place within a watershed: (1) The equations used in hydrologic models are only approximate representations of the real world and must introduce some error arising from model structure. (2) Spatial heterogeneities in system responses may not be well reproduced by catchment average parameters. (3) The accuracy with which a model can be calibrated or validated is very dependent on errors in the observations of both inputs and outputs.

6.2.1 Implications of Hypothesis 2

Although the ANN-AGNPS model is not able to accurately predict NPS pollution loadings, it still can be used as an agricultural NPS pollution management

tool. There are alternative descriptions for NPS water pollution loading performance as forwarded in Hypothesis 2. These alternative descriptions can provide resource planners with vital information needed in identifying NPS pollution contributing lands and aid in the selection of BMPs for contributing lands in minimizing water quality impacts. The descriptions include an ordinal ranking of sub-watersheds relative to the NPS contribution of sediment and Total-Nitrogen and a nominal or identification description for a pre-determined cut-off value identifying which of the sub-watersheds within the larger watershed contribute significant NPS pollutants to the watershed outlet. Even with insignificant correlation between simulated model results and observed recordings, the model is capable of generating results that are accurate in relative terms.

The capacities and limitations of the model must be aligned with water quality management requirements mandated by policy. Overstating the capabilities of models to assist in water quality planning and management will lead to failure in achieving desired goals of pollution mitigation.

Implementation of the re-authorized Coastal Zone Management Act (CZMA) requires two levels of possible model application. The policy first requires that land areas and practices which threaten coastal water quality be identified. Second it requires quantitative estimations of pollution reduction effects for economically achievable management measures.

This research has demonstrated that the ANN-AGNPS water quality model is best capable of performing the first task of identifying lands within a watershed that

contribute agricultural pollutants to the watershed outlet. The model is incapable of accurately simulating agricultural pollution loading required in the second task. Therefore, quantitative estimations of potential reduction between alternative management measures is beyond the capacity of this model.

The Soil Conservation Service has chosen the AGNPS model as a NPS pollution simulation model to be used in carrying out programs required by the CZMA. However, as shown in this research, the model to be used by the federal government's lead technical agency will not perform the tasks required by the legislation. The SCS is obviously asking too much of the available technology. To ensure policy success, management requirements must become more aligned with capabilities of the technology. In the case of the re-authorized CZMA, quantitative estimations of NPS pollution loading from alternative management measures should be replaced with qualitative ordinal comparisons of alternative management measures. The requirement of qualitative descriptions of pollution loading in order to identify optimal management measures need not jeopardize attainment of overall policy goals.

6.3 Future Research Needs

This research involved the initial development of a computer-based distributed-parameter agricultural NPS simulation model. It used as a starting point the single rainfall event AGNPS model, and integrated into it available and tested algorithms for estimating daily changes in physical parameters influencing the generation and routing of water, sediment and nutrients. It is realized by the researcher that the encoding of algorithms into a computer program accomplishes only one intermediate step in the

model development process. The next steps of model verification and validation procedures were initiated in a single watershed under a limited number of rainfall events in a single growing season. The simulation results and conclusions drawn from the results are also limited to the particular agricultural environment and time-span in which data was collected. Continued research into the verification of the model as well as the initial conclusions presented in this research can only be achieved by comparing simulation results to collected data for additional agricultural watersheds which vary in size, cropping patterns, and physical characteristics for soils, slopes, channel network, and meteorology.

Upon simulation of multiple different agronomic, physical and meteorological agricultural conditions, the appropriateness of the ANN-AGNPS model's algorithms must be assessed. Sensitivity analyses can be used to isolate weaknesses in model performance. Sub-processes found to be error-prone can be re-calibrated to observed data or alternative algorithms incorporated and re-tested.

This research also involved the evaluation of GIS-generated input parameters of the ANN-AGNPS model. Even though significant differences between GIS and map interpretation/field survey methods did not produce significant differences in the model output results, continued research is needed to develop spatial data processing methods that generate more accurate data from the available digital data source. Improvements in the generation of topography-related parameters, such as hillslope, hillslope length, channel slope, channel side slope and channel length are particularly needed. The use of statistical probabilities in assigning flow direction for minimal

and constant sloping terrain is a new research area in stream network generation requiring more work. Further, the incorporation of secondary physical environmental and landscape characterization data, such as soil types, hillslope position and other geomorphic-based relationships can potentially be used to improve the generation of topographic parameters.

Determining the shape and scale of distributed-parameter computational units is a research area requiring more investigation. The artificial square boundaries of the grid cell can create discontinuities in the representation of "ground" data. Research into the analytic capabilities of GIS to generate distributed-parameter geometries that better fit the natural boundaries of the physical and agronomic environment is needed.

The integrated computer tool, GIS and simulation modeling, represents the future of resource management planning. This research focused on the use of GIS and simulation models for describing agricultural NPS pollution. It was demonstrated that these tools have inherent limitations, affecting the accuracy of NPS pollution estimation . The research undertaken represents the first step in identifying limitations in the tools. It thus provides an initial blueprint for refining analytic techniques and procedures in GIS and simulation modeling. As this technology matures through more testing and validation, confidence in its use will increase as conservation planners become better aware of the integrated tool's capabilities and limitations. Ultimately, this will result in better formulated policies and more successfully implemented programs.

APPENDIX A

BbB2 BARNES; FINE-LOAMY; 5 0.05 B 0.28 5.0 2.0
7.0 1.45 23.0 22.0 3.5 0.0 5.0
17.0 1.45 30.0 14.0 3.5 0.0 6.0
27.0 1.45 22.0 23.0 3.5 0.0 5.0
29.0 1.45 23.0 22.0 0.0 0.0 5.0
60.0 1.55 23.0 22.0 0.0 0.0 5.0

Va VALLERS-WINGER; SILTY-CLAY-LOAMS; 5 0.05 B 0.26 5.0 2.0
11.0 1.45 29.0 15.0 5.5 0.0 6.0
21.0 1.25 10.0 31.0 5.5 0.0 9.0
31.0 1.3 22.0 22.0 5.5 0.0 6.0
36.0 1.45 29.0 15.0 0.0 0.0 6.0
60.0 1.5 28.0 15.0 0.0 0.0 7.0

SuA SVEA; FINE-LOAMY; 4 0.05 B 0.3 5.0 2.0
10.0 1.2 23.0 22.0 6.5 0.0 5.0
20.0 1.2 14.0 30.0 6.5 0.0 6.0
21.0 1.35 22.0 23.0 0.0 0.0 5.0
60.0 1.2 23.0 22.0 0.0 0.0 5.0

Pf PARNELL and FLOM; FINE; 5 0.05 C 0.28 5.0 2.0
22.0 1.25 14.0 33.0 8.0 0.0 3.0
32.0 1.25 5.0 42.0 8.0 0.0 3.0
42.0 1.3 22.0 25.0 8.0 0.0 3.0
55.0 1.25 14.0 33.0 0.0 0.0 3.0
60.0 1.3 14.0 33.0 0.0 0.0 3.0

TaA TARA; FINE-SILTY; 5 0.5 B 0.3 5.0 2.0
19.0 1.45 25.0 22.0 6.0 0.0 3.0
29.0 1.45 19.0 28.0 6.0 0.0 3.0
37.0 1.45 25.0 22.0 0.0 0.0 3.0
43.0 1.45 25.0 22.0 0.0 0.0 3.0
60.0 1.48 22.0 22.0 0.0 0.0 6.0

BaA BARNES; FINE-LOAMY; 5 0.5 B 0.28 5.0 2.0
7.0 1.45 23.0 22.0 3.5 0.0 5.0
17.0 1.45 30.0 14.0 3.5 0.0 6.0
27.0 1.45 22.0 23.0 3.5 0.0 5.0
29.0 1.45 23.0 22.0 0.0 0.0 5.0
60.0 1.55 23.0 22.0 0.0 0.0 5.0

HdA TARA; FINE-LOAMY; 5 0.5 C 0.3 5.0 2.0
8.0 1.4 25.0 22.0 5.5 0.0 3.0
18.0 1.4 12.0 31.0 5.5 0.0 7.0
28.0 1.4 20.0 27.0 5.5 0.0 3.0
38.0 1.4 25.0 22.0 0.0 0.0 3.0
60.0 1.45 25.0 23.0 0.0 0.0 3.0

BuB2 BUSE; FINE-LOAMY; 2 0.5 B 0.33 5.0 2.0
1.0 7.00 1.45 22.0 22.0 2.0 0.0
60.0 7.45 1.55 20.0 22.0 0.0 0.0

SuB SVEA; FINE-LOAMY; 4 0.05 B 0.3 5.0 2.0
10.0 1.2 23.0 22.0 6.5 0.0 5.0
20.0 1.2 14.0 30.0 6.5 0.0 6.0
21.0 1.35 22.0 23.0 0.0 0.0 5.0
60.0 1.2 23.0 22.0 0.0 0.0 5.0

D1B DOLAND; FINE-LOAMY; 3 0.05 B 0.32 5.0 2.0
8.0 1.38 25.0 22.0 5.0 0.0 3.0
32.0 1.43 25.0 22.0 0.0 0.0 3.0
60.0 1.58 21.0 24.0 0.0 0.0 5.0

Pa PARNELL; FINE; 5 0.05 C 0.28 5.0 2.0
2.0 1.25 14.0 33.0 8.0 0.0 3.0
32.0 1.25 5.0 42.0 8.0 0.0 3.0
42.0 1.3 22.0 25.0 8.0 0.0 3.0
55.0 1.25 14.0 33.0 0.0 0.0 3.0
60.0 1.3 14.0 33.0 0.0 0.0 3.0

Top Row:

Map Symbol
Soil Name
Soil Texture
Number of Soil Layers
Soil Albedo
Hydraulic Soils Group
USLE K Factor
Initial Nitrogen Concentration (ppm)
Initial Phosphorus Concentration (ppm)

Subsequent Rows:

Soil Layers (in)
Bulk Density (gm/cc)
Percent Sand
Percent Clay
Percent Organic Matter
Cation Exchange Capacity

APPENDIX B

Field SB 1

Soybeans Soybeans
1 2 Soybeans 0 7
10/15/90 Tillage disk;_large_offset
04/20/91 Tillage cult;_field_(16-18)
04/21/91 Fertilize
60.0 30.0 30.0 20.0
04/21/91 Tillage harrow_(spike)
04/22/91 Plant planter:_row
06/16/91 Tillage cult;_field_(shovel)
09/28/91 Harvest/Cut Harvest
42.0 0.0 0.0
2 2 Soybeans 0 5
10/15/91 Tillage disk;_1-way_(18-22)
05/06/92 Tillage cult;_field_(16-18)
05/07/92 Fertilize
60.0 50.0 30.0 50.0
05/08/92 Plant planter:_row
11/06/92 Harvest/Cut Harvest
65.0 0.0 0.0

Field SB 2

Corn Soybeans
2 2 Corn 0 7
10/20/90 Tillage disk;_1-way_(18-22)
04/12/91 Tillage disk;_large_offset
04/14/91 Fertilize
120.0 60.0 60.0 50.0
04/17/91 Plant planter:_row
06/15/91 Tillage cult;_row
07/02/91 Tillage cult;_row
10/01/91 Harvest/Cut Harvest
120.0 0.0 0.0
2 2 Soybeans 0 5
10/15/91 Tillage disk;_1-way_(18-22)
05/06/92 Tillage cult;_field_(16-18)
05/07/92 Fertilize
60.0 50.0 30.0 50.0
05/08/92 Plant planter:_row
11/06/92 Harvest/Cut Harvest
65.0 0.0 0.0

Field SB 3

Corn Soybeans
2 2 Corn 0 7
10/20/90 Tillage disk;_1-way_(18-22)
04/12/91 Tillage disk;_large_offset
04/14/91 Fertilize
120.0 60.0 60.0 50.0
04/17/91 Plant planter:_row
06/15/91 Tillage cult;_row
07/02/91 Tillage cult;_row
10/01/91 Harvest/Cut Harvest
120.0 0.0 0.0
2 2 Soybeans 0 4
05/05/92 Tillage disk;_1-way_(18-22)
05/06/92 Fertilize
75.0 50.0 60.0 50.0
05/07/92 Plant planter:_row
11/05/92 Harvest/Cut Harvest
65.0 0.0 0.0

Field SB 4

Corn Soybeans
2 2 Corn 0 7
10/20/90 Tillage disk;_1-way_(18-22)
04/12/91 Tillage disk;_large_offset
04/14/91 Fertilize
120.0 60.0 60.0 50.0
04/17/91 Plant planter:_row
06/15/91 Tillage cult;_row
07/02/91 Tillage cult;_row
10/01/91 Harvest/Cut Harvest
120.0 0.0 0.0
2 2 Soybeans 0 5
10/15/91 Tillage disk;_1-way_(18-22)
05/06/92 Tillage cult;_field_(16-18)
05/07/92 Fertilize
60.0 50.0 30.0 50.0
05/08/92 Plant planter:_row
11/06/92 Harvest/Cut Harvest
65.0 0.0 0.0

Field SB 6

Soybeans Soybeans
1 2 Soybeans 0 7
10/15/90 Tillage disk;_large_offset
04/20/91 Tillage cult;_field_(16-18)
04/21/91 Fertilize
60.0 30.0 30.0 20.0
04/21/91 Tillage harrow_(spike)
04/22/91 Plant planter:_row
06/16/91 Tillage cult;_field_(shovel)
09/28/91 Harvest/Cut Harvest
42.0 0.0 0.0
2 2 Soybeans 0 5
10/15/91 Tillage disk;_1-way_(18-22)
05/06/92 Tillage cult;_field_(16-18)
05/07/92 Fertilize
60.0 50.0 30.0 50.0
05/08/92 Plant planter:_row
11/06/92 Harvest/Cut Harvest
65.0 0.0 0.0

Field SB 6

Corn Soybeans
2 2 Corn 0 7
10/20/90 Tillage disk;_1-way_(18-22)
04/12/91 Tillage disk;_large_offset
04/14/91 Fertilize
120.0 60.0 60.0 50.0
04/17/91 Plant planter:_row
06/15/91 Tillage cult;_row
07/02/91 Tillage cult;_row
10/01/91 Harvest/Cut Harvest
120.0 0.0 0.0
2 2 Soybeans 0 4
05/05/92 Tillage disk;_1-way_(18-22)
05/06/92 Fertilize
75.0 50.0 60.0 50.0
05/07/92 Plant planter:_row
11/05/92 Harvest/Cut Harvest
65.0 0.0 0.0

Field C1

Soybeans Corn
1 2 Soybeans 0 7
10/15/90 Tillage disk;_large_offset
04/20/91 Tillage cult;_field_(16-18)
04/21/91 Fertilize
60.0 30.0 30.0 20.0
04/21/91 Tillage harrow_(spike)
04/22/91 Plant planter:_row
06/16/91 Tillage cult;_field_(shovel)
09/28/91 Harvest/Cut Harvest
42.0 0.0 0.0
2 2 Corn 0 6
10/17/91 Tillage chisel_(2_in_shovel)
05/05/92 Tillage cult;_field_(16-18)
05/01/92 Fertilize
120.0 60.0 60.0 50.0
05/01/92 Plant planter:_row
06/25/92 Tillage cult;_row
11/02/92 Harvest/Cut Harvest
150.0 0.0 0.0

Field C2

Soybeans Corn
1 2 Soybeans 0 7
10/15/90 Tillage disk;_large_offset
04/20/91 Tillage cult;_field_(16-18)
04/21/91 Fertilize
60.0 30.0 30.0 20.0
04/21/91 Tillage harrow_(spike)
04/22/91 Plant planter:_row
06/16/91 Tillage cult;_field_(shovel)
09/28/91 Harvest/Cut Harvest
42.0 0.0 0.0
2 2 Corn 0 5
05/07/92 Tillage disk;_1-way_(18-22)
05/08/92 Fertilize
100.0 60.0 60.0 50.0
05/10/92 Plant planter:_row
06/28/92 Tillage cult;_row
11/17/92 Harvest/Cut Harvest
150.0 0.0 0.0

Field C3

Corn Corn
1 2 Corn 0 7
10/20/90 Tillage disk;_1-way_(18-22)
04/12/91 Tillage disk;_large_offset
04/14/91 Fertilize
120.0 60.0 60.0 50.0
04/17/91 Plant planter:_row
06/15/91 Tillage cult;_row
07/02/91 Tillage cult;_row
10/01/91 Harvest/Cut Harvest
120.0 0.0 0.0
2 2 Corn 0 5
05/07/92 Tillage disk;_1-way_(18-22)
05/08/92 Fertilize
100.0 60.0 60.0 50.0
05/10/92 Plant planter:_row
06/28/92 Tillage cult;_row
11/17/92 Harvest/Cut Harvest
150.0 0.0 0.0

Field C4

Soybeans Corn
1 2 Soybeans 0 7
10/15/90 Tillage disk;_large_offset
04/20/91 Tillage cult;_field_(16-18)
04/21/91 Fertilize
60.0 30.0 30.0 20.0
04/21/91 Tillage harrow_(spike)
04/22/91 Plant planter:_row
06/16/91 Tillage cult;_field_(shovel)
09/28/91 Harvest/Cut Harvest
42.0 0.0 0.0
2 2 Corn 0 6
10/17/91 Tillage chisel_(2_in_shovel)
05/01/92 Tillage cult;_field_(16-18)
05/01/92 Fertilize
120.0 60.0 60.0 50.0
05/05/92 Plant planter:_row
06/25/92 Tillage cult;_row
11/02/92 Harvest/Cut Harvest
150.0 0.0 0.0

Field C5

Soybeans Corn
1 2 Soybeans 0 7
10/15/90 Tillage disk;_large_offset
04/20/91 Tillage cult;_field_(16-18)
04/21/91 Fertilize
60.0 30.0 30.0 20.0
04/21/91 Tillage harrow_(spike)
04/22/91 Plant planter:_row
06/16/91 Tillage cult;_field_(shovel)
09/28/91 Harvest/Cut Harvest
42.0 0.0 0.0
2 2 Corn 0 5
05/07/92 Tillage disk;_1-way_(18-22)
05/08/92 Fertilize
100.0 60.0 60.0 50.0
05/10/92 Plant planter:_row
06/28/92 Tillage cult;_row
11/17/92 Harvest/Cut Harvest
150.0 0.0 0.0

Field C6

Soybeans Corn
1 2 Soybeans 0 7
10/15/90 Tillage disk;_large_offset
04/20/91 Tillage cult;_field_(16-18)
04/21/91 Fertilize
60.0 30.0 30.0 20.0
04/21/91 Tillage harrow_(spike)
04/22/91 Plant planter:_row
06/16/91 Tillage cult;_field_(shovel)
09/28/91 Harvest/Cut Harvest
42.0 0.0 0.0
2 2 Corn 0 6
10/15/91 Tillage chisel_(2_in_shovel)
05/06/92 Tillage disk;_1-way_(18-22)
05/07/92 Fertilize
120.0 60.0 60.0 50.0
04/17/92 Plant planter:_row
06/29/92 Tillage cult;_row
11/14/92 Harvest/Cut Harvest
170.0 0.0 0.0

Field C7

Corn Corn
1 2 Corn 0 7
10/20/90 Tillage disk;_1-way_(18-22)
04/12/91 Tillage disk;_large_offset
04/14/91 Fertilize
120.0 60.0 60.0 50.0
04/17/91 Plant planter:_row
06/15/91 Tillage cult;_row
07/02/91 Tillage cult;_row
10/01/91 Harvest/Cut Harvest
120.0 0.0 0.0
2 2 Corn 0 6
10/17/91 Tillage chisel_(2_in_shovel)
05/01/92 Tillage cult;_field_(16-18)
05/01/92 Fertilize
120.0 60.0 60.0 50.0
05/05/92 Plant planter:_row
06/25/92 Tillage cult;_row
11/02/92 Harvest/Cut Harvest
150.0 0.0 0.0

Field C8

Soybeans Corn
1 2 Soybeans 0 7
10/15/90 Tillage disk;_large_offset
04/20/91 Tillage cult;_field_(16-18)
04/21/91 Fertilize
60.0 30.0 30.0 20.0
04/21/91 Tillage harrow_(spike)
04/22/91 Plant planter:_row
06/16/91 Tillage cult;_field_(shovel)
09/28/91 Harvest/Cut Harvest
42.0 0.0 0.0
2 2 Corn 0 6
10/17/91 Tillage chisel_(2_in_shovel)
05/01/92 Tillage cult;_field_(16-18)
05/01/92 Fertilize
120.0 60.0 60.0 50.0
05/05/92 Plant planter:_row
06/25/92 Tillage cult;_row
11/02/92 Harvest/Cut Harvest
120.0 0.0 0.0

Field C9

Soybeans Corn
1 2 Soybeans 0 7
10/15/90 Tillage disk;_large_offset
04/20/91 Tillage cult;_field_(16-18)
04/21/91 Fertilize
60.0 30.0 30.0 20.0
04/21/91 Tillage harrow_(spike)
04/22/91 Plant planter:_row
06/16/91 Tillage cult;_field_(shovel)
09/28/91 Harvest/Cut Harvest
42.0 0.0 0.0
2 2 Corn 0 6
10/17/91 Tillage chisel_(2_in_shovel)
05/01/92 Tillage cult;_field_(16-18)
05/01/92 Fertilize
120.0 60.0 60.0 50.0
05/05/92 Plant planter:_row
06/25/92 Tillage cult;_row
11/02/92 Harvest/Cut Harvest
150.0 0.0 0.0

Field C10

Soybeans Corn
1 2 Soybeans 0 7
10/15/90 Tillage disk;_large_offset
04/20/91 Tillage cult;_field_(16-18)
04/21/91 Fertilize
60.0 30.0 30.0 20.0
04/21/91 Tillage harrow_(spike)
04/22/91 Plant planter:_row
06/16/91 Tillage cult;_field_(shovel)
09/28/91 Harvest/Cut Harvest
42.0 0.0 0.0
2 2 Corn 0 5
11/09/91 Tillage chisel_(2_in_shovel)
05/05/92 Tillage disk;_1-way_(18-22)
05/05/92 Plant planter:_row
05/05/92 Fertilize
50.0 50.0 50.0 50.0
11/06/92 Harvest/Cut Harvest
120.0 0.0 0.0

Field C11

Corn Corn
1 2 Corn 0 7
10/20/90 Tillage disk;_1-way_(18-22)
04/12/91 Tillage disk;_large_offset
04/14/91 Fertilize
120.0 60.0 60.0 50.0
04/17/91 Plant planter:_row
06/15/91 Tillage cult;_row
07/02/91 Tillage cult;_row
10/01/91 Harvest/Cut Harvest
120.0 0.0 0.0
2 2 Corn 0 5
11/09/91 Tillage chisel_(2_in_shovel)
05/05/92 Tillage disk;_1-way_(18-22)
05/05/92 Plant planter:_row
05/05/92 Fertilize
50.0 50.0 50.0 50.0
11/06/92 Harvest/Cut Harvest
120.0 0.0 0.0

Field W1

Soybeans Spring_Wheat
1 2 Soybeans 0 7
10/15/90 Tillage disk;_large_offset
04/20/91 Tillage cult;_field_(16-18)
04/21/91 Fertilize
60.0 30.0 30.0 20.0
04/21/91 Tillage harrow_(spike)
04/22/91 Plant planter:_row
06/16/91 Tillage cult;_field_(shovel)
09/28/91 Harvest/Cut Harvest
42.0 0.0 0.0
2 2 Spring_Wheat 0 4
10/15/91 Tillage chisel_(2_in_shovel)
04/25/92 Plant drill;_conventional
04/26/92 Fertilize
129.0 50.0 0.0 0.0
08/15/92 Harvest/Cut Harvest
60.0 0.0 0.0

Field W2

Soybeans Spring_Wheat
1 2 Soybeans 0 7
10/15/90 Tillage disk;_large_offset
04/20/91 Tillage cult;_field_(16-18)
04/21/91 Fertilize
60.0 30.0 30.0 20.0
04/21/91 Tillage harrow_(spike)
04/22/91 Plant planter:_row
06/16/91 Tillage cult;_field_(shovel)
09/28/91 Harvest/Cut Harvest
42.0 0.0 0.0
2 2 Spring_Wheat 0 4
04/21/92 Tillage disk;_1-way_(18-22)
04/22/92 Plant drill;_conventional
04/24/92 Fertilize
50.0 50.0 0.0 0.0
08/10/92 Harvest/Cut Harvest
58.0 0.0 0.0

Field W3

Soybeans Spring_Wheat
1 2 Soybeans 0 7
10/15/90 Tillage disk;_large_offset
04/20/91 Tillage cult;_field_(16-18)
04/21/91 Fertilize
60.0 30.0 30.0 20.0
04/21/91 Tillage harrow_(spike)
04/22/91 Plant planter:_row
06/16/91 Tillage cult;_field_(shovel)
09/28/91 Harvest/Cut Harvest
42.0 0.0 0.0
2 2 Spring_Wheat 0 4
04/21/92 Tillage disk;_1-way_(18-22)
04/22/92 Plant drill;_conventional
04/24/92 Fertilize
50.0 50.0 0.0 0.0
08/10/92 Harvest/Cut Harvest
58.0 0.0 0.0

Field W4

Soybeans Spring_Wheat
1 2 Soybeans 0 7
10/15/90 Tillage disk;_large_offset
04/20/91 Tillage cult;_field_(16-18)
04/21/91 Fertilize
60.0 30.0 30.0 20.0
04/21/91 Tillage harrow_(spike)
04/22/91 Plant planter:_row
06/16/91 Tillage cult;_field_(shovel)
09/28/91 Harvest/Cut Harvest
42.0 0.0 0.0
2 2 Spring_Wheat 0 4
04/21/92 Tillage disk;_1-way_(18-22)
04/22/92 Plant drill;_conventional
04/24/92 Fertilize
50.0 50.0 0.0 0.0
08/10/92 Harvest/Cut Harvest
58.0 0.0 0.0

Field F1

Spring_Wheat Spring_Wheat
1 2 Spring_Wheat 0 4
04/10/90 Fertilize
75.0 70.0 55.0 70.0
04/16/91 Tillage cult;_field_(shovel)
04/17/91 Plant drill;_conventional
08/04/91 Harvest/Cut Harvest
38.5 0.0 0.0
2 2 Spring_Wheat 0 4
04/10/92 Fertilize
75.0 70.0 55.0 70.0
04/16/92 Tillage cult;_field_(shovel)
04/17/92 Plant drill;_conventional
08/04/92 Harvest/Cut Harvest
38.5 0.0 0.0

APPENDIX C

Table C1 40 Acre Grid Cell Interpreted Model Input Parameter Values

Cell #	Flow Direct-ion	Rec. Cell	Hill Slope	Slope Length	Channel Slope	Channel Length	Channel Side Slope	Mann. N	Soils	Fields
1	5	4	2.1	100	1.05*	660*	10.0*	0.045	SaA	W1
2	5	5	1.7	100	0.85*	660*	10.0*	0.045	Pf	W2
3	5	10	3.6	125	1.0	900	5.6	0.033	BbB2	C1
4	5	11	1.3	100	0.65*	1320*	10.0*	0.045	BbB2	W3
5	5	12	2.4	100	1.2*	660*	10.0*	0.045	Ta	C2
6	5	13	2.4	100	2.0	1050	10.0*	0.080	Pf	SB3
7	5	14	6.2	125	3.1*	660*	10.0*	0.045	BbB2	SB3
8	5	9	3.3	125	1.55*	660*	10.0*	0.045	Va	SB2
9	4	18	3.1	125	1.1	2100	10.0*	0.033	BbB2	C1
10	5	18	3.4	125	2.5	1360	8.6	0.080	BbB2	SB6
11	5	19	3.1	125	1.6	1400	10.0*	0.080	BbB2	C2
12	5	20	1.4	100	2.0	1100	10.0*	0.080	BbB2	SB3
13	5	21	2.5	100	1.2	1500	5.6	0.080	HdA	SB3
14	5	22	4.0	125	1.3	1325	9.6	0.080	TaA	C4
15	7	15	1.2	100	0.6*	660*	10.0*	0.045	BuB2	C4
16	3	18	0.9	125	0.45*	660*	10.0*	0.045	SuA	SB5
17	4	24	2.8	100	1.1	2117	3.4	0.033	Pf	C6
18	5	24	3.8	100	1.4	1502	7.0	0.033	BbB2	C6
19	5	25	1.1	100	0.55*	1320*	10.0*	0.045	TaA	W4
20	5	26	1.6	100	1.1	1500	10.4	0.080	TaA	C5
21	7	21	2.4	125	0.8	800	9.6	0.080	BbB2	SB4
22	3	24	4.1	125	1.1	1200	10.0*	0.033	BbB2	C6
23	3	25	1.5	100	0.5	1700	3.9	0.080	BbB2	C6
24	5	28	1.6	125	0.3	1400	10.4	0.033	Pf	W4
25	7	25	0.8	100	0.9	1000	10.4	0.033	TaA	C5
26	1	23	1.1	100	0.55*	660*	10.0*	0.045	BaA	C9

* Approximated Input Parameter Values

Table C2 10 Acre Grid Cell Interpreted Model Input Parameter Values

Cell #	Flow Direct-ion	Rec. Cell	Hill Slope	Slope Length	Channel Slope	Channel Length	Channel Side Slope	Mann. N	Soils	Fields
1	5	2	2.0	100	1.0*	330*	10.0*	0.045	BbB2	W1
2	6	12	2.1	100	1.05*	738*	10.0*	0.045	BbB2	W1
3	5	14	2.3	100	1.15*	330*	10.0*	0.045	BbB2	W1
4	5	15	0.7	100	.35*	330*	10.0*	0.045	BbB2	W2
5	5	16	2.3	100	1.15*	330*	10.0*	0.045	BbB2	W2
6	5	17	1.4	100	0.7*	330*	10.0*	0.045	BbB2	W2
7	5	18	0.8	100	0.4*	330*	10.0*	0.045	BbB2	W2
8	5	19	1.4	100	0.7*	330*	10.0*	0.045	BbB2	SB1
9	5	20	1.6	100	0.8*	330*	10.0*	0.045	BbB2	SB1
10	5	21	1.5	100	0.75*	330*	10.0*	0.045	BbB2	SB1
11	5	22	0.5	100	0.25*	330*	10.0*	0.045	TaA	SB1
12	5	24	1.8	100	0.9*	330*	10.0*	0.045	BbB2	C1
13	4	26	7.1	100	3.55*	466*	10.0*	0.045	BbB2	C1
14	5	26	1.2	100	0.6*	660*	10.0*	0.045	BbB2	C1
15	5	27	1.1	100	0.55*	660*	10.0*	0.045	BbB2	W3
16	5	28	1.4	100	0.7*	660*	10.0*	0.045	BbB2	C2
17	5	29	1.4	100	0.7*	660*	10.0*	0.045	BbB2	C2
18	5	30	1.0	100	0.5*	660*	10.0*	0.045	BbB2	C2
19	5	31	1.1	100	0.55*	660*	10.0*	0.045	BbB2	C3
20	5	32	2.1	100	1.05*	660*	10.0*	0.045	SaA	C3
21	5	33	3.3	125	1.65*	660*	10.0*	0.045	BbB2	C3
22	5	34	6.2	125	3.3	540	10.0*	0.080	BbB2	C3
23	5	35	4.6	125	2.3*	330*	10.0*	0.045	HdA	SB2
24	4	38	1.1	100	0.6	762	10.0*	0.033	BbB2	C1
25	5	38	0.8	100	0.4*	660*	10.0*	0.045	BbB2	C1
26	4	40	2.0	100	1.0*	933*	10.0*	0.045	BbB2	C1
27	5	40	1.8	100	0.9*	660*	10.0*	0.045	BbB2	SB6
28	6	40	1.2	100	0.6*	738*	10.0*	0.045	TaA	C2
29	5	42	1.4	100	0.7*	660*	10.0*	0.045	TaA	C2
30	5	43	1.1	100	0.55*	660*	10.0*	0.045	Pf	C2

Table C2 10 Acre Grid Cell Interpreted Model Input Parameter Values (continued)

Cell #	Flow Direct-ion	Rec. Cell	Hill Slope	Slope Length	Channel Slope	Channel Length	Channel Side Slope	Mann. N	Soils	Fields
31	5	44	0.8	100	0.4*	660*	10.0*	0.045	BbB2	SB3
32	5	45	1.2	100	1.1	743	10.0*	0.045	BbB2	SB#
33	5	46	4.9	125	2.45*	660*	10.0*	0.045	BbB2	SB3
34	5	47	7.2	125	2.2	708	10.0*	0.080	BbB2	SB3
35	5	48	5.2	125	1.5	870	10.0*	0.080	BbB2	SB2
36	5	49	2.8	100	1.4*	330*	10.0*	0.045	SuA	SB2
37	3	38	0.8	100	0.4*	330*	10.0*	0.045	BbB2	C1
38	5	51	1.0	100	1.0	778	10.0*	0.033	BbB2	C1
39	5	52	1.6	100	0.8*	660*	10.0*	0.045	BbB2	C1
40	5	53	3.0	125	0.7	812	10.0*	0.080	BbB2	SB6
41	5	54	2.0	100	1.0*	660*	10.0*	0.045	BbB2	C2
42	5	55	1.3	100	0.65*	660*	10.0*	0.045	BbB2	C2
43	5	56	1.2	100	1.1	801	10.0*	0.080	BbB2	C2
44	5	57	1.0	100	0.5*	660*	10.0*	0.045	BbB2	SB3
45	5	58	2.3	100	2.3	690	10.0*	0.080	BbB2	SB3
46	5	59	1.5	100	0.75*	660*	10.0*	0.045	BbB2	SB3
47	5	60	3.5	125	1.2	674	10.0*	0.080	BbB2	SB3
48	5	61	4.4	125	2.2	667*	9.6	0.080	BbB2	C4
49	7	48	2.8	100	1.4*	660*	10.0*	0.045	BuB2	C4
50	7	49	1.6	100	0.8*	330*	10.0*	0.045	TaA	C4
51	3	52	1.6	100	0.8*	330*	10.0*	0.045	SuB	C1
52	4	66	3.1	125	0.7	697	5.6	0.080	BbB2	C1
53	5	66	3.0	125	1.5*	660*	10.0*	0.045	BbB2	SB6
54	5	67	2.8	100	1.4*	660*	10.0*	0.045	BbB2	C2
55	5	68	2.3	100	2.0	627	9.6	0.080	BbB2	C2
56	5	69	2.3	100	1.15*	660*	10.0*	0.045	SuA	C2
57	5	70	1.2	100	0.6*	660*	10.0*	0.045	BbB2	SB3
58	3	59	1.7	100	0.85*	330*	10.0*	0.045	BbB2	SB3
59	5	72	2.1	100	1.05*	660*	10.0*	0.045	Pf	F1

Table C2 10 Acre Grid Cell Interpreted Model Input Parmater Values (continued)

Cell #	Flow Direct-ion	Rec. Cell	Hill Slope	Slope Length	Channel Slope	Channel Length	Channel Side Slope	Mann. N	Soils	Fields
60	7	59	2.0	100	1.0*	330*	10.0*	0.045	TaA	F1
61	5	74	1.4	100	0.7*	660*	10.0*	0.045	D1B	C4
62	7	61	1.6	100	0.8*	660*	10.0*	0.045	TaA	C4
63	7	62	1.6	100	0.8*	330*	10.0*	0.045	BuB2	C4
64	3	65	1.9	100	0.95*	330*	10.0*	0.045	BbB2	SB5
65	3	66	4.0	125	2.0*	660*	10.0*	0.045	BbB2	SB5
66	4	78	2.3	100	1.2	845	3.4	0.080	Pf	C6
67	5	78	3,9	125	1.95*	660*	10.0*	0.045	BbB2	C6
68	5	79	1.3	100	0.75*	660*	10.0*	0.045	BbB2	C6
69	5	80	2.1	100	1.4	712	8.6	0.033	TaA	C6
70	5	81	1.0	100	0.5*	660*	10.0*	0.045	BbB2	W4
71	5	82	1.0	100	0.5*	660*	10.0*	0.045	TaA	W4
72	6	82	0.8	100	0.7	707	9.6	0.080	Pf	C5
73	5	84	0.6	100	0.3*	660*	10.0*	0.045	TaA	C5
74	6	84	1.4	100	1.0	670	9.6	0.080	BbB2	SB4
75	7	74	1.6	100	0.8*	330*	10.0*	0.045	BbB2	SB4
76	3	77	1.8	100	0.9*	330*	10.0*	0.045	SuA	C7
77	3	78	3.5	125	1.75*	660*	10.0*	0.045	BbB2	C6
78	4	88	2.3	100	0.6	743	3.4	0.033	Pf	C6
79	5	88	4.6	125	2.3*	660*	10.0*	0.045	Pf	C6
80	5	89	2.1	100	0.7	670	10.0*	0.033	BbB2	C6
81	4	91	1.1	100	0.55*	738*	10.0*	0.045	Pa	W4
82	5	91	1.4	100	0.6	590	9.6	0.080	TaA	W4
83	7	82	1.1	100	0.55*	660*	10.0*	0.045	TaA	C5
84	6	92	1.2	100	0.8	1192	10.0*	0.033	TaA	C5
85	3	86	2.1	100	1.05*	330*	10.0*	0.045	BbB2	C7
86	3	87	2.3	100	1.15*	660*	10.0*	0.045	SuA	C6
87	3	88	1.7	100	1.7	551	10.0*	0.033	Pf	C6
88	3	89	1,8	100	0.7	699	3.4	0.033	BbB2	C6

Table C2 10 Acre Grid Cell Interpreted Model Input Parameter Values (continued)

Cell #	Flow Direct-ion	Rec. Cell	Hill Slope	Slope Length	Channel Slope	Channel Length	Channel Side Slope	Mann. N	Soils	Fields
89	4	99	1.6	100	0.5	818	3.4	0.033	Pf	C6
90	5	99	3.0	125	1.5*	330*	10.0*	0.045	BbB2	W4
91	5	100	2.9	100	0.8	682	10.0*	0.080	TaA	W4
92	7	91	1.7	100	0.8	987	10.0*	0.033	Pf	C5
93	7	92	1.6	100	0.8*	330*	10.0*	0.045	DlB	C5
94	3	95	2.3	100	1.15*	330*	10.0*	0.045	SuA	C7
95	3	96	1.8	100	1.7	693	10.0*	0.033	BaA	C6
96	1	87	2.8	100	1.1	745	10.0*	0.033	BbB2	C6
97	3	98	2.2	100	1.1*	330*	10.0*	0.045	BbB2	C6
98	3	99	2.1	100	1.05*	660*	10.0*	0.045	BbB2	C6
99	3	100	3.6	125	0.4	670	10.4	0.080	BbB2	C10
100	5	108	0.8	100	0.2	853	10.4	0.080	Pf	C11
101	7	100	0.4	100	0.2*	330*	10.0*	0.045	TaA	C5
102	3	103	0.3	100	0.15*	330*	10.0*	0.045	HdA	C8
103	3	104	1.1	100	0.55*	660*	10.0*	0.045	BaA	C9
104	1	96	0.9	100	0.45*	330*	10.0*	0.045	BbB2	C9
105	1	97	0.6	100	0.3*	330*	10.0*	0.045	Pf	C9
106	2	103	0.2	100	0.1*	466*	10.0*	0.045	HdA	C8
107	1	103	0.2	100	0.1*	330*	10.0*	0.045	BbB2	C9

* Approximated Input Parameter Values

Table C3 40 Acre Grid Cell GIS-Generated Model Input Parameter Values

Cell Number	Direct.	Rec. Cell	Hillside Slope	Slope Length	Channel Slope	Channel Length	Channel Side Slope	Mann. N	Soils	Fields
1	5	2	0.27	100	0.27	660	10.0	0.045	BbB2	W1
2	5	8	0.22	100	0.19	1320	10.0	0.045	BbB2	W1
3	6	8	2.21	100	2.40	933	10.0	0.045	BbB2	W3
4	5	10	1.67	100	1.57	660	10.0	0.045	Bbb2	C2
5	5	11	1.84	100	0.46	660	10.0	0.045	Bbb2	C3
6	3	7	1.66	100	2.07	660	10.0	0.045	BbB2	C3
7	6	12	0.79	100	0.38	933	10.0	0.045	Va	SB2
8	5	15	2.67	100	0.01	1501	10.0	0.033	BbB2	W1
9	5	8	0.90	100	2.57	660	10.0	0.045	BbB2	W3
10	5	15	3.32	125	2.28	1320	10.0	0.045	BbB2	C2
11	4	18	2.30	100	4.10	1475	10.0	0.045	BbB2	SB3
12	5	18	2.40	100	1.94	1171	10.0	0.033	BbB2	SB3
13	7	12	2.51	100	2.50	933	10.0	0.045	BbB2	C4
14	3	8	1.99	100	0.90	760	10.0	0.033	SuA	SB5
15	5	20	4.83	125	1.90	1293	10.0	0.033	Pf	C6
16	3	17	3.43	125	1.67	933	10.0	0.045	SuA	C6
17	5	22	2.01	100	2.01	67	10.0	0.033	TaA	W4
18	6	22	0.56	100	0.51	1492	10.0	0.033	BbB2	C5
19	7	18	3.29	125	3.14	660	10.0	0.045	BbB2	SB4
20	3	21	4.44	125	3.06	732	10.0	0.033	BbB2	C6
21	3	16	1.41	100	0.36	1186	10.0	0.033	Pf	C6
22	2	24	1.35	100	0.61	993	10.0	0.033	BbB2	W4
23	1	20	0.71	100	0.07	933	10.0	0.045	BaA	C9

Table C4 10 Acre Grid Cell GIS-Generated Model Input Parameter Values

Cell Number	Direct.	Rec. Cell	Hillside Slope	Slope Length	Channel Slope	Channel Length	Channel Side Slope	Mann. N	Soils	Fields
1	6	2	1.40	100	1.40	466	10.0	0.045	BbB2	W1
2	5	12	0.49	100	0.49	738	10.0	0.045	BbB2	W1
3	7	2	2.75	100	1.57	396	10.0	0.045	Pf	W1
4	6	13	3.30	125	3.30	330	10.0	0.045	BbB2	W1
5	5	15	1.72	100	1.72	330	10.0	0.045	BbB2	W2
6	4	17	1.59	100	1.59	466	10.0	0.045	BbB2	W2
7	5	17	1.76	100	1.76	330	10.0	0.045	BbB2	W2
8	4	20	2.04	100	2.04	466	10.0	0.045	BbB2	SB1
9	5	20	1.15	100	1.15	330	10.0	0.045	BbB2	SB1
10	4	22	2.73	100	2.73	466	10.0	0.045	BbB2	SB1
11	4	23	1.56	100	1.56	466	10.0	0.045	BbB2	SB1
12	4	25	3.43	125	3.78	589	10.0	0.033	BbB2	C1
13	7	12	0.12	100	0.22	487	10.0	0.033	BbB2	C1
14	5	26	1.47	100	1.47	330	10.0	0.033	BbB2	C1
15	5	27	2.70	100	2.40	348	10.0	0.033	BbB2	W3
16	5	28	1.15	100		660	10.0	0.033	BbB2	W3
17	5	29	1.75	100	1.75	738	10.0	0.033	BbB2	C2
18	5	30	1.81	100	1.81	330	10.0	0.033	BbB2	C2
19	6	30	1.59	100		466	10.0	0.033	SaA	C3
20	6	31	0.66	100	0.66	738	10.0	0.033	SaA	C3
21	3	22	2.51	100	0.17	330	10.0	0.033	BbB2	C3
22	6	33	3.61	125	2.40	623	10.0	0.033	BbB2	C3
23	5	35	1.22	100	2.02	738	10.0	0.033	HdA	SB2
24	7	23	1.03	100	1.03	466	10.0	0.033	BbB2	SB2
25	5	37	0.52	100		370	10.0	0.033	BbB2	C1
26	4	39	0.17	100	0.17	738	10.0	0.045	Pf	C1
27	5	39	2.22	100	2.21	660	10.0	0.045	BbB2	SB6
28	5	40	1.15	100	1.25	755	10.0	0.045	BbB2	W3
29	3	30	1.48	100	0.01	466	10.0	0.045	TaA	C2
30	5	42	1.98	100	1.57	599	10.0	0.045	Pf	C2

Table C4 10 Acre Grid Cell GIS-Generated Model Input Parameter Values (continued)

Cell Number	Direct.	Rec. Cell	Hillslide Slope	Slope Length	Channel Slope	Channel Length	Channel Side Slope	Mann. N	Soils	Fields
31	5	43	2.02	100	1.99	697	10.0	0.045	BbB2	SB3
32	5	44	2.57	100	2.80	480	10.0	0.045	BbB2	SB3
33	4	46	4.68	125	2.37	660	10.0	0.045	BbB2	SB3
34	5	46	5.71	125		330	10.0	0.033	BbB2	SB3
35	6	46	3.13	125	3.11	728	10.0	0.045	BbB2	SB2
36	7	35	0.01	100	0.01	330	10.0	0.045	SaA	SB2
37	5	49	0.67	100	0.01	728	10.0	0.033	BbB2	C1
38	5	50	2.97	100	2.97	330	10.0	0.045	BbB2	C1
39	5	51	1.49	100	0.99	738	10.0	0.045	BbB2	SB6
40	5	52	1.88	100	1.88	660	10.0	0.045	BbB2	C2
41	5	53	0.74	100	0.56	784	10.0	0.045	BbB2	C2
42	5	54	3.83	125	3.83	660	10.0	0.045	BbB2	C2
43	4	56	2.81	100	4.10	734	10.0	0.045	BbB2	SB3
44	4	57	4.66	125	3.87	747	10.0	0.045	BbB2	SB3
45	5	57	4.55	125	2.72	665	10.0	0.045	BbB2	SB3
46	6	57	3.92	125	0.18	673	10.0	0.033	BbB2	SB3
47	6	58	3.06	125	2.50	462	10.0	0.045	BbB2	C4
48	5	60	2.15	100	2.15	330	10.0	0.045	BbB2	C4
49	4	62	1.72	100	0.01	345	10.0	0.033	SaA	C1
50	5	62	4.61	125	0.31	713	10.0	0.033	BuB2	C1
51	5	63	0.50	100	0.01	462	10.0	0.045	BbB2	SB6
52	6	63	2.47	100		738	10.0	0.045	BbB2	C2
53	5	65	0.48	100	0.65	660	10.0	0.045	BbB2	C2
54	5	66	2.54	100	2.54	660	10.0	0.045	BbB2	C2
55	5	67	2.22	100	2.22	746	10.0	0.045	BbB2	SB3
56	3	57	2.89	100	1.14	330	10.0	0.045	BbB2	SB3
57	5	69	2.47	100	1.46	416	10.0	0.033	BbB2	SB3
58	6	69	2.01	100	2.99	420	10.0	0.033	TaA	F1
59	5	71	3.75	125	3.08	348	10.0	0.045	D1B	C4

Table C4 10 Acre Grid Cell GIS-Generated Model Input Parameter Values (continued)

Cell Number	Direct.	Rec. Cell	Hillside Slope	Slope Length	Channel Slope	Channel Length	Channel Side Slope	Mann. N	Soils	Fields
60	5	72	3.72	125	0.01	660	10.0	0.045	TaA	C4
61	6	72	2.59	100	2.59	416	10.0	0.045	BuB2	C4
62	3	63	1.95	100	1.95	330	10.0	0.045	BbB2	SB5
63	4	75	3.35	125	3.71	955	10.0	0.033	Pf	C6
64	7	63	4.23	125	2.33	330	10.0	0.045	BbB2	C6
66	5	77	2.92	100	0.60	660	10.0	0.045	BbB2	C6
67	4	79	2.84	100	2.57	738	10.0	0.045	BbB2	W4
68	5	79	3.89	125	0.01	330	10.0	0.045	TaA	W4
69	5	80	1.00	100	0.51	696	10.0	0.033	Pf	C5
70	6	80	1.54	100	1.46	466	10.0	0.045	TaA	C5
71	6	81	1.61	100	1.56	738	10.0	0.045	TaA	SB4
72	7	71	3.46	125	3.46	738	10.0	0.045	BbB2	SB4
73	2	85	2.30	100	2.30	466	10.0	0.045	BbB2	SB5
74	3	75	3.98	125	0.10	272	10.0	0.033	BbB2	C6
75	4	87	2.92	100	2.77	784	10.0	0.033	Pf	C6
76	5	87	2.38	100	0.01	466	10.0	0.045	Pf	C6
77	6	87	3.37	125	2.95	738	10.0	0.045	BbB2	C6
78	3	79	1.88	100	1.85	330	10.0	0.045	Pa	W4
79	5	90	0.26	100	0.01	430	10.0	0.033	TaA	W4
80	7	79	0.37	100	1.75	314	10.0	0.033	TaA	C5
81	6	91	2.04	100	2.35	933	10.0	0.045	TaA	C5
82	7	91	1.62	100	1.55	660	10.0	0.045	TaA	SB4
83	7	82	1.57	100	1.57	330	10.0	0.045	BbB2	SB4
84	3	85	1.40	100	1.40	330	10.0	0.045	BbB2	C7
85	3	86	3.45	125	3.45	660	10.0	0.045	SuA	C6
86	3	87	2.56	100	1.77	660	10.0	0.033	BbC2	C6
87	3	88	0.36	100	0.01	696	10.0	0.033	BbB2	C6
88	3	89	0.01	100	0.01	484	10.0	0.033	Pf	C6

Table C4 10 Acre Grid Cell GIS-Generated Model Input Parameter Values (continued)

Cell Number	Direct.	Rec. Cell	Hillside Slope	Slope Length	Channel Slope	Channel Length	Channel Side Slope	Mann. N	Soils	Fields
89	5	97	4.62	125		131	10.0	0.033	BbB2	W4
90	5	98	3.26	125	3.48	41	10.0	0.033	TaA	W4
91	6	98	1.09	100	1.09	933	10.0	0.045	Pf	C5
92	4	100	0.88	100	0.88	466	10.0	0.045	SuA	C7
93	2	101	3.38	125	2.89	466	10.0	0.045	BaA	C6
94	1	86	3.26	125	2.87	660	10.0	0.045	BbB2	C6
95	3	96	2.57	100	2.57	330	10.0	0.045	BbB2	C6
96	3	97	3.20	125	2.74	666	10.0	0.045	BbB2	C6
97	3	98	4.86	125	0.35	616	10.0	0.033	BbB2	C10
98	5	102	0.01	100	0.01	707	10.0	0.033	Pf	C11
99	3	100	0.93	100	0.93	330	10.0	0.045	HdA	C8
100	3	101	0.90	100	0.90	660	10.0	0.045	BuA	C9
101	1	94	1.74	100	1.77	466	10.0	0.045	BbB2	C9

APPENDIX D

Gauge Site Channel Cross Section Measurements

Cross Section D1

Horizontal Distance	Vertical Height
0.0	2.80
10.0	2.57
20.0	1.45
25.0	0.36
26.0	0.21
27.0	0.00
28.0	0.06
29.0	0.94
34.0	1.64
44.0	2.36
54.0	2.80

Cross Section D2

Horizontal Distance	Vertical Height
0.0	1.46
10.0	1.27
20.0	1.00
25.0	0.80
26.0	0.00
28.0	0.82
33.0	1.16
53.0	1.21
63.0	1.46

Cross Section S3

Horizontal Distance	Vertical Height
0.0	3.82
10.0	3.77
20.0	1.72
25.0	0.47
26.0	0.00
28.0	0.32
33.0	1.44
53.0	1.95
63.0	3.25

Cross Section K4

Horizontal Distance	Vertical Height
0.0	2.60
10.0	2.54
20.0	2.16
25.0	1.83
30.0	0.00
34.0	2.25
39.0	2.41
49.0	2.45
59.0	2.50

Cross Section K5

Horizontal Distance	Vertical Height
0.0	1.24
10.0	1.23
15.0	1.22
20.0	1.22
23.0	0.00
25.0	1.49
30.0	1.64
35.0	1.72
45.0	1.75

Cross Section K6

Horizontal Distance	Vertical Height
0.0	1.40
10.0	0.57
20.0	0.26
26.0	0.00
28.0	0.24
33.0	0.57
38.0	1.40

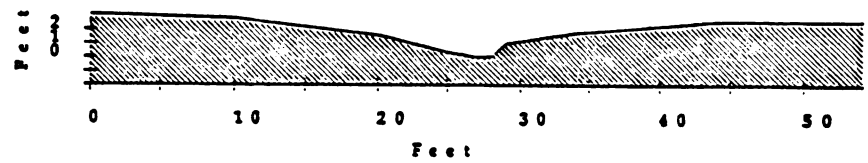

Cross Section D1

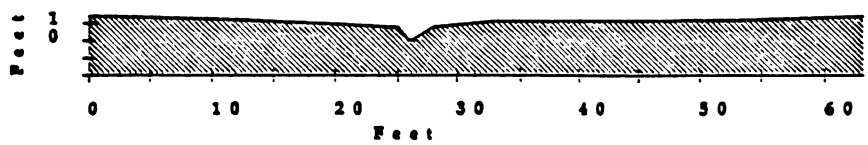

Cross Section D2

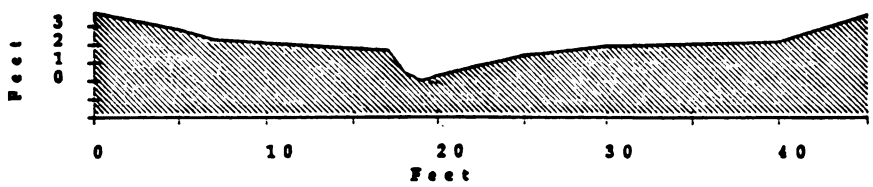

Cross Section S3

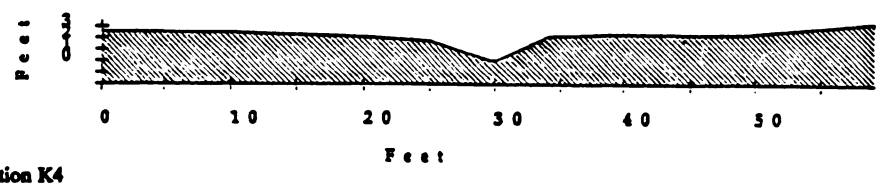

Cross Section K4

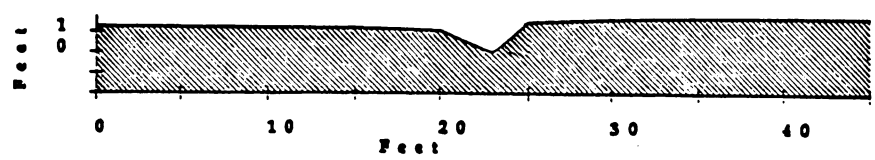

Cross Section K5

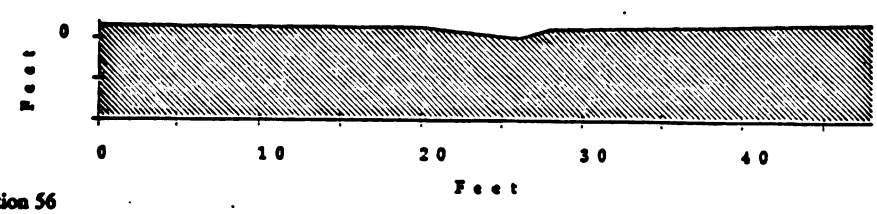

Cross Section 56

FIGURES D Channel Cross Sections

APPENDIX E

1992 Growing Season Weather Records

Day	Month	Year	Precip (mm)	Max. Temp. (C)	Min. Temp. (C)	Solar Radiation (ly/day)	EI
6	4	92	4.38	14.30	5.20	286.64	0.0
7	4	92	0.25	8.20	-2.00	402.93	0.0
8	4	92	2.54	12.30	-3.30	334.22	0.0
9	4	92	0.0	9.90	-0.50	399.05	0.0
10	4	92	1.02	2.10	-0.80	95.60	0.02
11	4	92	0.25	0.60	-5.90	418.97	0.0
12	4	92	0.0	0.40	-9.20	338.88	0.0
13	4	92	0.0	6.90	-1.40	378.10	0.0
14	4	92	0.0	7.60	2.00	134.66	0.0
15	4	92	2.03	9.60	5.40	154.57	0.05
16	4	92	0.0	9.90	3.40	213.02	0.0
17	4	92	0.0	7.60	0.30	246.72	0.0
18	4	92	13.46	11.30	6.70	49.57	2.05
19	4	92	2.29	14.90	4.10	387.15	0.1
20	4	92	3.05	4.50	0.20	92.41	0.06
21	4	92	2.54	0.50	-1.90	120.60	0.06
22	4	92	0.0	1.60	-1.00	250.95	0.0
23	4	92	0.0	3.90	0.20	196.38	0.0
24	4	92	0.0	7.30	0.00	262.67	0.0
25	4	92	0.0	5.10	0.30	214.83	0.0
26	4	92	0.0	10.40	-0.90	290.09	0.0
27	4	92	0.0	15.70	-3.90	607.07	0.0
28	4	92	0.0	27.40	6.00	539.67	0.0
29	4	92	0.0	26.50	4.60	510.43	0.0
30	4	92	0.0	33.30	10.80	562.59	0.0
1	5	92	0.0	29.00	14.20	538.62	0.0
2	5	92	0.0	20.20	6.40	586.46	0.0
3	5	92	0.0	18.70	-0.10	593.28	0.0
4	5	92	0.0	16.70	2.70	578.71	0.0

Day	Month	Year	Precip	Max. Temp.	Min. Temp.	Solar Radiation	EI
5	5	92	0.0	17.40	-1.30	624.83	0.0
6	5	92	0.0	24.40	4.60	635.09	0.0
7	5	92	0.0	29.50	10.20	623.36	0.0
8	5	92	0.0	30.10	12.30	620.26	0.0
9	5	92	0.0	30.30	13.70	488.45	0.0
10	5	92	2.54	24.50	13.40	257.84	0.5
11	5	92	20.07	21.70	11.90	358.53	23.97
12	5	92	1.78	19.40	6.50	567.15	0.04
13	5	92	0.0	12.90	0.80	260.86	0.0
14	5	92	0.0	23.30	3.40	526.38	0.0
15	5	92	0.0	26.10	9.30	534.05	0.0
16	5	92	7.87	25.10	14.40	460.69	5.67
17	5	92	1.78	16.40	8.60	403.19	0.55
18	5	92	0.0	24.50	6.90	664.14	0.0
19	5	92	0.0	32.00	14.00	500.43	0.0
20	5	92	0.0	29.90	16.00	578.10	0.0
21	5	92	0.0	27.80	18.10	414.22	0.0
22	5	92	0.25	21.50	6.10	197.93	0.0
23	5	92	0.0	13.70	3.60	672.93	0.0
24	5	92	0.0	12.60	4.10	371.29	0.0
25	5	92	14.99	10.30	3.20	252.41	5.55
26	5	92	0.0	16.50	1.80	507.50	0.0
27	5	92	0.0	19.00	2.90	507.24	0.0
28	5	92	0.51	20.50	5.80	603.36	0.02
29	5	92	0.0	23.20	6.80	692.93	0.0
30	5	92	0.0	25.60	6.20	689.22	0.0
31	5	92	0.0	25.60	11.10	521.46	0.0
1	6	92	0.0	25.20	12.10	559.91	0.0
2	6	92	0.0	25.30	8.50	515.34	0.0

Day	Month	Year	Precip	Max. Temp.	Min. Temp.	Solar Radiation	EI
3	6	92	0.0	27.60	10.70	562.84	0.0
4	6	92	10.67	20.00	9.90	640.52	8.56
5	6	92	8.13	20.10	8.60	237.59	2.13
6	6	92	0.76	15.30	6.80	479.74	0.0
7	6	92	6.86	17.70	1.30	412.76	0.04
8	6	92	6.60	18.50	11.10	407.67	0.04
9	6	92	0.0	22.50	14.30	413.53	0.0
10	6	92	0.0	26.90	10.90	634.57	0.0
11	6	92	0.0	30.20	12.50	660.60	0.0
12	6	92	0.0	31.40	13.10	548.36	0.0
13	6	92	0.0	30.50	15.10	616.90	0.0
14	6	92	2.28	27.00	16.30	265.09	0.06
15	6	92	11.17	21.00	14.30	459.22	6.18
16	6	92	51.82	24.50	15.40	332.59	249.55
17	6	92	12.45	19.30	15.90	226.98	22.98
18	6	92	4.06	25.10	16.10	571.72	1.94
19	6	92	0.25	15.70	9.40	206.90	0.0
20	6	92	0.0	17.80	3.90	641.72	0.0
21	6	92	2.29	17.90	6.00	526.12	0.23
22	6	92	1.27	19.10	12.00	264.22	0.14
23	6	92	0.0	23.70	9.60	614.14	0.0
24	6	92	1.02	22.40	12.60	646.90	0.02
25	6	92	0.0	18.60	9.00	392.15	0.0
26	6	92	0.0	20.20	4.90	713.45	0.0
27	6	92	0.0	24.70	7.10	541.55	0.0
28	6	92	0.0	25.80	13.40	458.53	0.0
29	6	92	0.0	19.70	12.10	652.33	0.0
30	6	92	31.50	15.30	11.60	123.19	55.71
1	7	92	0.0	17.00	12.90	211.64	0.0

Day	Month	Year	Precip	Max. Temp.	Min. Temp.	Solar Radiation	EI
2	7	92	13.46	15.10	12.70	146.55	3.11
3	7	92	0.0	20.20	10.00	623.28	0.0
4	7	92	0.0	20.10	8.80	653.45	0.0
5	7	92	0.0	22.00	6.90	675.00	0.0
6	7	92	0.76	22.10	8.40	378.97	0.06
7	7	92	0.0	25.90	13.90	358.79	0.0
8	7	92	0.0	25.40	15.70	625.54	0.0
9	7	92	3.56	25.80	13.80	463.28	1.32
10	7	92	8.89	20.70	12.20	347.50	6.82
11	7	92	4.83	18.70	9.70	214.31	1.85
12	7	92	24.89	23.60	14.60	419.12	80.92
13	7	92	0.0	20.10	11.60	264.91	0.0
14	7	92	0.0	23.90	8.20	655.34	0.0
15	7	92	2.29	24.30	14.10	467.41	.33
16	7	92	0.0	21.50	10.80	414.74	0.0
17	7	92	0.0	22.50	12.40	616.03	0.0
18	7	92	0.0	24.40	10.10	553.36	0.0
19	7	92	3.81	21.90	13.60	486.64	2.41
20	7	92	0.0	21.10	9.20	610.60	0.0
21	7	92	0.0	22.70	10.10	490.26	0.0
22	7	92	13.72	18.50	10.00	402.07	6.19
23	7	92	0.0	20.70	6.30	606.21	0.0
24	7	92	0.0	20.30	12.60	252.59	0.0
25	7	92	0.0	27.30	17.00	330.60	0.0
26	7	92	0.0	26.00	11.20	604.83	0.0
27	7	92	0.0	28.60	12.30	519.40	0.0
28	7	92	0.76	23.20	13.00	582.07	0.01
29	7	92	0.0	21.00	11.60	496.29	0.0
30	7	92	0.51	22.50	11.00	443.71	0.0

Day	Month	Year	Precip	Max. Temp.	Min. Temp.	Solar Radiation	EI
31	7	92	0.0	26.50	9.00	525.60	0.0
1	8	92	0.51	29.40	11.60	427.50	0.01
2	8	92	1.27	23.40	8.60	546.38	0.07
3	8	92	0.25	21.40	8.40	556.55	0.0
4	8	92	0.0	20.80	7.00	441.55	0.0
5	8	92	0.0	23.70	9.50	580.26	0.0
6	8	92	3.56	22.70	17.00	271.81	2.63
7	8	92	1.52	28.00	17.40	460.43	0.03
8	8	92	0.0	31.20	14.30	576.29	0.0
9	8	92	0.0	30.50	18.20	457.50	0.0
10	8	92	0.0	25.40	13.00	621.81	0.0
11	8	92	0.0	22.90	7.40	338.36	0.0
12	8	92	0.0	19.20	8.70	332.76	0.0
13	8	92	0.0	21.40	7.50	458.36	0.0
14	8	92	0.0	22.40	4.20	574.74	0.0
15	8	92	0.0	22.70	7.20	592.67	0.0
16	8	92	0.0	24.90	10.00	506.03	0.0
17	8	92	3.81	24.40	12.80	326.81	3.34
18	8	92	0.0	24.40	7.40	569.40	0.0
19	8	92	0.0	25.20	6.40	535.09	0.0
20	8	92	0.0	29.10	14.60	521.90	0.0
21	8	92	6.86	22.50	17.10	211.29	8.59
22	8	92	0.0	29.00	19.20	450.43	0.0
23	8	92	1.02	27.30	14.50	329.14	0.01
24	8	92	27.43	15.10	12.00	112.76	19.01
25	8	92	5.33	15.40	7.50	167.76	0.05
26	8	92	0.25	18.00	3.90	347.07	0.0
27	8	92	0.25	19.90	9.00	480.86	0.0
28	8	92	0.0	24.40	10.60	460.34	0.0

Day	Month	Year	Precip	Max. Temp.	Min. Temp.	Solar Radiation	EI
29	8	92	0.25	18.40	13.60	253.02	0.0
30	8	92	0.0	20.10	6.90	489.14	0.0
31	8	92	0.0	20.10	3.20	514.48	0.0
1	9	92	13.97	17.90	10.0	131.03	3.48
2	9	92	0.25	24.90	11.80	376.98	0.0
3	9	92	0.0	22.00	6.70	497.41	0.0
4	9	92	0.25	26.00	14.80	378.53	0.0
5	9	92	6.35	24.90	13.00	426.64	3.57
6	9	92	0.0	21.80	6.10	389.22	0.0
7	9	92	2.29	16.30	7.60	129.74	0.01
8	9	92	6.35	16.60	2.20	383.19	0.0
9	9	92	0.76	17.80	8.60	359.05	0.0
10	9	92	0.25	17.80	6.40	409.48	0.0
11	9	92	0.0	24.20	5.30	453.79	0.0
12	9	92	0.0	22.70	13.40	267.84	0.0
13	9	92	0.0	24.40	10.40	378.97	0.0
14	9	92	0.0	22.80	6.70	414.57	0.0
15	9	92	1.27	23.90	10.60	137.93	0.05
16	9	92	0.0	25.80	10.50	220.60	0.0
17	9	92	0.25	14.60	9.70	155.52	0.0
18	9	92	0.24	14.10	2.20	353.88	0.0
19	9	92	0.0	20.60	1.90	391.55	0.0
20	9	92	0.0	26.30	8.30	426.21	0.0
21	9	92	0.0	21.70	8.00	416.76	0.0
22	9	92	0.0	13.80	-1.00	426.98	0.0
23	9	92	0.0	25.10	5.40	405.86	0.0
24	9	92	0.0	25.10	13.20	401.72	0.0
25	9	92	0.0	24.80	10.80	379.83	0.0
26	9	92	0.0	18.30	3.60	320.43	0.0

Day	Month	Year	Precip	Max. Temp.	Min. Temp.	Solar Radiation	EI
27	9	92	0.0	21.50	0.30	321.55	0.0
28	9	92	0.0	12.40	-2.30	406.55	0.0
29	9	92	0.0	22.90	-1.50	353.45	0.0
30	9	92	0.0	27.60	4.60	385.09	0.0
1	10	92	0.0	31.50	2.50	391.90	0.0
2	10	92	0.0	30.20	3.80	378.97	0.0
3	10	92	0.0	22.30	2.80	377.50	0.0
4	10	92	0.0	21.60	8.20	365.86	0.0
5	10	92	0.0	24.60	10.80	289.31	0.0
6	10	92	0.0	12.20	4.50	216.29	0.0
7	10	92	4.32	9.50	5.30	72.93	0.72
8	10	92	6.09	10.40	5.30	74.05	0.02
9	10	92	0.0	11.00	6.10	67.50	0.0
10	10	92	0.0	14.10	-0.70	300.69	0.0
11	10	92	0.0	21.10	-3.70	303.79	0.0
12	10	92	0.0	12.00	3.50	322.33	0.0
13	10	92	0.0	11.80	0.30	253.45	0.0
14	10	92	0.0	5.20	-3.40	215.34	0.0
15	10	92	0.0	5.50	-6.90	167.59	0.0
16	10	92	1.52	1.20	-3.20	134.57	0.0

BIBLIOGRAPHY

Abbott, M.B., J.C. Bathurst, J.A. Cunge, P.E. O'Connell and J. Rasmussen. 1986. "An Introduction to the European Hydrological System (Systeme Hydrologique Europeen: SHE), 2: Structure of a Physically-Based, Distributed Modeling System". Journal of Hydrology. 87: 61-77.

Aha, A.V., J.E. Mopcroft and J.D. Ullman. 1983. Data Structures and Algorithms. Addison-Wesley. Reading, Massachusetts.

Ahuja, L.R. 1982. "Release of a Soluble Chemical from Soil to Runoff". Transactions ASAE. 25: 948-956.

Alberts, E.E., M.A. Weltz and F. Ghidey. 1989a. "Plant Growth Component". USDA-Water Erosion Prediction Project: Hillslope Profile Model Documentation. L.J. Lane and M.A. Nearing (eds). NSERL Report No. 2. USDA-ARS National Soil Erosion Research Laboratory. West Lafayette, Indiana. 8.1-8.38.

Alberts, E.E., J.M. Laflen, W.J. Rawls, J.R. Simanton and M.A. Nearing. 1989b. "Soil Component". USDA-Water Erosion Prediction Project: Hillslope Profile Model Documentation. L.J. Lane and M.A. Nearing (eds). NSERL Report No. 2. USDA-ARS National Soil Erosion Research Laboratory. West Lafayette, Indiana. 6.1-6.15.

Aller, L., T. Bennett, J.H. Lehr, R.J. Petty and G. Hackett. 1987. DRASTIC: A Standardized System for Evaluating Ground Water Pollution Potential Using Hydrogeologic Settings. EPA/600/2-87/035. Environmental Protection Agency. Ada, Oklahoma.

Arnold, J.G., J.R. Williams, A.D. Nicks and N.B. Sammons. 1990. SWRBB: A Basin Scale Simulation Model for Soil and Water Resources Management. Texas A&M Press.

Ashof, M.S. and D.K. Borah. 1992. "Modeling Pollutant Transport in Runoff and Sediment". Transactions ASAE. 35(6): 1789-1797.

Associated Press. Sept. 3, 1993. "Plan Would Merge and Purge Department of Agriculture".

Bagnold, R.A. 1966. "An Approach to the Sediment Transport Problem From General Physics". USGS Professional Paper. 422-J.

Bailey, G.W., R.R. Swank and H.P. Nicholson. 1974. "Predicting Pesticide Runoff from Agricultural Lands: A Conceptual Model". Journal of Environmental Quality. 3: 95-102.

Band, L.E. 1986. "Topographic Partition of Watersheds with Digital Elevation Models". Water Resources Research. 22(1): 15-24.

Baumer, O. 1989. Personal Communication. in: "Soil Component". 6.1-6.15. USDA-Water Erosion Prediction Project: Hillslope Profile Model Documentation. L.J. Lane and M.A. Nearing (eds). NSERL Report No. 2. USDA-ARS National Soil Erosion Research Laboratory. West Lafayette, Indiana.

Beasley, D.B, L.F. Huggins and E.F. Monke. 1980. ANSWERS: A Model for Watershed Planning. Transactions ASAE. 23(4): 938-944.

Bennett, J.P. 1974. "Concepts of Mathematical Modeling of Sediment Yield". Water Resources Research. 10(3): 485-492.

Betson, R.P. 1964. "What is Watershed Runoff?". Journal of Geophysical Research. 69: 1541-1552.

Beven, K 1993. "Prophecy, Reality and Uncertainty in Distributed Hydrologic Modeling". Advances in Water Resources. 16(1): 41-52.

Beven, K. 1989. "Changing Ideas in Hydrology: The Case of Physically-Based Models". Journal of Hydrology. 105: 157-172.

Beven, K. 1985. "Distributed Models". Hydrological Forecasting. M.G. Anderson and T.P. Burt (eds). John Wiley & Sons. New York. 405-437.

Binger, R.L., C.E. Murphree and C.K. Mutchler. 1989. "Comparison of Sediment Yield Models on Watersheds in Mississippi". Transactions ASAE. 32(2): 529-534.

Bodman. G.B and E.A. Coleman. 1944. "Moisture and Energy Conditions During Downward Entry of Water into Soils". Soil Science Society of America Proceeding. 8: 116-122.

Bolan, N.S., N.J. Barrow and A.M. Posner. 1985. "Describing the Effect of Time on Sorption of Phosphate by Iron and Aluminum Hydroxides". Journal of Soil Science. 36(2): 187-197.

Borg, H. and D.W. Williams. 1986. "Depth Development of Roots with Time: An Empirical Description". Transactions ASAE. 29(1): 194-197.

Boyer, J.M. 1993. "An Object-Oriented Approach to General Purpose River Basin Management". Proceedings of the Federal Interagency Workshop on Hydrologic Modeling: Demands for the 90's. USGS Water-Resources Investigations Report 93-4018. 4.16-4.21.

Braden, J. and D. Uchtmann. 1985. "Agricultural Nonpoint Pollution Control: An Assessment". Journal of Soil and Water Conservation. 40(1): 23-26.

Brakensiek, D.L., W.J. Rawls and G.R. Stephenson. 1986. "Determining the Saturated Hydraulic Conductivity of a Soil Containing Rock Fragments". Soil Science Society of America Journal. 50:834-835.

Brakensiek, D.L., R.L. Engleman and W.J. Rawls. 1981. "Variation Within Texture Classes of Soil Water Parameters". Transactions ASAE. 24(2): 335-339.

Brakensiek. D.L. 1966. "Hydrodynamics of Overland Flow and Nonprismatic Channels". Transactions ASAE. 9(1): 119-122.

Brooks, R.H. and A.T. Corey. 1964. "Hydraulic Properties of Porous Media". Hydrology Paper 3. Colorado State University. Fort Collins, Colorado.

Center for Resource Economics. 1990. 1990 Farm Bill: Environmental and Consumer Provisions. Volume 1: Statutory Language. Island Press. Washington D.C.

Chien, S.H. and W.R. Clayton. 1980. "Application of Elovich Equation to the Kinetics of Phosphate Release and Sorption in Soils". Soil Science Society of America Journal. 4(2): 265-268.

Chorley, R.J. 1978. "The Hillslope Hydrological Cycle". Hillslope Hydrology. M.J. Kirkby (ed). John Wiley & Sons. New York. 1-32.

Chow, V.T., D.R. Maidment and L.W. Mays. 1988. Applied Hydrology. McGraw Hill. New York.

Chu, S.T. 1978. "Infiltration During an Unsteady Rain". Water Resources Research. 14(3): 461-466.

Clark, E.H., J.A. Haverkamp and W. Chapman. 1985. Eroding Soils: The Off-Farm Impacts. The Conservation Foundation.

Crawford, N.H. and A.S. Donigian. 1973. Pesticide Transport and Runoff Model for Agricultural Lands. Office of Research and Development. USEPA. EPA-600/2-74-013.

Cronshey, R.G., F.D. Theurer and R.L. Glenn. 1993. "GIS-Water Quality Computer Model Interface: A Prototype". Proceedings, Geographic Information Systems and Environmental Modeling. Breckenridge, Colorado.

Crowder, B.M., M.O. Ribaudo and C.E. Young. 1988. Agriculture and Water Quality. USDA-ERS. Ag. Info. Bulletin No. 548. Washington D.C.

Daniel, T.C., D.R. Edwards and A.N. Sharpley. 1993. "Effect of Extractable Soil Surface Phosphorus on Runoff Water Quality". Transactions ASAE. 36(4): 1079-1085.

Dawes, W.R. and D.L. Short. 1988. TOPOG: Series Topographic Analysis and Catchment Drainage Modeling Package. Australian Centre of Catchment Hydrology. CSIRO Division of Water Resources. Canberra, Australia.

Dillaha, T.A. and D.B. Beasley. 1983. "Distributed Parameter Modeling of Sediment Movement and Particle Size Distribution". Transactions ASAE. 26(6): 1766-1772.

Dissmeyer, G.E. and G.R. Foster. 1981. "Estimating the Cover-Management Factor (C) in the Universal Soil Loss Equation of Forest Conditions". Journal of Soil and Water Conservation. 36(4): 235-240.

Djokic, D. 1993. "Towards General Purpose Spatial Decision Support System Using Existing Technologies". Proceedings, Geographic Information Systems and Environmental Modeling. Breckenridge, Colorado.

Donigian, A.S. and N.H. Crawford. 1976. Modeling Nonpoint Pollution from the Land Surface. Office of Research and Development. USEPA. EPA-600/3-76-083.

Dunne, T., T.R. Moore and C.H. Taylor. 1975. "Recognition and Prediction of Runoff Producing Zones in Humid Regions". Hydrologic Science Bulletin. 20: 305-327.

Ellison, W.D. 1947. "Soil Erosion Studies". Agricultural Engineering. 28: 145-146.

Emmerich, W.E., D.A. Woolhiser and E.D. Shirley. 1989. "Comparison of Lumped and Distributed Models for Chemical Transport of Surface Runoff". Journal of Environmental Quality. 18: 120-126.

Emmett, W.W. 1978. "Overland Flow". Hillslope Hydrology. M.J. Kirkby (ed). John Wiley & Sons. New York. 145-177.

Engel, B.A. 1993a. "Methodologies for Development of Hydrologic Response Units Based on Terrain, Land Cover and Soils Data". Proceedings, Geographic Information Systems and Environmental Modeling. Breckenridge, Colorado.

Engel, B.A., R. Srinivasan and C. Rewerts. 1993b. "A Spatial Decision Support System for Modeling and Managing Agricultural Nonpoint Source Pollution". Geographic Information Systems and Environmental Modeling. M.F. Goodchild, B.O. Parks and L.T. Steyaert (eds). Oxford University Press. Oxford. 231-237.

ESRI. 1991. Users Manual. Environmental Systems Research Institute. Redlands, California.

Evans, B.M and W.L. Myers. 1990. "A GIS-Based Approach to Evaluating Regional Groundwater Pollution Potential with DRASTIC". Journal of Soil and Water Conservation. 45(2): 242-245.

Fairfield, J. and P. Leymaire. 1991. "Drainage Networks from Grid Digital Elevation Models". Water Resources Research. 27: 709-717.

Foster, G.R., G.A. Weesies, K.G. Renard, J.P. Porter and D.C Yoder. 1991. "Conservation Practice Factor". Predicting Soil Erosion by Water: A Guide to Conservation Planning with the Revised Universal Soil Loss Equation (RUSLE). USDA-ARS.

Foster, G.R., L.J. Lane, M.A. Nearing, S.C. Finkner and D.C. Flanagan. 1989. "Erosion Component". USDA-Water Erosion Prediction Project: Hillslope Profile Model Documentation. L.J. Lane and M.A. Nearing (eds). NSERL Report No. 2. USDA-ARS National Soil Erosion Research Laboratory. West Lafayette, Indiana. 10.1-10.12.

Foster, G.R. 1982. "Modeling the Erosion Process". Hydrologic Modeling of Small Watersheds. C.T. Haan, H.P. Johnson and D.L. Brakensiek (eds). ASAE Monograph No. 5. St. Joseph, Michigan. 297-382.

Foster, G.R. 1981. "The Overland Flow Process Under Natural Conditions". Biological Effects in the Hydrological Cycle. Proc. of the Third International Seminar for Hydrology Professors. Purdue University. West Lafayette, Indiana.

Foster, G.R., L.J. Land, J.D. Nowlin, J.M. Laflen and R.A. Young. 1980. "A Model to Estimate Sediment Yield from Field-Sized Areas: Development of Model". CREAMS: A Field-Scale Model for Chemicals, Runoff and Erosion from Agricultural Management Systems. USDA-ARS. Conservation Research Report No. 26. 36-64.

Foster, G.R., L.D. Meyer and C.A. Onstad. 1977. "A Runoff Erosivity Factor and Variable Slope Length Exponents for Soil Loss Estimates". Transactions ASAE. 20(4): 678-682.

Foster, G.R. 1976. "Sedimentation, General". Proceedings of the National Symposium on Urban Hydrology, Hydraulics and Sediment Control. University of Kentucky, Lexington.

Foster, G.R. and L.D. Meyer. 1972. "A Closed-Form Soil Erosion Equation for Upland Areas". Sedimentation: Symposium to Honor Professor H.A. Einstein. H.W. Shen (ed). Ft. Collins, CO.

Freeman, G.T. 1991. "Calculating Catchment Area with Divergent Flow Based on a Regular Grid". Computer and Geosciences. 17: 413-422.

Freeze, R.A. 1974. "Streamflow Generation". Reviews of Geophysics and Space Physics. 12(4): 627-647.

Freezor, D.R., M.C. Hirschi and B.J. Lesikar. 1989. "Effect of Cell Size on AGNPS Prediction". ASAE Paper No. 89-2662. New Orleans, Louisiana.

Frere, M.H., J.D. Ross and L.J. Lane. 1980. "The Nutrient Submodel". CREAMS: A Field-Scale Model for Chemicals, Runoff and Erosion from Agricultural Management Systems. USDA-ARS. Conservation Research Report No. 26. 65-87.

Frere, M.H., C.A. Onstad and H.N. Holton. 1975. ACTMO: An Agricultural Chemical Transport Model. ARS-H-3. Agricultural Research Service, USDA. Washington D.C.

Gao, X., S. Sorooshian and D.C. Goodrich. 1993. "Linkage of a GIS to a Distributed Rainfall-Runoff Model". Geographic Information Systems and Environmental Modeling. M.F. Goodchild, B.O. Parks and L.T. Steyaert (eds). Oxford University Press. Oxford. 182-187.

Ghebreiyessus, Y. and J.M. Gregory. 1987. "Crop Canopy Functions for Soil Erosion Prediction". Transactions ASAE 30(3): 676-682.

Goodchild, M.F. 1993. Geographic Information Systems and Environmental Modeling. Geographic Information Systems and Environmental Modeling. M.F. Goodchild, B.O. Parks and L.T. Steyaert (eds). Oxford University Press.

Goodrich, D.C., Woolhiser, D.A. and Keefer, T.O. 1991. "Kinematic Routing Using Finite Elements on a Triangular Irregular Network". Water Resources Research. 27(6): 995-1003.

Grayson, R.B., I.D. Moore and T.A. McMahon. 1992a. "Physically-Based Hydrologic Modeling - II: Is the Concept Realistic?". Water Resources Research. 26(10): 2659-2666.

Grayson, R.B., I.D. Moore and T.A. McMahon. 1992b. "Physically-Based Hydrologic Modeling - I: A Terrain-Based Model for Investigative Purposes". Water Resources Research. 26(10): 2639-2658.

Green, W.H. and G.A. Ampt. 1911. "Study of Soil Physics: 1. Flow of Air and Water Through Soils". Journal Agricultural Science. 4: 1-24.

Griner, A.J. 1993. Development of a Water Supply Protection Model in a GIS. Geographic Information Systems and Water Resources, Proceedings. J.M. Harlin and K.J. Lanfear (eds). AWRA. Bethesda, Maryland. 371-378.

Haith, D.A. and L.L. Shoemaker. 1987. "Generalized Watershed Loading Functions for Stream Flow Nutrients". Water Resources Bulletin. 23(3): 471-478.

Halliday, S.L. and M.L. Wolfe. 1991. "Assessing Ground Water Pollution Potential from Nitrogen Fertilizer Using a Geographic Information System". Water Resources Bulletin. 27(2): 237-245.

Hamed, K. and B.A. Engel. 1993. "Soil Erosion Estimation Within the Animal Science Watershed". Class Report for AGEN 526. Agricultural Engineering Department. Purdue University. West Lafayette, Indiana.

Hamlett, J.M. and G.W. Petersen. 1992. "Geographic Information Systems for Nonpoint Pollution Ranking of Watershed". Water Resources Update. The Universities Council of Water Resources. 87: 21-25.

Harlin, J.M. and K.J. Lanfear (eds). 1993. Symposium on Geographic Information Systems and Water Resources. AWRA Tech. Publ. Series. TPS-93-1. Bethesda, Maryland.

Hearne, G.A., M. Wireman, A. Campbell, S. Turner and G.P. Ingersoll. 1991. Vulnerability of Ground Water in the Greater Denver Area. USGS. Water Resources Investigations Report 91-4143. Denver, Colorado.

Henderson, F.M. and R.A. Wooding. 1965. "Overland Flow and Groundwater Flow from a Steady Rainfall of Infinite Duration". Journal Geophysical Research. 69(8): 1531-1539.

Hession, C.W. and V.O. Shanholtz. 1988. "A Geographic Information System for Targeting Nonpoint Source Agricultural Pollution". Journal of Water Conservation. 43(3): 264-266.

Hewlett, J.D and A.R. Hibbert. 1967. "Factors Affecting the Response of Small Watersheds to Precipitation in Humid Areas". Proceedings of the International Symposium on Forest Hydrology. Pennsylvania State University. Pergamon.

Hjelmfelt, A.T. and C.R. Amerman. 1980. "The Mathematical Basin Model of Merrill Benard". Proceedings of International Symposium on the Hydrological Regime. Helsinki. AISH Publ. No. 130.

Holtan, H.N, G.J. Stiltner, W.H. Henson and N.C. Lopez. 1975. USDAHL-74 Model of Watershed Hydrology. USDA-ARS Tech. Bull. No. 1518. Washington D.C.

Holtan, H.N. and N.C. Lopez. 1971. USDAHL-70 Model of Watershed Hydrology. USDA Technical Bulletin 1435. Washington D.C.

Holton, H.N. 1961. A Concept for Infiltration Estimates in Watershed Engineering. USDA Bulletin. Washington D.C.

Hoogenboom, G., J.W. White, J.W. Jones and D.J. Boote. 1990. BEANGRO Version 1.00: Dry Bean Crop Growth Simulation Model User's Guide. University of Florida, Florida Agricultural Experiment Station Journal No. N-00379. Gainesville, Florida.

Horton, R.E. 1933. "The Role of Infiltration in the Hydrological Cycle". Transaction American Geophysical Union. 14: 446-460.

Huggins, L.F. and J.R. Burney. 1982. "Surface Runoff, Storage and Routing. Hydrologic Modeling of Small Watersheds. C.T. Haan, H.P. Johnson and D.L. Brakensiek (eds). ASAE Monograph No. 5. St. Joseph, Michigan. 169-228.

Hutchinson, D.E. and H.W. Pritchard. 1976. "Resource Conservation Glossary". Journal of Soil and Water Conservation. 31(4).

Ingram, J.J and D.A. Woolhiser. 1981. "Chemical Transfer into Overland Flow". Proceedings ASCE Symposium of Watershed Management. Boise, Idaho.

Jenson, S.K. and J.O. Domingue. 1988. "Extracting Topographic Structure from Digital Elevation Model Data for Geographic Information System Analysis". Photogrametric Engineering and Remote Sensing. 54: 1593-1600.

Jones, J.W., K.J. Boote, G. Hoogenboom, S.S. Jagtap and G.G Wilkerson. 1989. SOYGRO V5.42: Soybean Crop Growth Simulation Model. University of Florida. Florida Agricultural Experimental Station Journal No. 8304. Gainesville, Florida.

Knisel, W.G (ed). 1980. CREAMS: A Field-Scale Model for Chemicals, Runoff and Erosion from Agricultural Management Systems. USDA-ARS. Conservation Research Report No. 26.

Lane, L.J. and M.A. Nearing (eds). 1989. USDA-Water Erosion Prediction Project: Hillslope Profile Model Documentation. NSERL Report No. 2. USDA-ARS National Soil Erosion Research Laboratory. West Lafayette, Indiana.

Larson, C.L., C.A. Onstad and H.H. Richardson. 1982. "Some Particular Watershed Models". Hydrologic Modeling of Small Watersheds. C.T. Haan, H.P. Johnson and D.L. Brakensiek (eds). ASAE Monograph No. 5. St. Joseph, Michigan. 410-436.

Lattenmaier, D.P., E. Hooper, C. Wagoner and K. Faris. 1991. "Trends in Stream Quality in the Continental United States: 1978-1987". Water Resources Research. Vol 27(3): 327-339.

Leavesley, G.H., P.J. Restrepo, L.G. Stannard and M.J. Dixon. 1993. "The Modular Hydrologic Modeling System: MHMS". Proceedings of the Federal Interagency Workshop on Hydrologic Modeling: Demands for the 90's. USGS Water-Resources Investigations Report 93-4018. 4.40-4.42.

Lee, D., T.A Dillaha and J.H. Sherrard. 1989. "Modeling Phosphorus Transport in Grass Buffer Strips". Journal of Environmental Engineering. 15(2): 409-427.

Lighthill, F.R. and G.B. Witham. 1955. "On Kinematic Waves: 1, Flood Movement in Long Rivers". Proceedings of the Royal Society of London.

Loague, K.M. and R.A. Freeze. 1985. "A Comparison of Rainfall-Runoff Modeling Techniques on Small Upland Catchments". Water Resources Research. 21(2): 229-248.

Loucks, D.P., J. Kindler and K. Fedra. 1985. "Interactive Water Resources Modeling and Model Use: an Overview". Water Resources Research. 21(2): 131-142.

Maidment, D.R. 1993. GIS and Hydrologic Modeling. Geographic Information Systems and Environmental Modeling. M.F. Goodchild, B.O. Parks and L.T. Steyaert (eds). Oxford University Press. Oxford. 147-167.

Maidment, D.R., D. Djokic and K.G. Lawrence. 1989. "Hydrologic Modeling on a Triangulated Irregular Network". Transactions American Geophysical Union. 70:1091-1099.

Massey, H.F. and M.L. Jackson. 1952. "Selective Erosion of Soil Fertility Constituents". Soil Science Society of America Proceedings. 45: 543-547.

McCool, D.K., G.R. Foster and G.A. Weesies. 1991. "Slope Length and Steepness Factors". Predicting Soil Erosion by Water: A Guide to Conservation Planning with the Revised Universal Soil Loss Equation (RUSLE). USDA-ARS.

Mein, R.G. and C.L. Larson. 1973. "Modeling Infiltration During a Steady Rain". Water Resources Research. 9(2): 384-394.

Menzel, R.G. 1980. "Enrichment Ratios for Water Quality Modeling". CREAMS: A Field-Scale Model for Chemicals, Runoff and Erosion from Agricultural Management Systems. USDA-ARS. Conservation Research Report No. 26. 486-492.

Meyer, L.D., G.R. Foster and M.J. Römkens. 1975. "Source of Soil Eroded by Water from Upland Slopes". Present and Prospective Technology for Predicting Sediment Yields and Sources. ARS-S-40. USDA-ARS. Washington D.C.

Meyer, L.D. and W.H. Wischmeier. 1969. "Mathematical Simulation of the Processes of Soil Erosion by Water". Transactions ASAE. 12(6): 754-758.

Mitchell, J.K, B.A. Engel, R. Srinivasan and S.S.Y. Wang. 1993. "Validation of AGNPS for Small Watersheds Using an Integrated AGNPS/GIS System". Symposium on Geographic Information Systems and Water Resources. J.M. Harlin and K.J. Lanfear (eds). AWRA. Mobile, Alabama. 89-100.

Moore, I.D. 1993a. "Hydrologic Modeling in GIS". Proceedings, Geographic Information Systems and Environmental Modeling. Breckenridge, Colorado.

Moore, I.D., A.K. Turner, P.P. Wilson, S.K. Jenson and L.E. Band. 1993b. "GIS and Surface-Subsurface Process Modeling". Geographic Information Systems and Environmental Modeling. M.F. Goodchild, B.O. Parks and L.T. Steyaert (eds). Oxford University Press. Oxford. 196-230.

Moore, I.D. and R.B. Grayson. 1991a. 'Terrain-Based Catchment Partitioning and Runoff Reduction Using Vector Elevation Data". Water Resources Research. 27(6): 1177-1191.

Moore, I.D., R.B. Grayson and A.R. Lanson. 1991b. "Digital Terrain Modeling: A Review of Hydrological, Geomorphological and Biological Applications". Hydrological Processes. 5: 3-10.

Moore, I.D. and J.L. Nieber. 1989. "Landscape Assessment of Soil Erosion and Nonpoint Source Pollution". Minnesota Academy of Sciences Journal. 55: 18-25.

Musgrave, G.W. 1955. "How Much of the Rain Enters the Soil?". USDA Water Yearbook of Agriculture. Washington D.C.

National Research Council. 1993. Ground Water Vulnerability Assessment: Predicting Relative Contamination Potential Under Conditions of Uncertainty. National Academy Press. Washington D.C.

Needham, S. and R.A. Young. 1993. "ANN-AGNPS: A Continuous Simulation Watershed Model". Proceedings of the Federal Interagency Workshop on Hydrologic Modeling Demands for the 90's. USGS Water Resource Investigation Report. 93-4018. 4.32-4.39.

Needham, S. and B.E. Vieux. 1989. "A GIS for AGNPS Parameter Input and Mapping Output". ASAE Paper No. 89-2673. New Orleans, Louisiana.

Negev, M. 1967. "A Sediment Model on a Digital Computer". Technical Report No. 76. Department of Civil Engineering. Stanford University. Stanford, California.

Novotny, V. and G. Chesters. 1981. Handbook of Nonpoint Pollution: Sources and Management. Van Nostrand Reinhold Environmental Engineering Series. New York.

Novotny, V., M. Chin and H.V. Tran. 1979. LANDRUN: An Overland Flow Mathematical Model, Users Manual, Calibration, and Use. International Joint Commission. Windsor, Ontario.

O'Callaghan, J.F. and D.M. Marks. 1984. "The Extraction of Drainage Networks from Digital Elevation Data". Computer Vision, Graphics and Image Processing. 28: 323-344.

Olivieri, L.J., G.M. Schaal, T.J. Logan, W.J. Elliot and B. Motch. 1991. "Generating AGNPS Input Using Remote Sensing and GIS". ASAE Paper No. 91-2662. Chicago, Illinois.

Onstad, C.A. and D.L. Brakensiek. 1968. "Watershed Simulation by Stream Path Analogy". Water Resources Research 4(5):965-971.

Otterby, M.A. and C.A. Onstad. 1978. Assessment of Upland Erosion and Sedimentation from Agricultural Nonpoint Sources in Minnesota. University of Minnesota, Dept. of Agricultural Engineering.

Panuska, J.C., I.D. Moore and L.A. Kramer. 1991. "Terrain Analysis: Integration into the Agricultural Nonpoint Source (AGNPS) Pollution Model". Journal of Soil and Water Conservation. 46(1): 59-64.

Philip, J.R. 1957. "The Theory of Infiltration: 1. The Infiltration Equation and Its Solution". Soil Science. 83: 345-357.

Quinn, P., K. Beven, P. Chevallier and O. Planchon. 1991. "The Prediction of Hillslope Flow Paths for Distributed Hydrological Modeling Using Digital Terrain Models". Hydrological Processes. 5: 59-79.

Rawls, W.J., L.R. Ahuja, D.L. Brakensiek and A. Shirmohammadi. 1993. "Infiltration and Soil Water Movement". Handbook of Hydrology. D.R. Maidment (ed). McGraw-Hill. New York.

Rawls, W.J., D.L. Brakensiek and N. Miller. 1983. "Green-Ampt Infiltration Parameters from Soils Data". Journal Hydraulic Div. ASCE. 109(1): 62-70.

Rawls, W.J., D.L. Brakensiek and K.E. Saxton. 1982. "Estimation of Soil Water Properties". Transactions ASAE. 25(5): 1316-1320.

Rawls, W.J., C.A. Onstad and H.H. Richardson. 1980. "Residue and Tillage Effects on SCS Runoff Curve Numbers". CREAMS: A Field Scale Model for Chemicals, Runoff, and Erosion from Agricultural Management Systems. W.G. Knisel (ed). USDA-ARS Conservation Research Report No. 26. Washington D.C. 405-425.

Renard, K.G., G.R. Foster, G.A. Weesies and J.P. Porter. 1991. "RUSLE: Revised Universal Soil Loss Equation". Journal of Soil and Water Conservation. 46(1): 30-33.

Renard, K.G. and G.R. Foster. 1983. "Soil Conservation: Principles of Erosion by Water". Dryland Agriculture. Agronomy Monograph No. 23. American Society of Agronomy. Madison, Wisconsin.

Renfro, G.W. 1975. "Use of Erosion Equations and Sediment Delivery Ratios for Predicting Sediment Yield". Present and Prospective Technology for Predicting Sediment Yields and Sources. ARS-S-40. USDA-ARS. Washington D.C.

Rewerts, C.C. and B.A. Engel. 1991. "ANSWERS on GRASS: Integrating a Watershed Simulation with a GIS". ASAE Paper No. 91-2621.

Richards, L.A. 1931. "Capillary Conduction of Liquids in Porous Mediums". Physics. 1: 318-333.

Ritchie, J.T., U. Singh, D. Godwin and L. Hunt. 1989. A User's Guide to CERES MAIZE - Version 2.10. Michigan State University, International Benchmark Sites Network for Agrotechnology Transfer and International Fertilizer Development Center, Muscle Shoals, Alabama.

Ritchie, J.T. 1972. "A Model for Predicting Evaporation from a Row Crop With Incomplete Cover". Water Resources Research. 8(5): 1204-1213.

Roehl, J.R. 1962. "Sediment Source Areas, Delivery Ratios, and Influencing Morphological Factors". International Association of Scientific Hydrology. Publication No. 59.

Römkens, M.J., R.A. Young, J.W. Poesen, K.K. McCool and S.A. El Swaify. 1991. "The USLE Soils Erodibility Factor". Predicting Soil Erosion by Water: A Guide to Conservation Planning with the Revised Universal Soil Loss Equation (RUSLE). USDA-ARS.

Ross, B.B., D.N. Contractor and V.O. Shanholtz. 1979. "A Finite-Element Model of Overland and Channel Flow for Assessing the Hydrologic Impact of Land-Use Change". Journal of Hydrology. 41: 11-30.

Rousseau, A., W.T. Dickinson, R.P. Rudra and G.J. Wall. 1988. "A Phosphorus Transport Model for Small Agricultural Watershed". Canadian Agricultural Engineering. 15: 213-220.

Rudra, R.P., W.T Dickinson, D.F. Clark and G.J. Wall. 1986. "GAMES: A Screening Model of Soil Erosion and Fluvial Sedimentation on Agricultural Watersheds". Canadian Water Research Journal. 11(4): 58-71.

Rundquist, D.C., D.A. Rodekohr, A.J. Peters, R.L. Ehrman, L. Di and G. Murray. 1991. "Statewide Groundwater Vulnerability Assessment in Nebraska Using the DRASTIC/GIS Model". Geocarto International. 2:51-57.

Saghafian, B. 1993. "Implementation of a Distributed Hydrologic Model within Geographic Resources Analysis Support System (GRASS)". Proceedings, Geographic Information Systems and Environmental Modeling. Breckenridge, Colorado.

Savabi, M.R., A.D. Nicks, J.R. Williams and W.J. Rawls. 1980. "Water Balance and Percolation". USDA-Water Erosion Prediction Project: Hillslope Profile Model Documentation. L.J. Lane and M.A. Nearing (eds). NSERL Report No. 2. USDA-ARS. National Soil Erosion Research Laboratory. West Lafayette, Indiana. 7.1-7.14.

Sharpley, A.N. and R.G. Menzel. 1987. "The Impact of Soil and Fertilizer Phosphorus on the Environment". Advances in Agronomy. 41: 297-324.

Sharpley, A.N. 1985. "Effect of Soil Properties on the Kinetics of Desorption". Soil Science Society of America Journal. 47: 462-467.

Sharpley, A.N., L.R. Ahuja and R.G. Menzel. 1981. "The Release of Soil P to Runoff in Relation to the Kinetics of Desorption". Journal of Environmental Quality. 10: 386-391.

Sharpley, A.N. 1980. "The Enrichment of Soil P in Runoff Sediment". Journal of Environmental Quality. 9(3): 521-526.

Shaw, R. 1991. "Managing the Land: A Technology Perspective". Journal of Soil and Water Conservation. 46(6): 406-408.

Singh, V.P. 1989. Hydrologic Systems: Watershed Modeling, Vol. II. Prentice Hall. Englewood Cliffs, New Jersey.

Singh, V.P. 1988. Hydrologic Systems: Rainfall-Runoff Modeling, Vol. I. Prentice Hall. Englewood Cliffs, New Jersey.

Smith, R.E. 1982. "Rational Models of Infiltration Hydrodynamics". Modeling Components of the Hydrologic Cycle. V.P. Singh (ed). Water Resources Publication. Littleton, Colorado. 107-126.

Smith, R.E. and J.R. Williams. 1980. Simulation of the Surface Water Hydrology. CREAMS: A Field Scale Model for Chemicals, Runoff, and Erosion From Agricultural Management Systems. W.G. Knisel (ed). USDA-ARS Conservation Research Report No. 26. 13-35.

Smith, R.E. and J.Y. Parlange. 1978. "A Parameter Efficient Hydrologic Infiltration Model". Water Resources Research. 14(3): 533-538.

Speight, J.G. 1980. "The Role of Topography in Controlling Throughflow Generation: A Discussion". Earth Surface Processes and Landforms. 5: 187-191.

Star, J. and J. Estes. 1990. Geographic Information Systems: An Introduction. Prentice Hall. Englewood Cliffs, New Jersey.

Steenhuis, T.S. 1979. "Simulation of the Action of Soil and Water Conservation Practices in Controlling Pesticides". D.A. Haith and R.C. Loehr. (eds). Effectiveness of Soil and Water Conservation Practices for Pollution Control. USEPA Report No. EPA-600/3-79-106. Athens, Georgia.

Steube, M.M. and D.M. Johnston. 1990. "Runoff Volume Estimation Using GIS Techniques". Water Resources Bulletin. 26(4): 611-620.

Stewart, B.A., D.A. Woolheiser, W.H. Wischmeier, J.H. Caro and M.H. Frere. 1975. Control of Pollution from Cropland. USEPA/600/2-75/026. Washington, D.C.

Storm, D.E., T.A. Dillaha, S. Mostaghimi and V.O. Shanholtz. 1988. "Modeling Phosphorus Transport in Surface Runoff". Transactions ASAE. 31(1): 117-127.

Stroo, H.F., K.L. Bristow, L.F. Elliott, R.I. Papendick and G.S. Campbell. 1985. "Predicting Rates of Wheat Residue Decomposition". Soil Science Society of America Journal. 53: 91-99.

Taylor, S.E. and O.J. Sexton. 1972. "Some Implications of Leaf Tearing in Musaceae". Ecology. 63: 143-149.

Unwin, D.J. and J. Wilson. 1990. A Short Course in GIS. Dept. of Geography. Univ. Waikato, New Zealand.

US Department of Commerce. Weather Bureau. 1961. US Dept. Comm. Weather Bur. Tech. Paper 40. Washington D.C.

USDA-SCS. 1991a. Digital Soils Data. USDA-SCS Bulletin. Fort Worth, Texas.

USDA-SCS. 1991b. Classification and Evaluation of Models in Support of the SCS 5-Year Water Quality and Quantity Plan of Operation. Washington D.C.

USDA-SCS. 1978. Predicting Rainfall Erosion Losses: A Guide to Conservation Planning. Washington D.C.

USDA-SCS. 1973. Soil Survey of Swift County, Minnesota. USDA Soil Conservation Service. Washington, D.C.

USDA-SCS. 1972. SCS National Engineering Handbook. Washington D.C.

USEPA. 1991a. Coastal Nonpoint Pollution Program: Program Development and Approval Guidance. Washington D.C.

USEPA. 1991b. Guidance for Water Quality-Based Decision. The TMDL Process. Office of Water. Washington D.C.

USEPA. 1988. National Water Quality Inventory: 1988 Report to Congress. Washington D.C.

USEPA. 1986. National Water Quality Inventory: 1986 Report to Congress. Washington D.C.

USGS. 1987. Digital Elevation Models: Data Users Guide. National Mapping Program, Technical Instructions, Data Users Guide 5. Reston, Virginia.

Vieux, B.E., N.S. Farajalla and N. Gaur. 1993a. "Integrated GIS and Distributed Stormwater Runoff Modeling". Proceedings, Geographic Information Systems and Environmental Modeling. Breckenridge, Colorado.

Vieux, B.E. and S. Needham. 1993b. "Nonpoint Pollution Model Sensitivity to Grid-Cell Size". Journal of Water Resource Planning and Management. 119(2): 141-157.

Vieux, B.E., L.P. Herndon and R. Liston. 1989. "GIS and Water Quality Modeling for Agricultural Resource Management Systems". ASAE Paper No. 89-2184. Montreal, Canada.

Vieux, B.E. 1988. Finite Element Analysis of Hydrologic Response Areas Using a Geographic Information System. Ph.D. Dissertation. Michigan State University.

Wendt, R.C. and E.E. Alberts. 1984. "Estimating Labile and Dissolved Inorganic Phosphate Concentrations in Surface Runoff". Journal of Environmental Quality. 13(4): 613-618.

Williams, J.R., A.D. Nicks and J.G. Arnold. 1985. "Simulator for Water Resources in Rural Basis". Journal of Hydraulic Engineering. 111(6): 970-986.

Williams, J.R., C.A. Jones and P.T. Dyke. 1984. "A Modeling Approach to Determining the Relationship Between Erosion and Soil Productivity". Transactions ASAE. 27(1): 129-142.

Williams, J.R. 1980. "SPNM: A Model for Predicting Sediment, Phosphorus, and Nitrogen Yields from Agricultural Basins". Water Resources Bulletin. 16(5): 843-848.

Williams, J.R. 1975. "Sediment Yield Prediction with Universal Equation Using Energy Factor". Present and Prospective Technology for Predicting Sediment Yields and Sources. ARS-S-40. USDA-ARS. Washington D.C.

Williams, J.R. and R.W. Haan. 1972. HYMO: Problem Oriented Computer Language for Hydrologic Modeling, User's Manual. USDA ARS-2-9. Washington D.C.

Wischmeier, W.H. and D.D. Smith. 1978. Predicting Rainfall Erosion Losses. Agriculture Handbook No. 537. USDA-Science and Education Administration. Washington D.C.

Wischmeier, W.H., C.B. Johnson and B.V. Cross. 1971. "A Soil Erodibility Nomograph for Farmland and Construction Sites". Journal of Soil and Water Conservation. 26(5): 189-193.

Wolfe, M.L. and C. Neale. 1988. "Input Data Development for a Distributed Parameter Hydrologic Model (FESHM)". Proceedings, Modeling Agricultural, Forest and Rangeland Hydrology Conference. ASAE. St. Joseph, Michigan.

Wood, E.F., M. Sivapalan, K. Beven and L. Band. 1988. "Effects of Spatial Variability and Scale with Implications to Hydrologic Modeling". Journal of Hydrology. 102: 29-47.

Wooding, R.A. 1965. "A Hydraulic Model for the Catchment Stream Problem I: Kinematic Wave Theory". Journal of Hydrology. 3: 254-267.

Woolhiser, D.A, R.E. Smith and D.C. Goodrich. 1990. KINEROS: A Kinematic Runoff and Erosion Model, Documentation and User Manual. USDA ARS-77. Washington D.C.

Woolhiser, D.A. 1982. "Physically-Based Models of Watershed Runoff". Rainfall-Runoff Relationship. V.P. Singh (ed). Water Resources Publication. Littleton, Colorado. 189-202.

Woolhiser, D.A. and J.A. Liggett. 1967. "Unsteady One-Dimensional Flow Over a Plane: the Rising Hydrograph". Water Resources Research. 3(3): 753-771.

Yalin, Y.S. 1963. "An Expression for Bed-Load Transportation". Journal of the Hydraulics Division. Proceedings of the ASCE. 89(HY3): 221-250.

Yoder, D.C, J.P. Porter, J.M Laflen, J.R. Simanton, K.G. Renard and D.K. McCool. 1991. "Cover-Management Factor". Predicting Soil Erosion by Water: A Guide to Conservation Planning with the Revised Universal Soil Loss Equation (RUSLE). USDA-ARS.

Yoon, J., G. Padmanabhan and L.H. Woodbury. 1993. "Linking Agricultural Nonpoint Source Pollution Model (AGNPS) to a Geographic Information System (GIS)". Geographic Information Systems and Water Resources, Proceedings. J.M. Harlin and K.J. Lanfear (ed). AWRA. Bethesda, Maryland. 79-88.

Young, R.A., R.S. Alessi and S. Needham. 1992. "Application of a Distributed Parameter Model for Watershed Assessment". Proceedings from Managing Water Resources During Global Change. AWRA. Reno, Nevada.

Young, R.A., C.A. Onstad, D.D. Bosch and W.P. Anderson. 1989. "AGNPS: A Nonpoint Source Pollution Model for Evaluating Agricultural Watersheds". Journal of Soil and Water Conservation. 44(2): 168-173.

Young, R.A. and C.A. Onstad. 1987. AGNPS: Agricultural Nonpoint Source Pollution Model, A Watershed Analysis Tool. USDA-ARS Report 35. Washington D.C.

Young, R.A. and J.L. Wiersma. 1973. "The Role of Rainfall Impacts in Soil Detachment and Transport". Water Resources Research. 9(6): 1629-1636.